A STUDY ON MATERIAL PROPERTIES OF AUTOCLAVED AERATED CONCRETE (AAC) AND ITS COMPLEMENTARY WALL ELEMENTS: THEIR COMPATIBILITY IN CONTEMPORARY AND HISTORICAL WALL SECTIONS

A THESIS SUBMITTED TO
THE GRADUATE SCHOOL OF NATURAL AND APPLIED SCIENCES
OF
MIDDLE EAST TECHNICAL UNIVERSITY

BY

SİMGE ANDOLSUN

IN PARTIAL FULFILLMENT OF THE REQUIREMENTS
FOR
THE DEGREE OF MASTER OF SCIENCE
IN
BUILDING SCIENCE
IN
ARCHITECTURE

SEPTEMBER, 2006

Approval of the Graduate School of Natural and Applied Sciences

_____

Prof. Dr. Canan Özgen
Director

I certify that this thesis satisfies all the requirements as a thesis for the degree of Master of Science

_____

Assoc. Prof. Dr. Selahattin Önür
Head of Department

This is to certify that we have read this thesis and that in our opinion it is fully adequate, in scope and quality, as a thesis for the degree of Master of Science .

_____	_____
Prof. Dr. Emine Caner Saltık	Inst. Dr. Ayşe Tavukçuoğlu
Co-Supervisor	Supervisor

Examining Committee Members

Prof. Dr. Şahinde Demirci	(METU, CHEM)	_____
Inst. Dr. Ayşe Tavukçuoğlu	(METU, ARCH)	_____
Prof. Dr. Emine Caner Saltık	(METU, ARCH)	_____
Assoc. Prof. Dr. Arda Düzgüneş	(METU, ARCH)	_____
Inst. Dr. Sema Onurlu	(METU, ARCH)	_____

I hereby declare that all information in this document has been obtained and presented in accordance with academic rules and ethical conduct. I also declare that, as required by these rules and conduct, I have fully cited and referenced all material and results that are not original to this work.

Name, Last name:

Signature :

ABSTRACT

A STUDY ON MATERIAL PROPERTIES OF AUTOCLAVED AERATED CONCRETE (AAC) AND ITS COMPLEMENTARY WALL ELEMENTS: THEIR COMPATIBILITY IN CONTEMPORARY AND HISTORICAL WALL SECTIONS

Andolsun, Simge
M.Sc., Department of Architecture
Supervisor : Inst. Dr. Ayşe Tavukçuoğlu
Co-supervisor : Prof. Dr. Emine Caner Saltık

September 2006; 105 pages

Examined in this study were some physical, mechanical, compositional and durability properties of AAC, its neighboring plasters and jointing adhesive, all of which were produced in Turkey. The compatibility of these materials inside the contemporary wall section and within historic fabric was discussed in terms of their material properties.

In addition to the literature survey, laboratory studies were conducted on two types of AAC as G2 and G4, its jointing adhesive and exterior finishing layers as base coat, under coat, finish coat, water repellent finish coat; and some historical traditional construction materials of Anatolia as timber, masonry and infill brick, lime based exterior and interior plasters. The results were evaluated in terms of

material properties of AAC, the compatibility of AAC and its complementary elements with each other and with the historic timber framed structures in Anatolia.

It was concluded that the use of AAC in repairs of historical structures could be discussed only if the original infill is lost. In addition, its cement-plasters should be avoided from the historic fabric since they introduce salt problems to the structure. In terms of vapor permeability and modulus of elasticity, water repellent finish coat was proper finishing for AAC, and AAC, especially G4, exhibited similarities with historic infill mud brick. Further studies on other compatibility parameters were, however, necessary to decide on the compatibility of AAC with its neighboring materials. Moreover, the integrity of AAC with the historic fabric needed improvement by increasing its pozzolanicity and/or producing a new intermediary repair mortar/plaster.

Keywords: autoclaved aerated concrete (AAC); cement-plasters; compatibility; material properties; timber framed historical structures

ÖZ

GAZBETON MALZEMESİ VE BÜTÜNLEYİCİ DUVAR ELEMANLARININ MALZEME ÖZELLİKLERİ ÜZERİNE BİR ÇALIŞMA: GÜNÜMÜZ VE TARİHİ DUVAR KESİTLERİNDEKİ UYUMLULUKLARI

Andolsun, Simge
Yüksek Lisans, Mimarlık Bölümü
Tez Yöneticisi : Öğr. Gör. Dr. Ayşe Tavukçuoğlu
Ortak Tez Yöneticisi : Prof. Dr. Emine Caner Saltık

Eylül, 2006; 105 sayfa

Bu çalışmada Türkiye' de üretilmekte olan gazbeton malzemesinin, komşu sıvalarının ve gazbeton yapıştırıcısının temel fiziksel, mekanik, bileşim ve dayanıklılık özellikleri incelenmiştir. Bu malzemelerin hem günümüz duvar kesiti, hem de tarihi doku içinde uyumlulukları malzeme özellikleri açısından tartışılmıştır.

Çalışmada kaynak araştırması ve laboratuvar analizleri yapılmıştır. Laboratuvar analizleriyle incelenen malzemeler şunlardır: biri dolgu, G2, diğeri taşıyıcı, G4, iki çeşit gazbeton bloğu, gazbeton yapıştırıcısı ve birbiri ardına uygulanan çimento esaslı dış sıvaları, serpme sıva, kaba sıva, ince sıva ve su geçirimsiz ince sıva; Anadolu'nun tarihi geleneksel yapı malzemelerinden ahşap, dolgu ve örgü tuğlası, kireç esaslı iç ve dış sıvalar. Bulgular, gazbetonun malzeme özellikleri açısından

değerlendirilmiş; gazbeton ve bütünleyici duvar elemanlarının birbirleriyle ve, onarım amaçlı kullanımlarında, Anadolu'daki tarihi ahşap karkas yapılarla uyumlulukları açısından yorumlanmıştır.

Sonuç olarak, gazbeton malzemesinin tarihi yapıların onarımında dolgu malzemesi olarak kullanımının yalnızca özgün dolgu malzemenin kaybedildiği durumlarda tartışılabileceği belirtilmiştir. Gazbetonun çimento esaslı sıvalarının ise, tarihi dokuya ciddi zararlar verecek tuz problemlerine sebep olacakları belirtilmiş ve bu sebeple onarım amaçlı kullanılmalarının uygun olmadığı vurgulanmıştır. Su buharı geçirimlilik özellikleri ve esneklik modülü değerleri açısından, su geçirimsiz ince sıvanın gazbeton için uygun bir bitirme olduğu ve gazbetonun, özellikle G4 ün, tarihi kerpiç dolgu ile benzerlikler gösterdiği görülmüştür. Diğer taraftan, gazbetonun komşu malzemelerle uyumluluğu konusunda karar verebilmek için diğer uyumluluk parametrelerinin de çalışılması gerekmektedir. Bundan başka, onarım amaçlı kullanımları için gazbetonun tarihi dokuyla bütünlüğünün geliştirilmesi gerektiği görülmüştür. Bu amaçla, gazbetonun kireç esaslı onarım harçlarıyla iyi bağlanabilmesi için puzolanik aktivitesinin geliştirilmesi ve/veya tarihi doku ile gazbeton arasında kullanılacak yeni bir onarım harcının üretilmesi önerilmiştir.

Anahtar kelimeler: gazbeton; çimento esaslı sıvalar; uyumluluk; malzeme özellikleri; ahşap karkas yapılar

To The Twins

ACKNOWLEDGEMENTS

First of all, I am thankful to my supervisor Dr. Ayşe Tavukçuoğlu for her invaluable supervision, support and encouragement besides her instructive critical viewpoint, unbelievable energy and sacrifices throughout the research and above all for her belief in me. I would also like to thank my co-supervisor Prof. Dr. Emine Caner Saltık for her support with her deep knowledge, experience and eagle eyed viewpoint on the subject matter.

I would like to thank to Prof. Dr. Şahinde Demirci for her support, guidance and instructive criticism during the preparation of the reports submitted to the Scientific Research Council. I am grateful to Mrs. Taliye Yaşar and to Mr. Okan Zimitoğlu for their generous help and careful work during the thin-section analysis. I would like to extend my gratitude to the staff of the Materials Conservation Laboratory especially to Res. Asst. Alp Güney and Res. Asst. Göze Akoğlu who helped me with unforgettable sacrifices.

I would like to thank to Mr. Aykut Haşimoğlu as the contact person of the AKG Gazbeton Company who provided the necessary sample material as well as many written sources and visual materials for the conduction of the study and, above all, for his open-minded attitude which made this study turn into a cooperative research project.

I would finally like to thank to my family who supported me throughout my lifetime with their never-ending patience, love and belief in me, which made me everything I am. I would also like to express my gratitude to Mr. Ahmet Uğursal, who once was my instructor and now my colleague, for his guidance during the very hard last two years of my study.

TABLE OF CONTENTS

PLAGIARISM…….. iii

ABSTRACT……. iv

ÖZ……. vi

DEDICATION……. viii

ACKNOWLEDGEMENTS…… ix

LIST OF TABLES…….. xiii

LIST OF FIGURES……..…….. xv

CHAPTER

1. INTRODUCTION

1.1. Argument……. 1

1.2. Objectives…… 3

1.3. Procedure……. 3

1.4. Disposition……... 5

2. LITERATURE REVIEW……... 6

2.1. Material Properties of Autoclaved Aerated Concrete…….. 6

2.1.1. Physical Properties …… 7

2.1.2. Mechanical Properties…… 13

2.1.3. Compositional Properties……... 17

2.1.4. Durability Properties…….. 19

2.1.5. Functional Properties…….…... 21

2.2. Material Properties of Cement Based Neighboring Plasters of AAC….. 22

2.3. Building AAC Walls……...…… 24

2.3.1. The Process of Laying Up AAC Walls…….…. 25

2.3.2. The Application Process of Renderings on AAC Walls…… 27

2.3.3. The Use of AAC in Repairs of Timber Framed Historic Structures……... 29

2.4. Material Properties of Historic Construction Materials in Anatolia…… 31
2.5. Compatibility Issue…….……. 36
3. MATERIAL AND METHOD…… 39
3.1. Determination of Basic Physical Properties…… 44
3.1.1. Determination of Effective Porosity, Bulk Density, Water Absorption Capacity…….……. 45
3.1.2. Determination of Drying Rate…… 47
3.1.3. Determination of Water Vapor Permeability……. 49
3.1.4. Determination of Capillary Suction…… 52
3.2. Determination of Basic Mechanical Properties…… 53
3.2.1. Determination of Modulus of Elasticity (Young's Modulus)…… 54
3.2.2. Determination of Uniaxial Compressive Strength, Point Load Index and Correction factor…….……... 55
3.3. Determination of Durability Properties……..……. 56
3.3.1. Determination of Saturation Coefficient…… 56
3.3.2. Determination of Wet to Dry Strength Ratio……. 57
3.4. Determination of the Compositional Properties…….. 58
3.4.1. Determination of the Pozzolanic Activity……. 59
3.4.2. Cross and Thin Section Analyses…….. 59
3.4.3. X-Ray Diffraction (XRD) Analyses ……. 60
4. RESULTS ……..…….. 61
4.1. Basic Physical Properties……. 61
4.1.1 Effective Porosity, Bulk Density, Water Absorption Capacity….. 61
4.1.2. Drying Rate…… 63
4.1.3. Water Vapor Permeability……. 67
4.1.4. Capillary Suction……..…….. 69
4.2. Basic Mechanical Properties…… 71
4.2.1. Modulus of Elasticity (Young's Modulus)…… 71

4.2.2. Uniaxial Compressive Strength, Point Load Strength Index and Correction factor……... 72
4.3. Durability Properties……... 72
4.3.1. Saturation Coefficient……... 72
4.3.2. Wet-to-dry Strength Ratio…… 73
4.4. Compositional Properties……..... 74
4.4.1. Pozzolanic Activity Measurements by Electrical Conductivity…... 74
4.4.2. Cross and Thin Section Analyses…….…… 74
4.4.3. X-Ray Diffraction (XRD) Analyses……. 75
5. DISCUSSION……. 80
5.1. Discussion on The Material Properties of AAC..... 80
5.2. Discussion on The Compatibility of Autoclaved Aerated Concrete (AAC) With its Complementary Wall Elements..... 83
5.3. The Compatibility of Autoclaved Aerated Concrete (AAC) and Its Complementary Wall Elements With Historic Building Materials……..... 86
6. CONCLUSION……... 89
LIST OF REFERENCES…….. 93
APPENDICES…… 104
A. BASIC PHYSICAL AND MECHANICAL PROPERTIES OF AAC, EXTERIOR FINISHING PLASTERS AND JOINTING ADHESIVE…... 104
B. DRYING RATE SAMPLES..... 104
C. THE MATERIAL PROPERTIES OF AAC, ITS COMPLEMENTARY WALL ELEMENTS AND HISTORICAL MATERIALS..... 105

LIST OF TABLES

TABLE

2.01 Density Classes of Autoclaved Aerated Concrete……... **7**

2.02 Porosity characteristics of AAC products which differ in density……. **10**

2.03 The water and gas permeability values for AAC samples with varying densities and porosities ……. **11**

2.04 The Capillary Water Absorption Coefficient (*A*) of AAC Samples With Respect to Their Bulk Density and Porosity Values ……. **12**

2.05 Compressive Strength Classes of AAC……... **13**

2.06 Classification of AAC According to Characteristic Compressive Strength ……... **13**

2.07 Mechanical Properties of AAC With Respect to its Density Values…….. **15**

2.08 Prediction Equations for Modulus of Elasticity of Aerated Concrete **16**

2.09 Typical Composition of AAC……. **17**

2.10 Product specifications of the manufacturer for the AAC masonry blocks..... **22**

2.11 The Mechanical Properties of Cement Based Neighboring Plasters of AAC…… **24**

2.12 Product Dimensions of AAC Masonry Blocks…… **25**

2.13 The Material Properties Of Some Historical Materials……... **38**

3.01 The Historical Materials Examined In The Study……... **43**

3.02 Samples cut from the AAC masonry wall prepared by the manufacturer…… **45**

4.01 The Bulk Density *(ρ),* Effective Porosity (*ϕ)* and Water Absorption Capacity (θ_{max}) values of: (a) AAC, its cement based plasters and jointing adhesive; and (b) and the historic materials of bricks, plasters and timbers..... **62**

4.02 The results showing the maximum density of water vapor flow rates (R_{Emax}) above θ_c, the total drying period (T_d) and the critical moisture content by volume (θ_c %): **(a)** for AAC (G2 and G4) and its plasters (BC, UC, FC and WRFC); and **(b)** for the historical materials (AdEP, AIP, KMB, AIB, ST and AT)..... **66**

4.03 The water vapor diffusion resistance index (μ) and the equivalent air thickness of water vapor permeability (*SD*) values for AAC, its cement based plasters and jointing adhesive **68**

4.04 The empirical and calculated *SD* values for the AAC samples in combination with its plasters..... **69**

4.05 The results of mechanical properties of AAC, its cement based plasters and jointing adhesive in terms of ultrasonic velocity (*UV*), modulus of elasticity (E_{mod}) and uniaxial compressive strength (*UCS*)..... **72**

4.06 Modulus of Elasticity values, E_{mod}, of cement-based plasters found in this study by indirect testing method [(1)] and examined by direct testing method by Felekoglu [(2)]..... **72**

4.07 The results on saturation coefficients (S) of AAC and its cement based plasters..... **73**

A Basic physical and mechanical properties of AAC, exterior finishing plasters and jointing adhesive..... **104**

B Drying rate samples..... **104**

C The Material Properties of AAC, its Complementary Wall Elements and Some Historical Materials in Anatolia..... **105**

LIST OF FIGURES

FIGURE

2.01 Pore Systems in Aerated Concrete: (a) artificial air pore; (b) inter-cluster air pore; (c) inter particle pore……. **9**

2.02 Schematic representation of volume parts in the structure of aircrete (a=anhydrite, h=hydrogarnet). Apparent density is 400 kg/m^3 in this case, and raw materials are: pure quartz sand, lime, portland cement, anhydrite and water …… **9**

2.03 Porosity Obtained by Image Analyses for AAC samples of GN, GH*, GH and GS, which have bulk densities of 390 kg/m^3, 490 kg/m^3, 610 kg/m^3, 630 kg/m^3 respectively. The denser the sample, the higher the proportion of micro pores…… **10**

2.04 Typical Adsorption and Desorption Isotherm of AAC…… **11**

2.05 Graphs showing (a) the relationship between the compressive strength and the density of AAC, (b) the influence of the moisture content on the compressive strength of AAC…….. **14**

2.06 Stress Strain Relationships of AAC cubes under compression in different directions relative to rising direction…… **15**

2.07 Strength of porous structures with different pore size of macro pores. Macro pore fraction is 0.4……. **15**

2.08 XRD Patterns of AAC……. **18**

2.09 Micrographs of Autoclaved Aerated Concrete with **(a)** sand and **(b)** fly ash fillers……..….. **18**

2.10 Relationships Between Volumetric Proportion of Air Void and Tensile Strength of Materials (or Pressure P per unit area)……. **20**

2.11 The Variation of thermal conductivity of AAC with **(a)** density and **(b)** moisture content. Thermal conductivity increases as the moisture content of AAC increases. Thermal conductivity also increases with the increasing density…….. **22**

2.12 Preparation of the adhesive mortar ……. **26**

2.13 Laying Up the AAC Walls…….. **26**

2.14 Laying the bed course of AAC Wall Construction…….. **27**

2.15 Typical application details of exterior finishing systems for AAC masonry, showing the order of layers and their recommended thickness: **(a)** successive application of cement-based plasters with various additives; **(b)** water repellent finish coat applied directly on base coat..... **28**

2.16 The Kindergarten in Safranbolu, **(a)** a view from the inside showing the use of AAC as an infill material substitute of the original stone infill **(b)** a view from the outside showing the application of the exterior cement based plasters over the timber framed structure with AAC infill…… **29**

2.17 Milli Egemenlik Evi, Safranbolu. (a) AAC partition wall in conjunction with the historic fabric (b) the use of AAC inside the timber skeleton (c) the view of the house from the exterior after the repair work.....……. **30**

2.18 Öğretmen Evi, Safranbolu (a) close view to the application of AAC inside the timber framed structure (b) the timber framed wall with AAC infill after the repair work..... **31**

3.01 A Plain-end AAC Masonry Block of 20 cm x 25 cm x 60 cm divided into 9 equal parts along the rising direction. The marked slices were taken out for the preparation of the test samples…… **41**

3.02 AAC plaster and jointing adhesive samples cast in the laboratory into 3.5x 3.5 x 3.5 cm formworks…… **42**

3.03 An AAC Wall with Already Applied Finishing Layers Provided by the Manufacturer…….. **42**

3.04 Representation for the section of a G2 type finished AAC masonry wall as prepared by the manufacturer for the laboratory tests…… **43**

3.05 AAC, AAC plaster, historic infill and masonry fired brick, and historic lime based interior and exterior plaster samples left for drying at 20°C and 40±5 % relative humidity……. **47**

4.01 Bulk density and effective porosity values for the 2.5 cm thick **(a)** G2 samples and **(b)** G4 samples taken from 2.5 cm, 5 cm., 7.5 cm and 10 cm depth from the wire-cut surfaces. The samples taken from the wire-cut surfaces until 2.5 cm depth have the lowest porosity…… **62**

4.02 The drying curves showing moisture content as a function of time for **(a)** AAC (G2 and G4), its plasters (BC, UC, FC and WRFC) and **(b)** some historic materials (AdEP, AIP, KMB, AIB, ST and AT)…….. **64**

4.03 The drying curves showing evaporation rate, R_E (kg/m^{2}h), versus moisture content (% by volume) **(a)** AAC (G2 and G4) and its plasters (BC, UC, FC and WRFC); **(b)** historical materials (AdEP, AIP, KMB, AIB, ST and AT)……. **65**

4.04 The results of evaporation rates (R_{Emax}) of AAC, its cement based plasters and some historical materials of infill brick (AIB), masonry brick (KMB), exterior plaster (AdEP), interior plaster (AIP) and timber samples from Safranbolu (ST) and Amasya (AT).....……. **66**

4.05 Charts showing the changes in (a) *SD* and (b) μ values through an AAC wall of 20 cm thickness having wire-cut surfaces at both sides which were plastered typically as shown in Figure 2.15a. Two segments taken from the wire-cut surfaces up to a depth of 1.25 cm were located in the chart at both sides of the AAC block in order to show the effect of the wire-cutting process. The rest are the 2.5 cm thick segments taken along the 20 cm thickness of an AAC block from one wire-cut surface to the other…… **68**

4.06 The trend lines for G4 and G2 samples showing: **(a)** water absorption per unit area (kg/m^2) versus square root time ($\sqrt{t}$) (s$^{0.5}$); and **(b)** moisture content (θ) (% by volume) versus square root time ($\sqrt{t}$) (s$^{0.5}$)…….. **70**

4.07 **(a)** The curve showing the moisture content at the level of capillary rise (gr/cm^3) versus square root time ($\sqrt{t}$) (s$^{0.5}$) **(b)** the trend line showing the moisture content at the level of capillary rise versus the level of capillary rise (mm), for G4 and G2 samples…….....…….. **70**

4.08 **(a)** The curve showing the level of capillary rise (*h*, mm) versus time (t) (sec); and **(b)** the trendline showing the level of capillary rise (*h*, mm) versus square root time ($\sqrt{t}$) (s$^{0.5}$)……...…….. **71**

4.09 The graphs showing the modulus of elasticity values, E_{mod}, of the initial state, after the first and second cycles of wetting and drying and when left in water for 20 days after being saturated under vacuum: for **(a)** G2; and **(b)** G4 samples……. **74**

4.10 Cross sections showing the pore size distribution of AAC. Longer side of the micrograph = 1 cm……. **76**

4.11 Thin section of G2 showing the porous structure mineral composition and the matrix in detail **(a)** under single nicol with x2.5 magnification; **(b)** under cross nicol with x2.5 magnification; and **(c)** under cross nicol with x10 magnification…….. **77**

4.12 Thin section of G4 showing the porous structure mineral composition and the matrix in detail **(a)** under single nicol with x2.5 magnification; **(b)** under cross nicol with x2.5 magnification; and **(c)** under cross nicol with x20 magnification…….. **78**

4.13 The XRD traces of **(a)** G2 and **(b)** G4 powder samples…….. **79**

CHAPTER 1

INTRODUCTION

In this chapter are presented the argument and objectives of the study on which this thesis is based, together with a brief overview of the procedure followed in conducting the study proper and of the contents of remaining chapters.

1.1. Argument

Within wall sections, the use of breathing, porous and lightweight materials improves thermal performance and thereby contributes to energy efficient building design. These lightweight materials also provide sound and fire insulation apart from being environmentally friendly and need less embodied energy in their production. Autoclaved Aerated Concrete (AAC) is one of the most commonly-used light-weight construction materials for contemporary buildings, especially due to its low density, unique thermal and breathing properties and high fire resistance (Taşdemir & Ertokat, 2002; Andolsun, Tavukçuoğlu and Caner-Saltık, 2005; Narayanan & Ramamurthy, 2000a). Moreover, such advantageous properties make it preferable for earthquake-resistant housing (Taşdemir & Ertokat, 2002). It is also used as an infill material in restorations of timber framed historical buildings. This material has, however, some disadvantages; for instance, its very high water absorption capacity makes it susceptible to deteriorations due to water. It is, therefore, essential to better understand and develop the material properties of AAC for use in both contemporary and historical buildings.

In today's AAC construction, many problems such as failures on finishing surfaces in the form of flakes, scales and cracks arise due to lack of knowledge on the material properties of AAC and, thereby, due to wrong selection of neighboring

materials. For instance, it is often used together with incompatible plasters leading to problems at the interfaces, such as condensation, which leads to increase in water content of the wall section and some faults appearing on the finishing. In the presence of moisture and/or water AAC is known to lose its inherent thermal, water vapor permeability and mechanical properties (Narayanan *et al*., 2000a; RILEM, 1993; Tada, 1986; Jacobs & Mayer, 1992; Frey, 1992; Lippe, 1992; Andolsun *et al*., 2005; Svanholm, 1983; CEB, 1978; Briesemann, 1976). In order to prevent such problems, it is essential to use waterproof and water vapor permeable plasters and/or finish coats in applications of AAC (Felekoğlu, 2004; Kuş, 2002). In addition, recently in Turkey, AAC has gained another field of application with its use as a repair material for timber framed historical structures instead of original mud brick, fired brick and stone infill. These applications also involve introduction of the complementary wall elements of AAC such as its cement-based plasters and jointing adhesive, into the historic structure. The compatibility of AAC and its complementary wall elements with the historic fabric, however, is still not known and requires extensive investigations.

Neighboring construction materials are considered to be compatible with each other if they are similar in terms of their physical and mechanical properties. Compatibility can, therefore, be defined in terms of water vapor permeability and the dynamic modulus of elasticity *(E_{mod})*. For instance, any compatible plaster/layer is expected to have E_{mod} no higher and water vapor permeability no lower than the base material (Sasse & Snethlage, 1997).

In the study, it was accepted that the failures recently appearing on the finishing surfaces of AAC both in contemporary and historic structures occur since the neighboring materials within wall sections are incompatible in terms of their material properties. Some important parameters of compatibility were then selected and studied for these materials in order to investigate the source of the

incompatibility problem. During the discussions, among the tested parameters, were emphasized the water vapor permeability properties and E_{mod} values, which were also stressed by Sasse and Snethlage (1997).

The outcome of this study was believed to be beneficial for the proper selection of neighboring materials and/or finishing systems in order to benefit from the advantageous properties of AAC in wall sections. This study also emphasizes that compatibility of the construction materials with each other, even within the overall structure, is essential for the long-term performance and sustainability of buildings.

1.2. Objectives

This research was conducted to better understand certain material properties of AAC manufactured in Turkey and the recommended complementary wall elements such as its cement based plasters and jointing adhesive. The study was also conducted to define the properties expected from a compatible neighboring material for AAC.

By comparative evaluations of the results, it was aimed to assess the compatibility of AAC masonry with the cement-based plasters and the jointing adhesive recommended for it. The compatibility of AAC and its complementary wall elements with the historic fabric was also aimed to be discussed for their use as repair materials in timber-framed historical structures.

1.3. Procedure

The study was conducted in 5 basic phases:

In the first phase, a comprehensive literature survey was done which provided the preliminary information needed for initiation of the study. The survey covered

material properties of AAC, plasters and historic construction materials of Anatolia. Testing standards related to the sampling and laboratory analyses were also included in order to establish experimental guidelines for the analyses. Some observations on failures on the finishing surfaces of AAC walls were also documented visually.

In the second, a set of laboratory experiments was adapted from current testing standards and recent experimental studies and then conducted in order to determine the basic physical, mechanical and compositional properties of AAC produced in Turkey and its neighboring cement based plasters. Some of the laboratory tests were also conducted on historic materials such as brick, plaster and timber.

In the third, the data obtained from the laboratory analyses on AAC was evaluated. The AAC material was defined in terms of its some basic physical, mechanical and compositional properties together with its weathering behavior in the presence of water. The properties expected from a compatible neighboring material for AAC were also defined especially with an emphasis on water vapor permeability properties and modulus of elasticity values.

In the fourth, AAC was compared with its complementary wall elements in terms of material properties in order to assess its compatibility within the AAC masonry wall section. The appropriateness of some typical exterior finishing systems was discussed with respect to the continuity of water vapor transmission along their finishing layers, compatibility of their modulus of elasticity values. The compatibility of AAC and its plasters with the neighboring historical materials within a timber framed historical building was also discussed for the case of their use as repair materials. During the comparative evaluations, the emphasis was again given on their water vapor permeability, dynamic modulus of elasticity *(E_{mod})* and drying behavior.

In the last phase, conclusions were drawn from the results for the definition of material properties of AAC and its plasters all of which were produced in Turkey. The compatibility of AAC and its neighboring materials both in contemporary and timber framed historical wall sections were assessed on the basis of water vapor permeability and modulus of elasticity values. Furthermore, the most proper finishing system/s for AAC were recommended. Some further studies were also suggested.

1.4. Disposition

The study is presented in six chapters, of which this introduction is the first.

In the second chapter, a brief literature review is given basically on material properties of Autoclaved Aerated Concrete (AAC), the recommended cement based plasters for it and some historical materials. The application procedures of the AAC wall system and the compatibility issue are also introduced here briefly.

In the third chapter, the sampling and experimental procedures of the laboratory tests conducted for the study are clearly described.

In the fourth chapter, the experimental results are presented in tables, figures and in diagrams.

In the fifth chapter, the results are discussed in terms of the material properties of AAC, in terms of the compatibility of AAC with its complementary wall elements and also in terms of the compatibility of AAC and its complementary wall elements within the historic fabric.

The last chapter, the conclusion, summarizes the findings of the study and offers recommendations for future research work.

CHAPTER 2

LITERATURE REVIEW

A brief literature review is given here on the material properties of Autoclaved Aerated Concrete (AAC), some contemporary cement based plasters specifically produced for AAC masonry and some historical materials, such as mortar, plaster, timber and infill mud brick and fired brick. In addition, building procedure of the AAC wall system was described including the construction of masonry itself and application of typical exterior finishing systems, plasters of which were examined in this study. A visual documentation of some AAC applications in repairs of historic structures was also made. Lastly, issue of compatibility was defined as the main focus of this study.

2.1. Material Properties of Autoclaved Aerated Concrete

In Turkish Standards, Autoclaved Aerated Concrete is defined as the lightweight concrete, which is produced from the mixture of fine grain siliceous aggregate and an inorganic binder (such as lime or cement) by the use of a pore-forming agent which decreases its unit weight and a following steam curing process which gives its mechanical strength (TSE, 1988; Çiçek, 2002). In another source, Autoclaved Aerated Concrete is described basically as a mortar with pulverized sand and/or industrial waste like fly ash as filler, in which air is entrapped artificially by chemical means (metallic powders like Al, Zn, H_2O_2) resulting in significant reduction in density (Narayanan & Ramamurthy, 2000b).

Under this title, was a brief literature review given on the material properties of Autoclaved Aerated Concrete (AAC) through references from selected sources.

Due to the fact that there is considerable lack of knowledge in literature on the material properties of AAC that is produced in Turkey, the data hereunder mostly belong to the AAC produced in other countries. They are classified under the headings of physical properties, mechanical properties, raw material properties, durability properties and functional properties.

2.1.1. Physical Properties

Many physical properties of AAC depend on its density. The density range for AAC is given as 300- 1800 kg/m^3 in a source (RILEM, 1993), while the range is stated to be between 100 and 800 kg/m^3 in another (Schober, 2005). The density classes stated in European Norms are as shown in Table 2.01 below (prEN 12602, 1999; Taşdemir *et.al*., 2002):

Table 2.01: Density Classes of Autoclaved Aerated Concrete (Taşdemir *et. al.,* 2002)

Density Class	**300**	**350**	**400**	**450**	**500**	**550**	**600**	**650**
Dry Density (kg/m^3)	>250 ≤300	>300 ≤350	>350 ≤400	>400 ≤450	>450 ≤500	>500 ≤550	>550 ≤600	>600 ≤650
Density Class	**700**	**750**	**800**	**850**	**900**	**950**	**1000**	
Dry Density (kg/m^3)	>650 ≤700	>700 ≤750	>750 ≤800	>800 ≤850	>850 ≤900	>900 ≤950	>950 ≤1000	

There is no other industrial product that covers such a range in apparent density. Up to 350 kg/m^3 in apparent density AAC can be used as load bearing construction material, the material lower in density is used for thermal insulation purpose. By varying the composition, AAC with wide range of densities can be manufactured for special applications. For this, there is no need for a change in production technology; only the pore volume to be produced by chemical reaction should be adjusted (Narayanan *et. al*., 2000a; Schober, 2005).

Density is related to *water/cementicious material* ratio of the mixture since it is related to the amount of aeration obtained. For a given density, *water/cement* ratio

increases with proportion of sand. For AAC with pozzolans, *water/solids* ratio appears to be more important than *water/cementicious material* ratio and does not depend on the method of pore-formation. A lower *water/solids* ratio leads to insufficient aeration, while a higher one results in rupture of the voids, which increases the density in both cases (Ramamurthy & Narayanan, in press). That is why; the water requirement of the mixture is determined according to the consistency of the fresh-mix rather than the predetermined *water/ cement* or *water/solids* ratio (Valore, 1954a; Rudnai, 1963).

The density of aerated concrete is also related to its compacity (t) and porosity (ϕ) (Rudnai, 1963). The compacity is the ratio of density to the specific weight can be calculated by subtracting the porosity from the hundred percent (100-ϕ). (Narayanan *et. al*., 2000a). Moreover, ultimate increase in density of AAC with changing relative humidity and temperature is attributed to the carbonation process and this increase is proportional with initial dry density (Hanečka, K., O. Koronthályová & P. Matiašovský, 1997).

Properties of AAC such as strength, permeability, diffusivity, shrinkage and creep are considerably related to its porosity and pore size distribution (Narayanan *et.al*., 2000a). In literature, three basic classifications exist on the porous system of Autoclaved Aerated Concrete (Narayanan *et. al.,* 2000b; Figure 2.01):

(1) artificial air pores, inter-cluster pores and inter-particle pores as shown in Figure 2.1 (Prim & Wittmann 1983),
(2) macro pores formed due the expansion of the mass caused by aeration, and micro pores which appear in the walls between the macro pores (Alexanderson, 1979),
(3) micro capillaries (<50nm) and macro capillaries (50 nm to 50 µm) (Tada & Nakano, 1983).

Schober describes the microstructure of AAC with the representation given in Figure 2.02 (Schober, 2005).

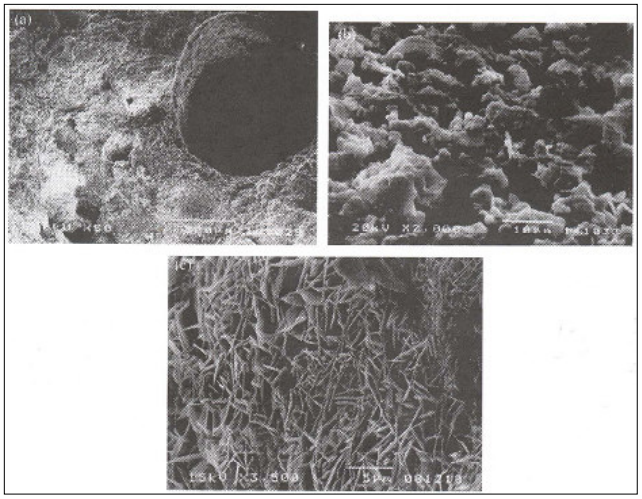

Figure 2.01. Pore Systems in Aerated Concrete: **(a)** artificial air pore; **(b)** inter-cluster air pore; **(c)** inter particle pore (Narayanan *et. al*., 2000b)

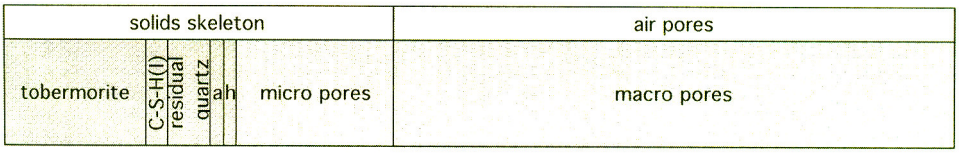

Figure 2.02. Schematic representation of volume parts in the structure of aircrete (a=anhydrite, h=hydrogarnet). Apparent density is 400 kg/m^3 in this case, and raw materials are: pure quartz sand, lime, portland cement, anhydrite and water (Schober, 2005).

Porosity and pore size distribution is closely related to apparent density. The variation of porosity values of AAC with respect to its apparent density values was given in Table 2.2. Here, the proportion of micro pores depends on *water/solid* ratio of raw materials mixture and it can be controlled by variations in this ratio (Schober, 2005).

As understood from Table 2.02, the proportion of micro pores increases with increasing density. This claim is also supported by the findings of Jacobs & Mayer (1992) who obtained the graph shown in Figure 2.03 by image analysis of AAC samples with different densities.

Table 2.02. Porosity characteristics of AAC products which differ in density (Schober, 2005, p.145)

Apparent Density kg/m^3	Macro Pores %	Micro Pores %	Total Porosity %
100	83	13	0.96
150	77	17	0.94
350	70	16	0.86
400	65	19	0.84
600	45	21	0.76
800	27	41	0.68

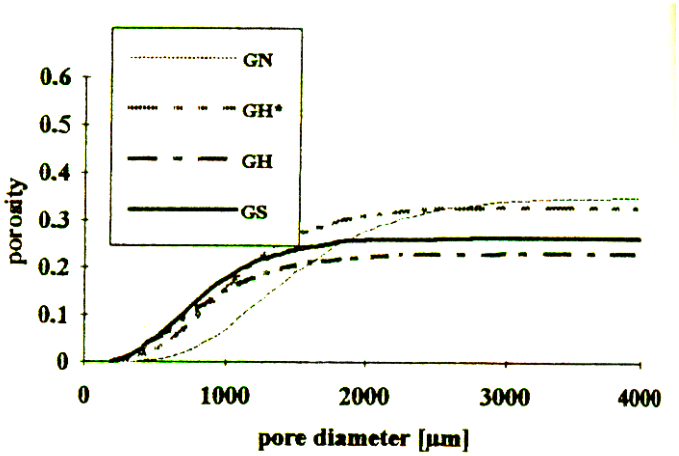

Figure 2.03. Porosity Obtained by Image Analyses for AAC samples of GN, GH*, GH and GS, which have bulk densities of 390 kg/m^3, 490 kg/m^3, 610 kg/m^3, 630 kg/m^3 respectively (Jacobs *et. al.*, 1992). The denser the sample, the higher the proportion of micro pores.

Being porous, there exist various moisture transport mechanisms in AAC. After autoclaving, AAC contains 30% water by weight of the material and it is lost after years. A typical adsorption and desorption isotherm of AAC was given in Figure 2.04 (RILEM, 1993; House, Alou & Wittmann, 1983).

The water vapor transfer is explained in terms of water vapor permeability and moisture diffusion coefficient whereas capillary suction and water permeability characterize the water transfer.

Water and gas permeability of AAC is said to be approximately the same and the artificial air pores have been found to have little influence on the permeability of both (Jacobs *et. al.*, 1992). This fact can clearly be seen in Table 2.03 reflecting the findings of Jacobs and Mayer (1992).

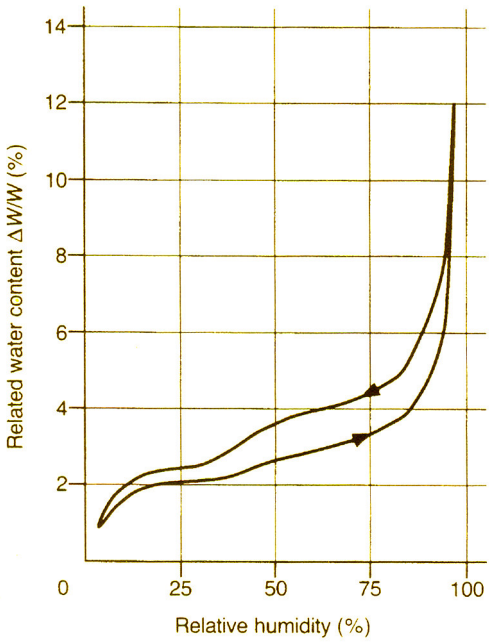

Figure 2.04. Typical Adsorption and Desorption Isotherm of AAC (RILEM, 1993; House *et. al.*, 1983)

Table 2.03. The water and gas permeability values for AAC samples with varying densities and porosities (Jacobs *et. al.*, 1992)

Bulk Density (kg/m^3)	Porosity (%)	Water permeability [$10^{-14}m^2$]	Gas permeability [$10^{-14}m^2$]
390	84.0	3.0±1.8	2.8±1.4
490	78.9	1.0±0.6	1.4±0.4
610	74.8	2.0±1.5	2.4±1.6
630	74.2	2.9±1.8	2.4±0.3

Jacobs and Mayer (1992) also found that gas permeability decreases sharply with increasing water content beyond the critical water content. On the other hand, they realized that water permeability increased with the increasing water content.

According to RILEM (1993), moisture diffusion coefficient *(μ)* value of AAC depends on its dry density and it is between 4 and 10. The same source gives the coefficient of water permeability (K) for AAC between 10^{-12} and 10^{-13} $m^{2,}$ which are higher when compared to the values obtained by Jacobs and Mayer (1992).

In dry state, the pores are empty and the water vapor diffusion is the dominant transport mechanism for AAC, however, if AAC is in contact with water, then capillary suction starts to predominate (Narayanan *et. al.,* 2000a). According to RILEM (1993), the capillary water absorption coefficient (a_w or *A*) is found to be between 4 and 8 $kg/m^2h^{0.5}$ when the experimental procedure described in RILEM TC 25- PEM: Protection and Erosion of Monuments (RILEM, 1980b) is applied. In another source, *A* values of AAC samples were given as listed in Table 4 with respect to their density and porosity values. Here, all sides of the AAC samples were covered with epoxy resin except their bottom and top surfaces (Pražák & Lunk, 1992):

Table 2.4. The capillary water absorption coefficient (*A*) of AAC samples with respect to their bulk density and porosity values (Pražák *et.al.*, 1992)

Bulk Density (kg/m^3)	Porosity (%)	*A* ($kg/m^2.s^{0.5}$)
390	81	0.038
500	79	0.061
650	74	0.066

Table 2.4 shows that the capillary water absorption coefficient *(A)* increases with the increasing density and with decreasing total porosity. This is because the proportion of micro pores (or capillaries) increases with decreasing total porosity and with increasing density as Table 2.2 indicates.

2.1.2. Mechanical Properties

According to European Norms, the compressive strength classes for AAC is as shown in Table 2.5 (prEN 12602, 1999; Taşdemir *et.al*., 2002)

Table 2.5. Compressive Strength Classes of AAC (prEN 12602, 1999; Taşdemir *et.al*., 2002)

Compressive Strength Class	**AAC 1,5**	**AAC 2**	**AAC 2,5**	**AAC 3**	**AAC 3,5**
UCS (Mpa)	1,5	2,0	2,5	3,0	3,5
Compressive Strength Class	**AAC 4**	**AAC 4,5**	**AAC 5**	**AAC 6**	**AAC 7**
UCS (Mpa)	4,0	4,5	5,0	6,0	7,0

AAC is also subdivided into classes by RILEM (1993) according to characteristic compressive strength as shown in Table 2.06:

Table 2.6. Classification of AAC According to Characteristic Compressive Strength (RILEM, 1993; p.4)

Property	**Low**	**Medium**	**High**
Compressive Strength (MPa)	<1.8	1.8- 4.0	>4.0
Young's Modulus (MPa)	<900	900- 2500	>2500
Density (kg/m^3)	200- 400	300- 600	500-1000
Thermal Conductivity (dry) (W/m K)	<0.10	0.06- 0.14	>0.12

The compressive strength values for AAC increase with density and they decrease with the moisture content as shown in Figure 2.5. In addition to the moisture content and dry density, compressive strength of AAC depends on the specimen size and shape, method of pore-formation, direction of loading, age and characteristics of ingredients used (Valore RC, 1954a; Pospisil, Jambor and Belko, 1992; Narayanan, 1999; Hanečka *et. al.,* 1997; Isu, Ishida and Mitsuda, 1995; Odler & Robler, 1985; Narayanan *et.al.,* 2000a) . Moreover, pore size distribution and microstructure is affective on compressive strength of AAC (Schober, 2005; Narayanan *et. al*., 2000a).

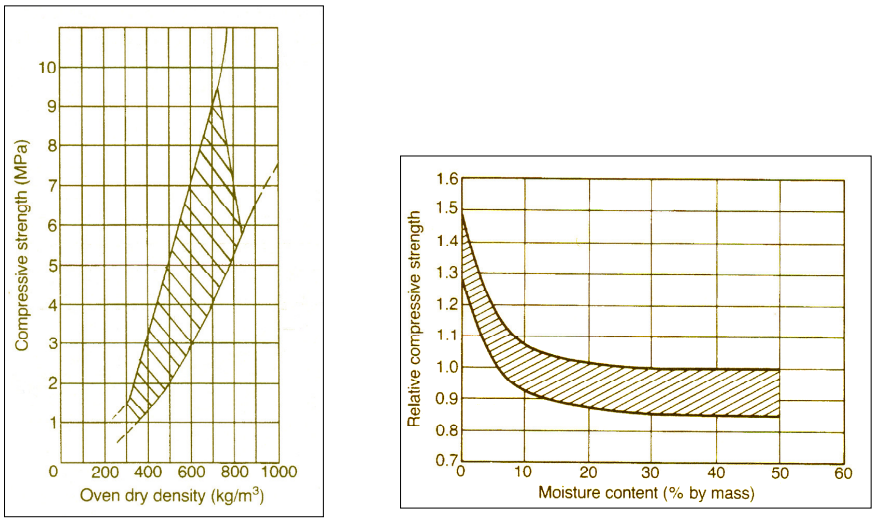

(a) **(b)**

Figure 2.5. Graphs showing (a) the relationship between the compressive strength and the density of AAC (CEB, 1978; Taşdemir *et. al.,* 2002), (b) the influence of the moisture content on the compressive strength of AAC (CEB, 1978; Briesemann, 1976; Svanholm, 1983; Taşdemir *et. al*., 2002)

The mechanical strength of AAC slightly varies depending on the direction of loading with respect to the rising direction. As the slurry of AAC rises, fission occurs in the pore walls leading to tiny cracks in horizontal direction which results in an anisotropy in strength and some other properties of AAC (Figure 2.06)

Schober (2005) also found that the influence of pore size is directly proportional to strength as shown in Figure 2.06 if the air pore porosity is within the range from 0.35 to 0.75. This relationship was shown in Figure 2.07. Modulus of Elasticity *(E_{mod})* values of AAC with respect to its dry density and compressive strength values are as shown in Table 2.07 (CEB, 1977; Narayanan *et. al.,* 2000a).

In literature, E_{mod} values are expressed as a function of *UCS* value by the Equations shown in Table 2.08. According to Valore (1954b), the ratio of direct tensile strength to compressive strength for AAC is between 0.15- 0.35, however, according to Legatski, this ratio was stated to be between 10% and 15%. The ratio of flexural strength to compressive strength is said to be between 0.22 and 0.27, and to be almost zero for very low density AAC (Valore, 1954b).

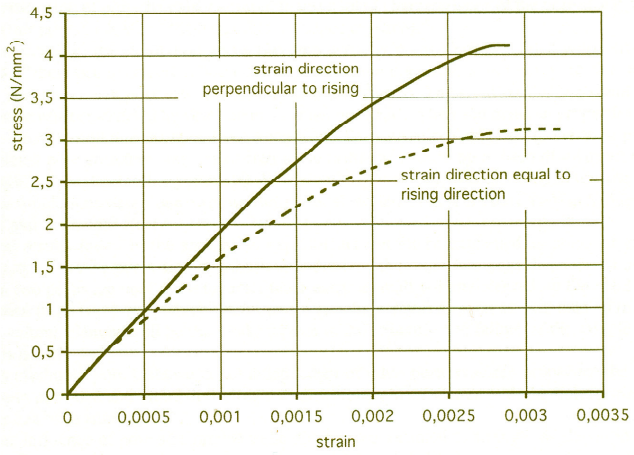

Figure 2.6. Stress Strain Relationships of AAC cubes under compression in different directions relative to rising direction.

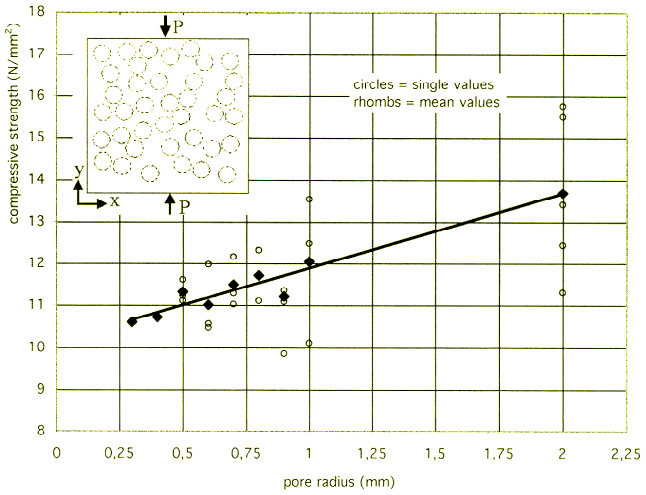

Figure 2.7. Strength of porous structures with different pore size of macro pores. Macro pore fraction is 0.4 (Schober, 2005).

Table 2.7. Mechanical Properties of AAC With Respect to its Density Values (CEB, 1977; Narayanan *et. al.,* 2000a)

Density (kg/m^3)	**Compressive Strength (Mpa)**	**Static Modulus of Elasticity (kN/mm^2)**
400	1.3-2.8	0.18-1.17
500	2.0-4.4	1.24-1.84
600	2.8-6.3	1.76-2.64
700	3.9-8.5	2.42-3.58

Table 2.8. Prediction Equations for Modulus of Elasticity of Aerated Concrete (Narayanan *et. al*., 2000a; p.326)

Modulus of Elasticity	**Notations**
6000 $(\alpha)^{1.5}S$	α- oven dry density in g/cm^3, *S* is the cube compressive strength in kg/cm^2 (Valore, 1954b)
1550 $S^{0.7}$	*S* is the cube compressive strength in kg/m^2 (Valore, 1954b)
3000 S_p	S_p is the prism strength in kg/cm^2 (Rudnai, 1963)
k γ_{dry} $(f_c)^{0.5}$	γ_{dry}- dry density in kg/m^3, f_c is the compressive strength in MPa, k is a constant ranging from 1.5 to 2.0 (CEB, 1977)
c_1 (ρ- c_2)	c_1 and c_2 – constants, ρ- dry density in kg/m^3, *E* is in MPa (Nielsen, 1983)

In addition, modulus of rupture can be estimated by the Equation 1 (RILEM, 1993; Narayanan *et.al*., 2000a).

$$MOR = 0.27 + 0.21 f_{ct} \quad \text{.....(1)}$$

where,

MOR: modulus of rupture (MPa)

f_{ct}: compressive strength (MPa)

Significant loss of absorbed water leads to drying shrinkage and it is crucial for AAC due to its high total porosity and specific surface of pores (Ziembika, 1977; Narayanan *et. al.*, 2000a). Higher percentage of pores together with low pore size leads to increase in shrinkage. According to Ziembika (1977) the shrinkage is related to volume and specific surface of micro pores of 75 to 1000Å pore size. On the other hand, Schubert (1983) claims that shrinkage is rather related to distribution of pores. The capillary suction theory of drying shrinkage of porous building materials states that the water in the pore exists in tension and this creates an attractive force between the pore walls (Tada, 1986). Nielsen (1983) pictures drying shrinkage as compression due to hydraulic vacuum in the pore water (Narayanan *et.al.,* 2000a).

2.1.3. Compositional Properties

The typical composition of AAC was given in Table 2.09 (RILEM, 1993).

Table 2.9. Typical Composition of AAC (RILEM, 1993; p.41).

element	Amount (%)
CaO	18- 36 %
SiO_2	32- 58 %
Al_2O_3	2.4 %
MgO	<2 %
Fe_2O_3	2 %
Alkalis	<1 %
Others	1-4 %
Weight loss	8-12 %

X- Ray Powder Diffraction studies showed that the main reaction product of AAC belong to the tobermorite group of calcium silicate hydrates (C-S-H) (Alexanderson, 1979; Tada *et.al.,* 1983; Mitsuda & Chan, 1977; Isu *et.al.,* 1995; Narayanan *et.al.,* 2000a). The reaction sequence is: Ca rich C-S-H→ C-S-H→ 11.3Å Tobermorite. The reaction product is a mixture of crystalline, semi-crystalline and near amorphous tobermorite, i.e. a material with varying degree of crystallinity, which is defined as the ratio of tobermorites to total calcium silicate hydrates (Alexanderson, 1979; Narayanan *et.al.,* 2000a). XRD patterns for powders of AAC with sand and for AAC with fly ash were given in Figure 2.08.

Scanning Electron Microscopy (SEM) showed that the microcapillaries in AAC are plate shaped crystals of 11.3 Å tobermorite with a double-chain silicate structure (Mitsuda, Kiribayashi, Sasaki & Ishida, 1992; Narayanan *et.al.*, 2000a). The growth rate and the degree of orientation of this structure cause differential pore distribution in gas forming and foaming methods (Tada *et.al*., 1983; Narayanan *et.al*., 2000a).

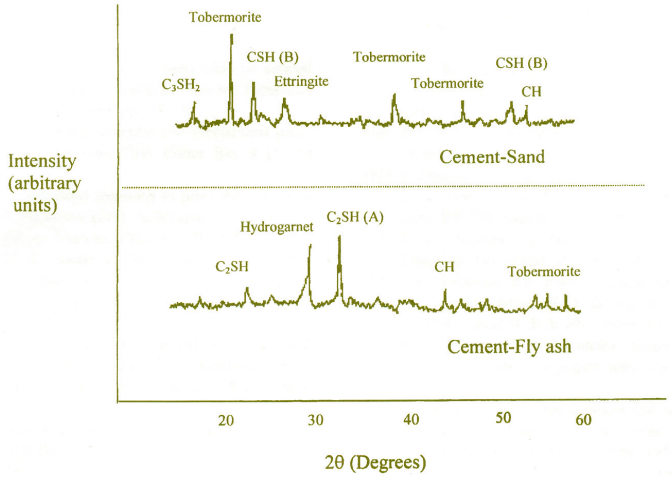

Figure 2.8. XRD Patterns of AAC (Narayanan *et.al*., 2000a)

AAC with fly ash and sand shows differences in terms of microstructure. AAC with sand shows a well-defined C-S-H (tobermorite) crystals and hexagonal $Ca(OH)_2$ crystals. The structure of AAC with fly ash does not show complete crystallinity. After 12 hours of autoclaving, it also becomes crystal, however, there is still some unreacted particles left and the reacted particles are farther apart than those formed with sand. This reduces the interlocking and thereby the strength. As a result, the drying shrinkage of AAC with fly ash happens to be higher than that with sand (Narayanan *et.al.,* 2000b) (Figure 2.09).

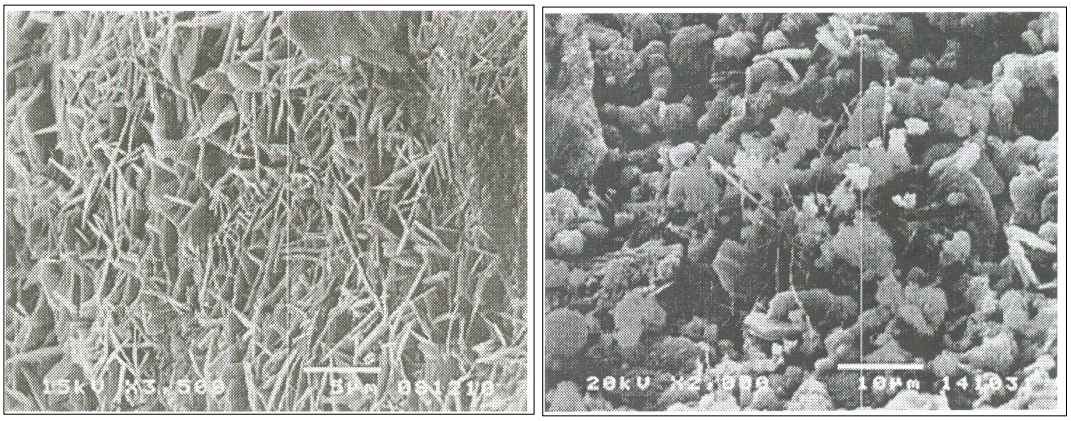

(a) **(b)**

Figure 2.09. Micrographs of Autoclaved Aerated Concrete with **(a)** sand and **(b)** fly ash fillers.

2.1.4. Durability properties

Autoclaved Aerated Concrete consists of tobermorite, which is more stable when compared to the other products formed in normally cured aerated concrete. However it has high porosity allowing penetration by liquids and gases which may lead to damage of the matrix (RILEM, 1993; Narayanan *et.al*, 2000a). Freeze-thaw reactions are reported to be significant as far as AAC is concerned at saturation degrees of 20-40%. At higher degrees of saturation, the sample becomes brittle and cracks completely (Roulet, 1983; Narayanan *et.al*, 2000a). Protective precautions using bitumen-based materials are necessary when sulphate attack is anticipated. Carbonation may lead to increase in density but it is not very serious unless exposure to CO_2 is too severe (CEB, 1977; Narayanan *et.al*, 2000a).

Carbonation is one of the main factors of the ageing deterioration of Autoclaved Aerated Concrete (AAC), where tobermorite-11Å and well-crystallized C-S-H, the main structural minerals of AAC, react with carbon dioxide under the existence of moisture and finally decomposed to silica gels and calcium carbonate (Matsushita *et.al.,* 2000a). Carbonation leads to degradation such as the decrease of strength, the increase of deflection and the growth of latticelike cracking, which are mainly caused by the carbonation shrinkage (Goodier & Matthews, 1997; Matsushita & Shibata. 2000; Matsushita, Aono & Shibata, 2004).

Two types of frost deteriorations are observed in external walls made from AAC in cold regions. One type of deterioration is surface scalling caused by freezing and thawing; the other is wide cracks caused by keeping the inner part of AAC at 0^oC (Senbu & Kamada, 1992). Senbu and Kamada analyzed the deteriorations of AAC by various test methods such as freezing thawing test, critical degree of saturation method and top surface freezing test. Depending on the capillary theory they concluded that ice forms in air voids while capillary water is kept unfrozen when deterioration occurs. The deterioration mechanism of AAC develops as the capillary pressure differential between ice in air voids and water in capillaries

increases. They also explained the formation of cracks on the top surfaces of AAC. When air voids are filled with ice, pressure (P) builds up inside them. This pressure depends on the capillary size and whether or not cracks occur is determined by comparing P per unit area and the tensile strength of the material. Figure 2.10 shows the relationship between the tensile strength of materials (or pressure P per unit area) and volumetric proportion of air voids. As understood from Figure 2.10, capillaries greater than 200 Å are thought to influence this deterioration mechanism (Senbu *et.al.*, 1992).

In agreement, Hama, Kamada, Tabata and Watanabe (1992) obtained a relation between the material properties of AAC and its frost resistance. They stated that AAC with higher density is comparatively more resistant to frost deteriorations. The time until crack formation has a correlation with only the water absorption for 24 hours, and the volume change has a correlation with the specific gravity and the air void size (Hama *et.al.*, 1992).

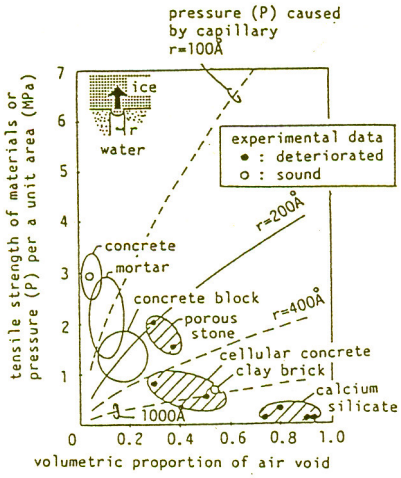

Figure 2.10. Relationships Between Volumetric Proportion of Air Void and Tensile Strength of Materials (or Pressure P per unit area)

2.1.5. Functional Properties

AAC is known with its unique thermal properties. Thermal conductivity depends on density, moisture content and ingredients of the material regardless of the curing process as the Figure 2.11 indicates. The amount of pores and their distribution are also critical for thermal insulation. Finer the pores, better the insulation. In addition, the thermal conductivity is influenced by the moisture content. A 1% increase in moisture by mass increases the thermal conductivity by 42% (Narayanan *et. al.*, 2000a).

In practice, the fire resistance of aerated concrete is more than or as good as ordinary dense concrete (Valore, 1954b; Rudnai, 1963; Narayanan *et.al*., 2000a). Hence, its use does not involve any risk of spread of flames. An important reason for such behavior is that the material is relatively homogenous, unlike normal concrete where presence of coarse aggregate leads to differential rates of expansion, cracking and disintegration (Leitch, 1980; Narayanan *et.al*., 2000a). The good fire resisting property of aerated concrete is due to the presence of high number of solid-air interfaces, which reduces the heat transfer. This coupled with their low thermal conductivity and diffusivity gives an indication that aerated concrete possesses better fire-resisting properties (Narayanan *et.al*., 2000a). Autoclaved Aerated Concrete has been shown to provide better insulation to sound transmitted by air than other solid building materials, eg. dense concrete, clay bricks, etc., under comparable conditions (RILEM, 1993).

The manufacturer of the AAC blocks examined in the study gives some of the material properties of their products as shown in Table 2.10 (www.akg-gazbeton.com)

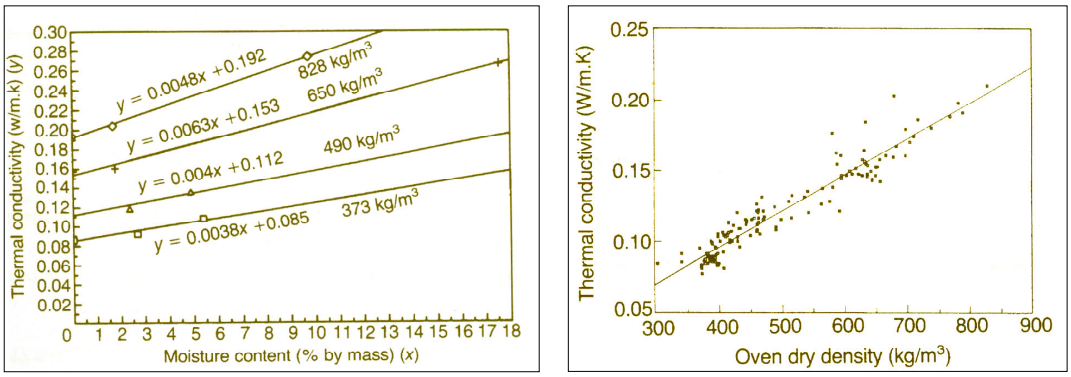

(a) **(b)**

Figure 2.11. The Variation of thermal conductivity of AAC with **(a)** density and **(b)** moisture content. Thermal conductivity increases as the moisture content of AAC increases. Thermal conductivity also increases with the increasing density (RILEM, 1993).

Table 2.10. Product specifications of the manufacturer for the AAC masonry blocks

Strength Category			**G2**	**G3**		**G4**
Average compressive strength (kgf/cm^2)			25	35		50
Maximum gross density- dry (kg/m^3)			400	500	600	700
Modulus of elasticity (kgf/cm^2)			12500	17500	22500	27500
Thermal Conductivity (W/mk)	**Bulk material**	**λd**	0.11	0.14	0.16	0.18
		λh	0.14	0.16	0.19	0.21
	Coursed wall	**λh**	0.15	0.17	0.20	0.23
Design value for dead load (kg/m^3)	**Coursed wall**		500	600	700	800
Water vapor diffusion resistance factor (μ)			5-10			

λd : Actual thermal conductivity of material under laboratory conditions

λh: Input value of thermal conductivity for heat loss/ gain calculations according to TS 825 and DIN 4108.

2.2. Material Properties of Cement Based Neighboring Plasters of AAC

The cement based contemporary neighboring plasters of AAC examined in this study were produced by the addition of special additives to ordinary pale cement based plasters. Felekoğlu (2004) studied on these plasters together with traditional

lime based and pale cement based plasters and concluded that these special additives add to durability and workability of the plaster as well as to its adherence with the AAC surfaces.

The need of water for these cement based plasters was much less when compared to traditional lime based plasters. They were able to reach higher values of workability with additions of relatively lower proportion of water and moreover, they had the ability to maintain their workability for longer periods of time without any addition of water. Moreover, the cement based plasters with additives were determined to be more workable and to be able to maintain this workability for longer periods of time when compared to plain cement based plasters. This was due to the presence of high proportion of air voids in their structure that lightened these plasters in their fresh state and increased their workability. During the application, these air voids were mentioned to drag increasing the ease and speed of the application process.

Felekoğlu (2004) determined the mechanical properties of the same cement based neighboring plasters of AAC, which were examined in this study, with direct testing methods of E_{mod} and *UCS*. He studied on the samples of 10cm x 10cm x 10cm and his results were given in Table 2.11. With the measurements of *UCS* and E_{mod} values, these cement based plasters with special additives were proved to perform better in terms of their mechanical properties when compared to the traditional lime based and pale cement based plasters under both normal and severe atmospheric conditions such as very high temperature. The plasters of AAC are also more resistive against freezing and thawing cycles when compared to the traditional lime based and pale cement based plasters due to the presence of many spherical air voids in their structure. In addition, when compared to the modulus of elasticity values of the traditional lime based and the pale cement based plasters, those for the plasters of AAC do not show any considerable difference.

The water absorption capacity values were also found to be parallel to the results of the capillary suction tests. Moreover, the cement based plasters of AAC were determined to lose less water when compared to the traditional lime based plasters during the curing period and this property makes them more resistant against drying shrinkage.

Table 2.11. The Mechanical Properties of Cement Based Neighboring Plasters of AAC (Felekoğlu, 2004).

Properties	BC	UC	FC	WRFC
UCS (MPa)	26.2	15.6	11.9	12.8
E_{mod} **(GPa)**	7.6	7.5	3	4.7

2.3. Building AAC Walls

In Turkey, both in construction and repair works, AAC masonry walls are constructed with the same procedure and they are finished with cement based contemporary plasters. In this section, basic types of AAC products are mentioned very briefly and the procedures of laying AAC masonry walls and of the rendering applications are described.

In Turkey, AAC is produced and used either as blocks or as steel reinforced panels. AAC blocks are of three basic types being masonry blocks, floor blocks and insulation blocks. AAC steel reinforced panels, on the other hand, are wall elements, roof and floor deck elements and complementary elements such as lintels (www.akg-gabeton.com).

Among these various AAC products, masonry blocks are the ones that are used both for repair and construction purposes and they have three basic types. These are plain-end blocks, tongue & groove blocks and U blocks. The manufacturer gives the dimensions of the masonry blocks as shown in Table 2.12.

Table 2.12. Product Dimensions of AAC Masonry Blocks (www.akg-gazbeton.com)

Type of the Masonry Block	Length (l) (cm)	Width (b) (cm)	Thickness (d)
Plain-end wall blocks	60	25	7.5- 35
Tongue and groove wall blocks	60	25	15- 35
U-blocks	60	25	17.5, 20, 25, 30

2.3.1. The Process of Laying Up AAC Walls

In this section, the construction of an AAC wall with AAC masonry blocks are described as recommended by the manufacturer in their website and product catalogues (www.akg-gazbeton.com).

For the right AAC wall construction, special care should be given to the procedure from the very beginning to the end. For instance, the plastic wrapping should be removed at least one full day for airing prior to the use of the material. Furthermore, a careful visual inspection of the material should be made before laying. If any of the units are soaked while in storage, they should be allowed to dry before use.

Firstly, the fine joint adhesive is prepared by a fairly simple procedure. Firstly, water is added to adhesive powder so that the water to powder ratio is 1:2. The batch is mixed using the beater accessory on a power drill operating at low speed as shown in Figure 2.12. The adhesive is ready within a few minutes and it has a working life of 4 to 5 hours. Since the paste irreversibly turns over and dries, the batch sizes should be prepared for each application accordingly.

Care should also be given while laying up the walls: For the jointing of the blocks either jointing adhesive or ordinary mason's mortar is used. If the jointing adhesive is used for jointing, it should be spread evenly over all faces of both bedand head joints. If the ordinary mason's mortar is used for jointing, the jointing faces should be moistened with brush just prior to buttering. In both cases, care

should be given to ensure that no cavity should be left in either bed or head joints. Moreover, vertical joints in alternate (stretcher) courses should overlap a minimum of 15cm. The use of full breaking courses where blocks in each course centered over joint of the course below is preferred as described in Figure 2.13.

Figure 2.12. Preparation of the adhesive mortar (www.akg-gazbeton.com)

Bed courses must invariably be laid in ordinary (mason's) mortar. The composition of the bedding mortar is one part cement and one part lime powder to six parts fine aggregate (sand). A damp-proof membrane should be placed under the mortar bedding, as shown in Figure 2.14 below, where the building plinth (or basement) is less than 30cm above grade.

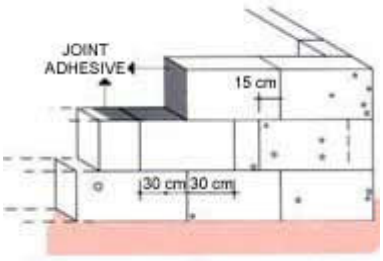

Figure 2.13. Laying Up the AAC Walls (www.akg-gazbeton.com)

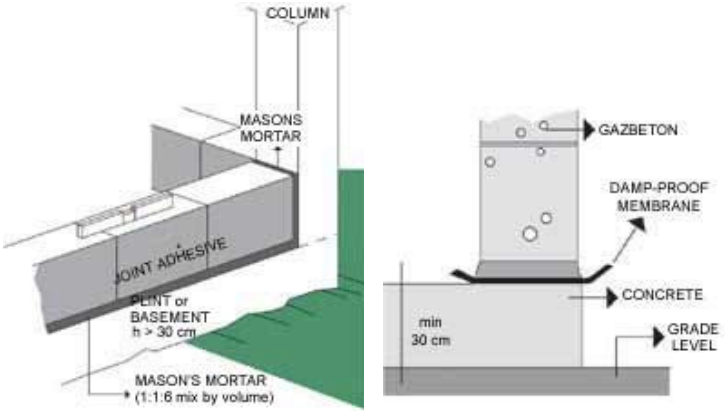

Figure 2.14. Laying the bed course of AAC Wall Construction (www.akg-gazbeton.com)

Care should be taken to ensure that the bed course is laid true (dead level) in both directions (length and crosswise). Block work walls with a damp-proof membrane under the bedding mortar should be duly anchored to vertical members of the structural system.

2.3.2. The Application Process of Renderings on AAC Walls

Before the application of the rendering, dust should be removed from the wall surfaces with a stiff brush in order to provide good adherence between the AAC and its plasters. All surfaces should then be wetted by sprinkling with a thick hairbrush in order to prevent absorption of water from the mortar mix. However surfaces should never be saturated with water. If the wall is wet for some reason, it should be left drying before the application of the plasters.

Base coat (BC) should be applied on AAC surfaces as the surface hardener and also for the provision of the water balance. The cement: sand: additive ratio of the BC is 1: 2: 1 and its application thickness is recommended not to exceed 4mm. It is not approved for the BC to cover the whole wall surface and the wall should be left for the BC to reach its ideal hardness. The wall surface should be rewetted prior to the application of the upper layers.

If the wall surface is flat enough, finish coat (FC) can directly be applied on BC. The cement: sand: additive ratio of the FC is 1: 4: 1 and its thickness of application recommended by the manufacturer is 8 to 10 mm. The plaster should be kept wet during the 2 to 3 days following its application. Wherever an undercoat (UC) is needed, the use of larger size aggregates is recommended. The cement: sand: additive ratio of the UC is 1: 3: 1 and its application thickness is 15 mm. As for the whole cement based plasters, the curing process is significant for these plasters. For instance, at least 5 days of curing period is necessary if the use of water repellent finish coat (WRFC) is preferred as the finish coat. The applications of these plasters should not be made under dense sunlight and they should not be exposed to extreme rain, frost and wind as well as sunlight.

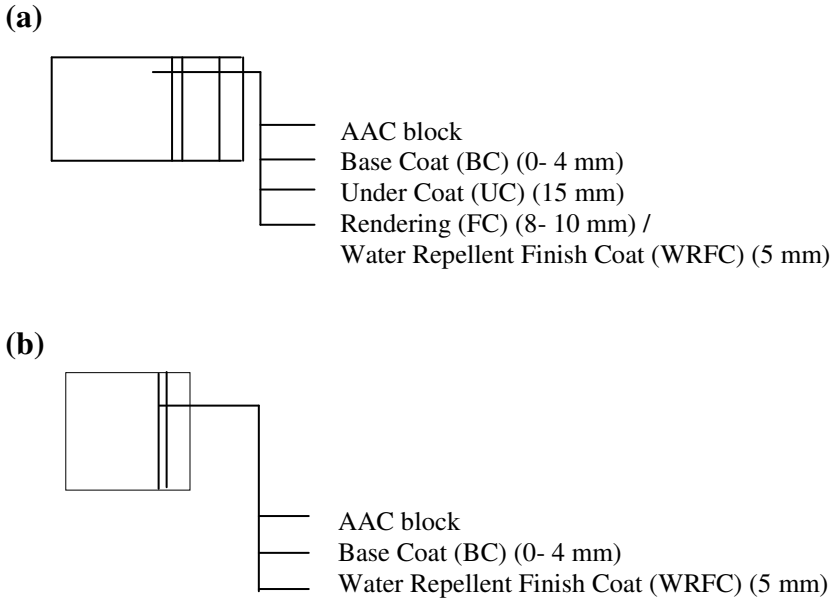

Figure 2.15. Typical application details of exterior finishing systems for AAC masonry, showing the order of layers and their recommended thickness: **(a)** successive application of cement-based plasters with various additives; **(b)** water repellent finish coat applied directly on base coat.

The typical application details of exterior finishing systems for AAC masonry, including plasters of BC, UC, FC, WRFC were given with their recommended thickness of application in Figure 2.15. JA, on the other hand, is applied with the

thickness ranging from 0.1 to 0.3 cm. As the application of WRFC needs more care and workmanship when compared to the successive application of BC, UC and FC/WRFC, the application detail shown in Figure 2.15a is preferred more often.

2.3.3. The Use of AAC in Repairs of Timber Frame Historic Structures

In Turkey, AAC started to be used as an infill material in timber framed historic structures for repair purposes. In these applications, the original stone, mud brick or fired brick infill is taken out and AAC is used as substitute of these original infill materials. Even timber studs are also substituted with new ones where the original studs seem very much deteriorated. The structure is then finished with cement-based plasters. Many of the timber frame historic structures in Safranbolu, a city in the north west of Turkey, which is in the World's Cultural List of UNESCO, are repaired with this technique (Figure 2.16). These repair works often result in failures on the finishing surfaces such as cracks and flakes within a month and the source of these failures are not known.

(a) **(b)**

Figure 2.16. The Kindergarten in Safranbolu, **(a)** a view showing the use of AAC as an infill material substitute of the original stone infill **(b)** a view from the outside showing the application of the exterior cement based plasters over the timber framed structure with AAC infill.

(a)

(b)

(c)

Figure 2.17. Milli Egemenlik Evi, Safranbolu. **(a)** AAC partition wall in contact with the historic fabric **(b)** the use of AAC inside the timber skeleton **(c)** the view of the house from the exterior after the repair work.

(a) **(b)**

Figure 2.18. Öğretmen Evi, Safranbolu (a) close view to the application of AAC inside the timber framed structure (b) the timber framed wall with AAC infill after the repair work

2.4. Material Properties of the Historic Construction Materials in Anatolia

In this section are presented the results of various studies conducted on the material properties of historical materials obtained from traditional structures in Turkey. The data collected from these studies were given in Table 2.13 to be used for comparisons during the discussions of compatibility.

Güdücü (2003) studied on the mud brick and mud plaster technology of Hittites by examining some burnt mud brick walls of Shapinuwa Hittite city in order to point out repair and conservation needs of those mud brick structures which underwent fire. She concluded that the ranges for the bulk density (ρ), effective porosity (ϕ) and water absorption capacity (θ_{max}) values of the mud brick samples were between 1.17 g/cm^3 and 1.57 g/cm^3, 35 % and 50 %, 39.1 % and 69.4 %

respectively. On the other hand, she determined the ρ, ϕ and θ_{max} values for mud plasters between 1.17 g/cm^3 and 1.32g/cm^3, 40.7 % and 56.2 %, 55.9 % and 76.8 % respectively. In addition, the only mud mortar she studied had the ρ, ϕ and θ_{max} values of 1.51 g/cm^3, 40.1 % and 44 % respectively. She also found that the water vapor diffusion resistance index (μ) values for mud brick samples varied between 0.57 and 0.99. On the other hand, the μ values of the two mud plasters studied were determined to be 0.51 and 0.64.

The modulus of elasticity (E_{mod}) values of mud brick samples were determined to be between 1.2 GPa and 2.1 GPa, while the those of mud plasters were lower with the values in the range of 0.6 GPa and 1.7 GPa. The point load strength index (I_s) values of mud brick samples were, on the other hand, between the values of 0.1 MPa and 1.5 MPa. Mud plasters had I_s values lower than those of mud brick samples with the values in the range of 0.02 MPa and 0.15 MPa.

Pozzolanic activity values for the aggregates of the mud brick samples, which were lower than 125 μ were found to be between 3 mS/cm and 5.7 mS/cm, while those for the aggregates of the mud plaster samples were between 1.8 mS/cm and 6.4 mS/cm.

Akkuzugil (1997) studied the plasters of timber framed traditional houses with adobe infill, situated in the historic center of Ankara, known as the Ulus district. She collected mud, lime and gypsum plasters from eight traditional houses and examined their characteristics with the emphasis on their water vapor permeability properties. The bulk density, effective porosity and water absorption capacity values of the mud plasters could not be determined due to their low resistance against water, however, the bulk densities of lime based plasters and the gypsum based plasters were determined to be between 1.28 g/cm^3 and 1.67 g/cm^3, 1.35 g/cm^3 and 1.70 g/cm^3 respectively. Their ϕ values were between 32.05 % and

47.82 %, 23.52 % and 41.38 % respectively. In addition, θ_{max} values of the lime based and gypsum based plasters were found to be between 21.94 % and 37.06 %, 13.90 % and 30.78 % respectively.

Akkuzugil (1997) also determined the water vapor diffusion resistance index (μ) values for the mud, lime and gypsum plasters and she concluded that lime coats had relatively higher μ values when compared to mud and gypsum coats with the values between 3.04 and 18.27. The μ values of mud and gypsum coats were, on the other hand, between 1.19 and 3.16, 2.88 and 13.33 respectively. A few samples of mud mortar had μ values between 1.92 and 2.70, while two mud brick samples studied had μ of 2.75 and 3.23.

Tuncoku (2001) studied the mortar technology of twenty-two stone and brick masonry structure of Anatolian Seljuk Period in Konya, Beyşehir and Akşehir in terms of their raw material composition, basic physical and mechanical properties and durability characteristics. The bulk density values of stone masonry mortars varied in the range of 1.39 g/cm^3- 1.85 g/cm^3. In the mortars of brick masonry, this range is between 1.25 g/cm^3 and 1.74 g/cm^3. The porosity values of stone masonry mortars were in the range of 27.36 %- 45.88 %, while the porosity values of brick masonry mortars varied between 27.81 % and 52.26 %. Tuncoku also examined the drying behaviors of the stone and brick masonry mortars and observed that all original mortars dried within five or six days. In the study, Tuncoku (2001) also examined masonry fired brick samples and found that their bulk density values varied between 1.18 g/cm^3 and 1.61 g/cm^3, while their ϕ values were in the range of 35.58 %- 56.91 %.

Within the scope of the same study, Tuncoku determined the mechanical properties of stone and brick mortars. In his study, while the E_{mod} values of stone mortars were between 0.71 GPa and 8.32 GPa, those of brick mortars were

between 0.7 GPa and 2.99 GPa. The point load strength index (I_s) values of the stone and brick mortars were also determined to be in the ranges of 0.52 MPa-1.38 MPa and 0.10 MPa- 0.59 MPa respectively.

Tuncoku, Caner Saltık & Böke (1993) studied the bricks of a XIIIth century mescid named as Sahipata Mescidi. The bricks were collected from the upper parts and from the roof structure. He observed that the bricks dried at 20^{o}C and 40% relative humidity in 10 days except the concrete bricks of later restoration interventions. He also determined the value ranges for the water absorption capacity, porosity and bulk density of the fired bricks as 15.2% - 36.7%, 28.1%-49.6% and 1.34 g/cm^3- 1.82 g/cm^3 respectively.

Tuncoku (1993) also studied fired bricks and mortars samples of a XIIIth century Anatolian Seljuk Monument, Tahir ile Zühre Mescidi in Konya. He determined that the bulk density, effective porosity and water absorption capacity values of fired bricks varied between 1.38 g/cm^3 and 1.47 g/cm^3, 45% and 48%, 30% and 35%. He also determined that the stone masonry mortars were denser with the value of 1.63 g/cm^3 when compared to the brick masonry mortars of 1.53 g/cm^3 density.

Caner (2003) studied on the technological characteristics of the Seljukid plaster samples from some historic structures in the archeological sites namely; Alanya castle, Kubadabad Palaces, Syedra Archeological Site, Aspendos Amphitheatre, Selinus Archeological Site- Şekerhane Köşk and Hasbahçe. She determined the value ranges for the bulk density, porosity and water absorption capacity of the plasters as 1.23 g/cm^3- 1.90 g/cm^3, 19.67%- 49.03% and 10.3%-39.8%.

Caner (2003) also studied the water vapor permeability and mechanical properties of the Seljukid plasters and she concluded that the μ values of the plasters ranged

between 1.79 and 9.22. The E_{mod} values were around 2.855 GPa with a few higher values. The pozzolanic activity of the plasters of the Alanya Byzantine plasters were found to be 42 mS/cm.

Esen, Tunç, Telatar, Tavukçuoğlu, Caner-Saltık & Demirci (2004) studied on the technological properties of the construction materials of XIVth century Çukur Hamam in Manisa. He examined 19 plasters, 6- brick masonry mortar, 4 stone masonry mortar, 3 fired bricks and a single stone sample. The bulk density and effective porosity values of the plasters were found to be between 0.97 g/cm^3-1.84 g/cm^3 and 29%- 59% respectively. The water vapor diffusion resistance index (μ) values of the plasters were found to vary between 2.3 and 16.2 and the equivalent air thickness of water vapor permeability (*SD*) values for these plasters were found to vary between 0.04 m and 0.15 m. The brick masonry mortars, on the other hand, had bulk density values between 1.52 g/cm^3 and 2.07 g/cm^3 and they had porosity values between 30% and 47%. Stone masonry mortars were determined to have bulk density values between 1.62 g/cm^3 and 2.22 g/cm^3 and their porosities were between 29% and 32%. Lastly, the fired brick samples were found to have average bulk density and effective porosity values of 1.67 g/cm^3 and 34% respectively.

Yıldırım Esen (2004) also determined the mechanical and compositional properties of the samples obtained from Çukur Hamam in Amasya. For instance, he observed that the E_{mod} values of the fired bricks ranged between 3.1 GPa and 5.2 GPa, while those of brick mortars were between 1.2 GPa and 3.6 GPa. In addition, lime plasters had E_{mod} values between 0.7 GPa and 2.9 GPa. On the other hand, the pozzolanic activity of the aggregates of stone and brick mortars were determined to be 9 mS/cm, while that of plasters were 7 mS/cm.

Akyazı (1998) studied Harçoğlu Konak in Bursa, which is an example of 18th century Anatolian traditional residential architecture. She examined the basic physical properties of lime plasters, horasan plasters, fired bricks and stones obtained from the building. Samples were collected from 6 different sections of the

residence namely, the *ılıklık* section of the bath, the *sıcaklık* section of the bath, the water tank, kitchen, mezzanine floor and the first floor. The bulk density of the fired bricks, horasan plasters and lime plasters varied between 1.57 g/cm^3 and 1.78 g/cm^3, 1.18 g/cm^3 and 1.43 g/cm^3, 0.98 g/cm^3 and 1.65 g/cm^3 respectively. Their effective porosity values were between 30.69% and 40.10%, 33.67% and 55.30%, 24.76% and 57.64% respectively. In addition their water absorption capacities were determined to be between 17.20% and 25.49%, 23.71% and 46.80%, 15.84% and 58.88%.

Akyazı (1998) also determined the water vapor permeability characteristics of the samples taken from the mezzanine and first floors and each space of the bath section in the Haraçoğlu Konak. She determined the μ values of the two fired brick samples as 9.062 and 12.845. The *SD* values of the lime plasters were between 0.051m and 0.113m and their μ values were between 6.444 and 23.704. The *SD* values of the horasan plasters varied between 0.052m and 0.152m, while their μ values were between 2.878 and 12.790. In addition, the three tested mud plasters interestingly had similar *SD* values (0.043m; 0.044m; 0.057m) for different thickness due to the variation in their μ values (3.043; 5.507; 2.519).

Akyazı (1998) also studied the elements of a typical timber skeleton wall with mud brick infill in terms of their water vapor permeability properties. She determined the *SD* values of mud and lime interior plasters, which were applied successively, as 0.44 m and 0.086 m respectively. The *SD* values of the successive exterior mud and horasan plasters were, on the other hand, 0.043 m and 0.060 m.

2.4. Compatibility Issue

Compatibility is an important concept both in the field of historic heritage preservation and also for the long-term performance of contemporary structures. In literature, it is possible to encounter different definitions of this concept especially in the field of heritage preservation. For instance, Teutonico, Charola , De Witte,

Grassegger, Koestler, Laurenzi Tabasso, Sasse, & Snethlage (1997) defined it as introduced treatments or materials which will not have negative consequences. Van Hees (2000) suggested a definition of compatibility related to repair mortars as follows: 'The new mortar should be as durable as possible, without (directly or indirectly) causing damage to the original material'. The common search for both of these definitions is that the new material introduced to the original fabric should not give harm to it (Valek, 2005). Broadening this perspective, it can be stated that materials can be used together unless they give harm to each other.

Compatibility issue has become a very recent field of interest. Sasse and Snethlage (1997) stated that 'reversibility' should be replaced by compatibility and retreatability measures in heritage preservation and arose the need for a better definition of compatibility.

Compatibility was expected to describe the properties and the behavior of both the new and the original material in relation with the original fabric after the intervention (Valek, 2005). Sasse and Snethlage proposed a set of compatibility criteria for the neighboring materials in terms of their material properties. By this way, compatibility gained a new definition in terms of these properties.

Dynamic modulus of elasticity *(E_{mod})*, water vapor diffusion resistance index *(μ)*, compressive strength, thermal dilatation coefficient, water uptake coefficient and pull off strength were among the compatibility parameters mentioned by Sasse and Snethlage (1997). μ and E_{mod} were two of the most critical compatibility criteria for the neighboring materials. From this point of view, any compatible plaster/layer was expected to have E_{mod} or μ no higher than the base material (Sasse *et al*., 1997). In this study, these two important parameters of compatibility were emphasized during the discussions on the compatibility of AAC and its cement based plasters not only with each other but also with the historic fabric. Drying behaviors of the materials and their durability properties supported these discussions.

Table 2.13. Material properties of some historical construction materials in Anatolia

VALUE	HISTORIC MUDBRICK	HISTORIC FIRED BRICKS	HISTORIC MORTARS	PLASTERS	TIMBER
ρ (gr/cm^3)	1.2-1.6 (Eriç, 1980) 1.17-1.57 for burnt mud brick (Güdücü, 2003)	1.34-1.82 (Tuncoku *et al.*, 1993); 1.38-1.47 (Tuncoku, 1993), 1.18- 1.61 for masonry brick (Tuncoku, 2001); average 1.67 (Yıldırım Esen *et al.*, 2004); 1.57-1.78 (Akyazı, 1998); 1.6 for infill brick; 1.30- 1.36 for masonry brick	1.51 for burnt mud-mortar (Güdücü, 2003); 1.39-1.85 for stone mortars; 1.25-1.74 for brick mortar (Tuncoku, 2001) 1.63 for stone masonry mortar, 1.53 for brick masonry mortar (Tuncoku, 1993); 1.52-2.07 for brick masonry mortars, 1.62-2.22 for stone masonry mortars (Yıldırım Esen *et al.*, 2004)	0.97–1.84 for lime plasters (Yıldırım Esen *et al.*, 2004); 1.28-1.67 for lime plasters, 1.35-1.70 for gypsum plasters (Akkuzugil, 1997); 1.17-1.32 for burnt mud plaster (Güdücü, 2003); 1.23-1.90 for Seljukid plasters (Caner, 2003); 1.18-1.43 for horasan plasters and 0.98-1.65 for lime plasters (Akyazı,1998); 1.66- 1.84 for exterior plasters from Adana; 1.1- 1.2 for exterior plasters from Ankara; 1.1 for interior plasters from Amasya;	0.5 for samples from Amasya and 0.2–0.4 for samples from Safranbolu
ϕ (%)	35- 50 for burnt mud brick (Güdücü, 2003)	45-48 (Tuncoku, 1993); 35.58-56.91 for masonry brick (Tuncoku, 2001); 28.1-49.6 (Tuncoku *et. al.* 1993); 34 (Yıldırım Esen *et al.*, 2004); 30.69-40.10 (Akyazı, 1998); 40.4- 40.7 for infill brick from Adana; 52.0- 54.2 for masonry brick;	40.1 for burnt mud-mortar (Güdücü, 2003), 27.36-45.88 for stone mortars; 27.81-52.26 for brick mortars (Tuncoku, 2001); 30-47 for brick masonry mortars, 29-32 for stone masonry mortars (Yıldırım Esen *et al.*, 2004)	32.05-47.82 for lime plasters; 23.52-41.38 for gypsum plasters (Akkuzugil, 1997); 40.7-56.2 for burnt mud plaster (Güdücü, 2003); 19.67-49.03 for Seljukid plasters (Caner, 2003); 33.67-55.30 for horasan plasters, 24.76-57.64 for lime plasters (Akyazı, 1998);29-59 (Yıldırım Esen *et al.*, 2004); 30-34 for exterior plasters from Adana; 54 for interior plasters from Amasya; 44-48 for exterior plasters from Ankara;	19-53 for samples from Safranbolu; 20-23 for samples from Amasya
θ_{max} (% by weight)	39.1-69.4 for burnt mud brick (Güdücü, 2003)	15.2-36.7 (Tuncoku *et. al.* 1993); 30-35 (Tuncoku, 1993); 17.20-25.49 (Akyazı, 1998); 38.5- 41.3 for masonry brick from Konya.; 24.6-25.1 for infill brick from Adana	44 for burnt mud mortar (Güdücü, 2003)	21.94-37.06 for lime plasters, 13.90- 30.78 for gypsum plasters (Akkuzugil, 1997); 55.9-76.8 for burnt mud plaster (Güdücü, 2003); 10.3-39.8 for Seljukid plasters (Caner, 2003); 23.71 and 46.80 for horasan plasters, 15.84-58.88 for lime plasters (Akyazı, 1998); 17.72- 19.38 for exterior plaster samples from Adana; 47.6-48.7 for interior plaster samples from Amasya; 36.0-43.6 for exterior plaster samples from Ankara;	78.6-137.4 for samples from Safranbolu; 37.6- 44.2 for samples from Amasya
SD (m)	0.26-0.32, S_o: 10 cm	0.91 & 1.29, S_o: 10 cm	0.033 for mud mortars of 0.0163 m thickness (Akkuzugil, 1997)	0.020-0.069 for Seljukid plasters (Caner, 2003); 0.04-0.15 for lime plasters (Yıldırım Esen *et al.*, 2004); 0.026-0.059 for lime coats, 0.014-0.051 for mud plasters, 0.013-0.050 for gypsum plasters (Akkuzugil, 1997); 0.052-0.152 for horasan, 0.051-0.113 for lime plasters, 0.043, 0.044 and 0.057 for mud plasters (Akyazı, 1998)	0.8, S_o: 10 cm
μ	2.75- 3.23 (Akkuzugil, 1997) 0.57-0.99 for burnt mud brick (Güdücü, 2003)	9.06 &12.85 (Akyazı, 1998)	1.92-2.70 for mud mortars (Akkuzugil, 1997)	2.3-16.2 for lime plasters (Yıldırım Esen *et al.*, 2004), 3.04-18.27 for lime plasters, 2.88-13.33 for gypsum plasters, 1.19-3.16 for mud plasters (Akkuzugil, 1997); 0.51 & 0.64 for burnt mud plaster (Güdücü, 2003); 1.79-9.22 for Seljukid plasters (Caner, 2003); 2.878 and 12.790 for horasan plasters, 6.444 and 23.704 for lime plasters and 3.043, 5.507 and 2.519 for mud plasters (Akyazı, 1998)	8 (Kumaran *et. al.*, 1994)
T_{drying} (days)	NA	~10 for historic bricks (Tuncoku *et. al.*, 1993); ~29 for masonry bricks; ~36 for infill bricks	5 or 6 for some stone and brick mortars (Tuncoku, 2001)	4 days for exterior plasters from Adana, 4 days for interior plasters from Amasya, 3 days for exterior plasters from Ankara	~43 days for Amasya timber, ~46 days for timber samples from Safranbolu
R_E (kg/m^2.h)	NA	0.0770 for infill brick samples from Adana; 0.1241 for masonry brick samples from Konya	NA	0.0745 for exterior plasters from Adana; 0.0782 for interior plaster samples from Amasya	0.1411 for samples from Safranbolu; 0.1637 for samples from Amasya
E_{mod} (GPa)	0.7 (METU-MCL studies Fall 04'-REST 556), 1.170- 2.068 (Güdücü, 2003)	3.1-5.2 for bricks (Yıldırım Esen *et al.*, 2004)	1.2-3.6 for brick mortars (Yıldırım Esen *et al.*, 2004), 0.71-8.32 for stone mortars, 0.70-2.99 for brick mortars (Tuncoku, 2001)	0.7-6.6 for lime plasters (Yıldırım Esen *et al.*, 2004); 0.6-1.7 for burnt mud plaster (Güdücü, 2003); 2.855 average for Seljukid plasters (Caner, 2003)	NA
UCS (Mpa)	5.69 Mpa (METU-MCL studies Fall 04'-REST 556), 0.3-2Mpa (Eriç, 1980), 0.5-2 Mpa for non stabilized earth (Olivier & Mesbah, 1993), 1Mpa for normal mud brick according to T.S. 2514 (Eriç, Anıl & Çorapçıoğlu, 1980)	17 (Kahya, 1991)	NA	NA	NA
$Is_{(50)}$(Mpa)	0.10- 1.51 for burnt mud brick (Güdücü, 2003)	NA	0.52-1.38 for stone mortars 0.10-0.59 for brick mortars (Tuncoku, 2001)	0.02-0.15 for burnt mud plasters (Güdücü, 2003)	NA
ΔEC (mS/cm)	3-5.7 for burnt mud brick (Güdücü, 2003)	NA	9 for the aggregates of stone and brick mortars (Yıldırım Esen *et al.*, 2004), 0.4-1.5 for brick mortars (Tuncoku, 2001); 1.7- 3.3 for stone mortars (Tuncoku, 2001)	7 for the aggregates of plasters (Yıldırım Esen *et al.*, 2004); 1.8- 6.4 for burnt mud plasters (Güdücü, 2003); 42 mS/cm for Alanya Byzantine plaster (Caner, 2003)	NA

CHAPTER 3

MATERIAL AND METHOD

In this section, the experimental methods of the study, the dimensions and the preparations of the related test materials are described. The laboratory analyses covered the determination of basic physical, mechanical and compositional properties of the test samples.

In the laboratory were examined two types of plain-end AAC masonry blocks, one produced as infill (G2) the other produced as load-bearing material (G4) (see Table 2.12). Other than that, complementary wall elements of AAC recommended by the manufacturer were examined in the study. They were the jointing adhesive (JA) of AAC and four types of cement-based plasters; Base Coat (BC), Under Coat (UC), Finish Coat (FC) and Water Repellent Finish Coat (WRFC). In addition, some representative samples of historical materials such as timber, infill and masonry fired bricks, lime based interior and exterior plasters were studied.

A Turkish AAC company provided the AAC blocks and the raw materials of the cement-based plasters such as cement, aggregates and some special additives. The plasters were produced in the laboratory out of these raw materials. Historical materials were, on the other hand, collected from traditional structures of Anatolia. They were from timber-framed structures with stone or mud brick or fired brick infill. A few additional samples were obtained from a fired brick masonry structure.

The G2 and G4 blocks examined in the study were produced in the factory from slurries of pure quartz sand, Portland cement, lime, gypsum and water. What made G2 and G4 differ from each other were the mixing proportions of these ingredients and the type of the Aluminum powder.

The AAC slurries prepared with special prescriptions were poured into shallow casting cars where they rised up to their final volume under controlled temperature and turned into AAC cakes. The AAC cakes were then wire-cut to size before autoclaving. Later, in the autoclaves, AAC cakes were kept under 12 atm pressure and 190°C for 12 hours until they gained their mechanical strength (www.akg-gazbeton.com).

AAC test samples were produced in the laboratory from the plain-end AAC blocks of 20cmx 25cmx 60cm according to the TS EN 678 (1995) and TS EN 453 (1988). These blocks had their rising direction along their 60 cm edges and their surfaces parallel to the rising direction were wire cut surfaces. The blocks were divided into 9 parts by wet cutting along their rising direction as shown in Figure 3.01 and only the marked slices were used for the preparation of the test samples. For each test, the necessary three samples were produced by cutting one sample from each of these three slices.

The plasters examined in the study constitute the most common exterior finishing system of AAC masonry walls, which consists of a base coat (BC), an undercoat (UC) and rendering (FC), applied successively as shown in Figure 2.15a. Water-repellent finish coat (WRFC), which is another cement-based plaster used instead of FC or directly on BC, as shown in Figure 2.15a and Figure 2.15b, was also examined.

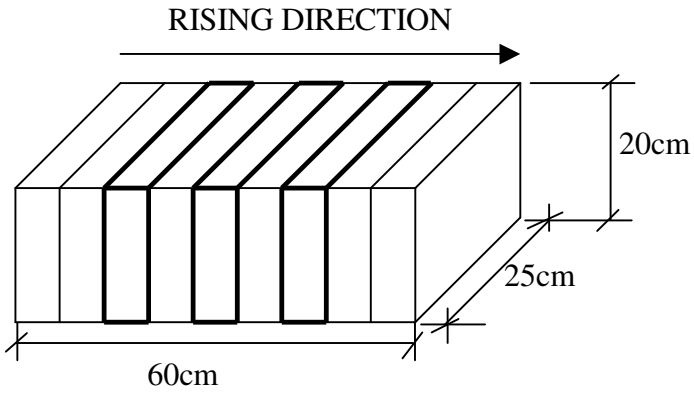

Figure 3.01. A Plain-end AAC Masonry Block of 20 cm x 25 cm x 60 cm divided into 9 equal parts along the rising direction. The marked slices were taken out for the preparation of the test samples.

The cement-based plaster samples to be examined in this study were prepared in the laboratory in the following proportions:

Base Coat (BC): 500 g aggregate, 250 g cement, 2.5 g BC additive, 200 ml water
Water Repellent Finish Coat (WRFC): 500 g aggregate, 166 g cement, 5 g WRFC additive, 110 ml water
Under Coat (UC): 750 g aggregate (0.3 mm), 250 g cement, 6 g UC additive, 170 ml water
Finish Coat (FC): 750 g silt, 250 g cement, 6 g FC additive, 200 ml water

The cement based plaster and the jointing adhesive samples were cast in the laboratory into formworks of 3.5 x 3.5 x 3.5 cm as shown in Figure 3.02 and they were examined after the curing period of 28 days.

Moreover, a G2 type AAC masonry wall was also prepared by the manufacturer together with its exterior finishing system consisting of BC, UC and FC. The wall was shown in Figure 3.03 and its cross section was given in Figure 3.04.

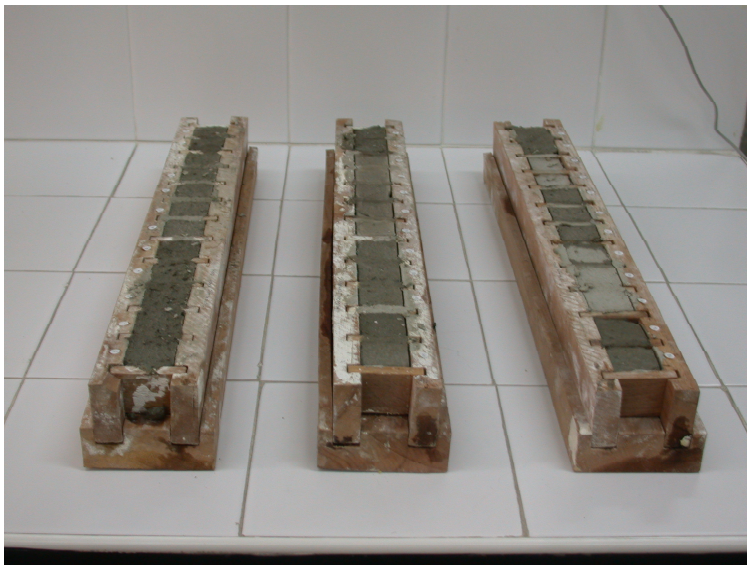

Figure 3.02 AAC plaster and jointing adhesive samples cast in the laboratory into 3.5x 3.5 x 3.5 cm formworks.

Figure 3.03. An AAC wall with already applied finishing layers provided by the manufacturer

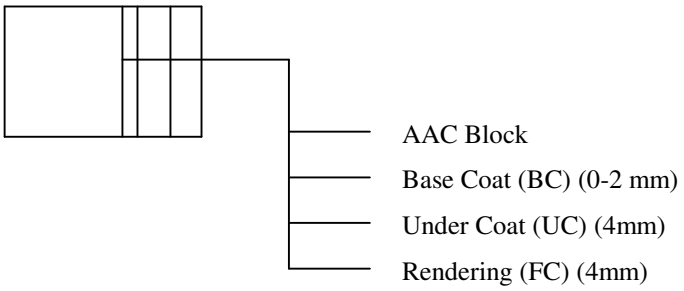

Figure 3.04 Representation for the section of a G2 type finished AAC masonry wall as prepared by the manufacturer for the laboratory tests.

The historical materials examined in the laboratory were given in Table 3.01. They were obtained from timber-framed structures with stone or mud brick or fired brick infill except the masonry fired brick samples (KMB). The masonry fired brick samples were obtained from the façade of Tahir ile Zühre Mescidi in Konya, which is a XIII. century mescid building.

Table 3.01. The historical materials examined in the study

code	explanation
AdIB	infill fired brick samples from Adana
KMB	masonry fired brick samples from Konya
AdEP	exterior lime based plaster samples from Adana
AIP	interior lime based plaster samples from Amasya
ST	timber samples from Safranbolu
AT	timber samples from Amasya

The timber samples from Safranbolu (ST) belong to a traditional timber framed residential structure. The timber samples from Amasya (AT) are from a timber framed structure with stone infill and AIP is its interior plaster over the stone infill. AdIB was the fired brick infill of a timber framed historical structure in Adana and the AdEP is its exterior plaster over the fired brick infill.

3.1. Determination of Basic Physical Properties

The basic physical properties examined in this study covered the determination of the following properties: bulk density *(ρ)*, effective porosity *(ϕ)*, water absorption capacity *(θ_{max})*, maximum vapor flow rate (R_{Emax}), critical moisture content (θ_c), water vapor diffusion resistance index (μ), equivalent air thickness of vapor permeability (*SD*) and the capillary water absorption coefficient (*A*). In this section were presented the dimensions of the test samples and the experimental methods used for the determination of these basic physical properties.

Bulk density (ρ), effective porosity (ϕ), water absorption capacity (θ_{max}) values of AAC, cement based plasters, jointing adhesive and historical materials were determined by the laboratory tests. For these tests, AAC samples were prepared as cubes of 5 cm x 5 cm x 5 cm from the AAC blocks of 20 cm x 25 cm x 60 cm (Figure 3.01). The plaster and the jointing adhesive samples were prepared as prisms of 2.5 cm x 3.5 cm x 3.5 cm from the cubes shown in Figure 3.02. The dimensions of the test samples prepared from the historical materials for these tests were given in Appendix B.

For the water vapor permeability tests; AAC, cement based plaster and jointing adhesive samples were used. In order to identify any variation in water vapor permeability along the thickness of AAC blocks, tests were conducted on eight 2.5 cm thick AAC samples of 2.5 cm x 5 cm x 5 cm which were taken from one wire-cut surface to another along the 20 cm thickness of the AAC blocks. 1.25 cm thick additional AAC samples of 1.25 cm x 5 cm x 5 cm were also prepared by cutting from the wire cut surfaces up to 1.25 cm depth and they were studied in order to assess the effect of the wire-cutting process on the water vapor permeability properties of AAC. In addition, samples of 1 cm x 3.5 cm x 3.5 cm were prepared from the cement based plasters (BC, UC, FC and WRFC) and the jointing adhesive by cutting from the cubes of 3.5 cm x 3.5 cm x 3.5 cm (Figure 3.02) for the water vapor permeability tests.

In order to comment on the adherence between the layers of a typical AAC exterior finishing system, water vapor permeability tests were also conducted on the samples cut from the finished AAC masonry wall prepared by the manufacturer (Figure 3.03). The samples cut from the finished AAC masonry wall were listed in Table 3.02.

Table 3.02. Samples cut from the AAC masonry wall prepared by the manufacturer

Sample	Thickness (cm) x Length (cm) x Width
AAC* + BC	1.46 x 5 x 5
AAC* + BC + UC	1.84 x 5 x 5
AAC* + BC + UC + FC	2.24 x 5 x 5

* G2 type autoclaved aerated concrete

The vapor flow rates (R_{Emax}), drying curves and critical moisture contents (θ_c) were determined for AAC, its cement based plasters and also for the historical materials listed in Table 3.01. The dimensions of the test samples examined in terms of their drying behaviors were given in Appendix B. Capillary suction tests were, on the other hand, conducted solely on AAC samples. The test samples were square prisms of 5 cm x 5 cm x 20 cm which were prepared from AAC blocks such that only their 5 cm x 5 cm square base was a wire cut surface.

3.1.1. Determination of Effective Porosity, Bulk Density and Water Absorption Capacity

All test samples except the timber ones were dried in the oven at 45°C to constant weight. The timber samples, on the other hand, were located in a humidity chamber of almost zero relative humidity to a constant weight. These weights were recorded as the dry weights of the samples (m_{dry}). The samples were then left in water for two days and their weights were recorded as the saturated weights in atmospheric pressure (m_{atm}). The test samples were then left in vacuum (HERAEUS vacuum chamber) under 0.132 atm (100 torr) pressure for half an

hour and they were fully saturated. The samples were then weighed and their weights were recorded as their saturated weights (m_{sat}). The weights of these saturated samples were also measured in water and recorded as their Archimedes weights (m_{arch}). All weights were measured with a balance sensitive to 0.0001 g and they were used in calculations for the determination of bulk density (ρ), effective porosity (ϕ) and water absorption capacity (θ_{max}) values. The results were expressed in tables and/or diagrams.

Effective Porosity (ϕ) is the percentage of volume occupied by the voids accessible to water within the total volume of the object. Effective porosity is expressed by the percentage of volume and calculated by the Equation 2 (RILEM, 1980a).

$$\phi\ (\%\ \text{volume}) = [(m_{sat} - m_{dry})/(m_{sat} - m_{arch})] \times 100 \quad \ldots\ldots\ldots\ldots\ldots\ldots\ (2)$$

where,

ϕ: effective porosity (% volume)

m_{sat} : saturated weight (gr)

m_{dry}: dry weight (gr)

m_{arch}: the weight of the saturated sample in water (gr)

The Bulk Density (ρ) is expressed by the ratio of the mass of the dry sample to its bulk volume and it is calculated by the Equation 3 (RILEM, 1980a).

$$\rho\ (g/\ cm^3) = m_{dry} / (m_{dry} - m_{arch}) \quad \ldots\ldots\ldots\ldots\ldots\ldots\ldots\ldots\ldots\ldots\ (3)$$

where,

ρ : bulk density (gr/cm^3)

m_{dry}: dry weight (gr)

m_{arch}: the weight of the saturated sample in water (gr)

Water Absorption Capacity (θ_{max}) is the maximum quantity of water absorbed by a porous material immersed in distilled water and is expressed as a percentage of the dry mass of the sample (Teutonico, 1988). Equation 4 calculates it.

$$\theta_{max}\ (\%\ \text{mass}) = [(m_{sat} - m_{dry})/m_{dry}] \times 100 \quad \ldots\ldots\ldots\ldots\ldots\ldots (4)$$

where,

θ_{max} : water absorption capacity (% mass)

m_{sat} : saturated weight (gr)

m_{dry}: dry weight (gr)

3.1.2. Determination of Drying Rate

Test samples were first dried in the oven at 45°C to constant weight and they were weighed (m_{dry}). The samples were kept in vacuum for 20 minutes under 0,132 atm (100 torr) pressure; they were saturated and weighed again (m_{sat}). The surfaces of the samples were then covered with paraffin so that only one surface for each was left open to evaporation as shown in Figure 3.5. Then the samples were weighed again in order to detect the weight of the paraffin and they were left for drying at 20°C and 40±5 % relative humidity. While the samples dry, their weights were recorded at regular intervals of 30-60 minutes, 2-4-6-12-14-14-24 hours and 1-1-1-3-3-3-5-5-6 days. All weight measurements were made with the sensitivity of 0.0001 grams.

The drying rate is expressed as the vapor flow rate (R_E) and it is calculated as a function of change in mass per unit time versus the surface area open to evaporation by the Equation 5 (RILEM, 1980a).

$$R_E\ (t) = dM / (A \times dt) \quad \ldots\ldots\ldots\ldots\ldots\ldots\ldots\ldots\ldots\ldots\ldots\ldots\ldots\ldots (5)$$

Figure 3.05. AAC, AAC plaster, historical infill and masonry fired brick, and historical lime based interior and exterior plaster samples left for drying at 20°C and 40±5 % relative humidity.

In Equation 5,

R_E: vapor flow rate (kg/m^2.h)

M: mass of the sample (kg)

t: time (s)

A: area of the surface open to evaporation (m^2)

Average moisture content of the samples (θ) at a definite time was calculated with Equation 6.

$$\theta = (m - m_{dry}) / (A \times \rho \times h) \quad \ldots\ldots\ldots\ldots\ldots\ldots\ldots\ldots\ldots\ldots (6)$$

where,

θ: average moisture content (m^3/m^3)

m: mass of the sample (kg)

m_{dry}: dry weight of the sample (kg)

A: area of the surface open to evaporation (m^2)

ρ: density of water (1000 kg/m^3)

Drying behaviors of the samples were expressed with the curves showing average moisture content (θ) versus time (t) and vapor flow rate (R_E) versus moisture content (θ).

The critical moisture content, θ_c, and the maximum vapor flow rate, R_{Emax}, of each material was determined by means of its drying curve showing its R_E values versus its θ. On this curve, the critical time when the sharp decline in R_E values started was noted as the θ_c level of each material. The R_{Emax} values were, on the other hand, obtained by calculating the mean of the R_E values recorded during the drying phase above θ_c. Critical moisture content, θ_c, level was defined in literature as the transition stage between the saturated and dry phases of porous materials (Massari and Massari, 1993; BS EN ISO, 2002; Torraca, 1988). Tavukçuoğlu and Grinzato (2006) stated that there was a relation between the thickness of the material and its θ_c. Therefore, comparisons over the critical moisture content values were made only for the samples with similar dimensions.

3.1.3. Determination of Water Vapor Permeability

The thickness of each test sample was measured on four sides by using a vernier caliper and the mean of these measurements was recorded as the width (S_o) of that sample. Waterproof cylindrical containers were then made ready for each test sample and their diameters were also measured with the vernier caliper. The cylindrical containers were filled with water so that 2 cm air space was left between the sample and the water surface. The containers were then covered with the samples and the edges were sealed with melted paraffin applied with a brush.

75 gr of calcium chloride ($CaCl_2$) was dissolved in 100 ml distilled water and the solution was poured into desiccators so that constant relative humidity of 50 % was provided in each dessicator. Samples were then placed into these desiccators

and they were weighed every day during the first week and every other day during the second week with a balance sensitive to 0.0001 g until the weight loss per unit time becomes constant.

Water vapor permeability is defined as the rate of water vapor transmission through unit area of flat material of unit thickness induced by unit vapor pressure difference between two specific surfaces, under specified temperature and humidity conditions (ASTM, 1993). Water vapor permeability is a material property and it is calculated with Equation 7.

$$SD=\mu So = (\Psi L \times A \times (P1-P2)/I)-SL \quad \ldots\ldots\ldots\ldots\ldots\ldots\ldots\ldots\ldots\ldots (7)$$

In Equation 7,

SD: equivalent air thickness of vapor permeability, m

μ: water vapor diffusion resistance coefficient, unitless

S_o: thickness of the sample, m

ΨL: constant= 6.89×10^{-6} (kg/mh (kg/m^2))

A: test area, m^2

P_1, P_2 : partial vapor pressures on the two sides of the sample, kg/m^2

I: weight change in unit time, kg/h

SL: thickness of air beneath the sample, m

The water vapor diffusion resistance index (μ) values were determined for BC, UC, FC, WRFC and JA by the Equation 7. Using their μ values, the *SD* values of these layers were then calculated for their thickness of application recommended by the manufacturer by the same equation. According to the classification in Turkish Standards (1999), *SD* values lower than 0.14m indicate high water vapor permeability; *SD* values between 0.14m and 1.4m indicate medium water vapor permeability and values higher than 1.4 m correspond to low water vapor permeability. The *SD* values of BC, UC, FC, WRFC and JA calculated for their

recommended thickness of application were then evaluated according to TSE (1999). The total *SD* values for the typical finishing systems of AAC were also evaluated and compared with each other with respect to this classification.

The total *SD* value was calculated for 10 cm thick AAC block together with each of its typical finishing systems shown in Figure 2.15. For these calculations, the μ value of each layer making up the wall section was multiplied by its thickness of application in order to obtain their *SD* values. The *SD* values individually obtained for each of these layers were then added together in order to calculate the total *SD* of the wall. Equation 8 summarized this calculation. In addition, the total *SD* value of a timber skeleton wall with mud brick infill finished with lime and mud plasters was calculated. Akyazı (1998) already determined the *SD* values of the exterior finishing layers of this wall (Section 2.4). Therefore, it was only needed to calculate the *SD* value of the mud brick infill. For this, the μ value that Akkuzugil (1997) determined for mud brick was multiplied by the thickness of the mud brick infill of the timber skeleton wall. The *SD* value of the mud brick infill was then added to the total *SD* value of its finishing system determined by Akyazı (1998) in order to calculate the total *SD* value of that historical wall section. The total *SD* value calculated for this historical wall section was then compared to that of 10 cm thick AAC block finished with its cement based plasters.

For calculating the total *SD* value of a timber skeleton wall with mud brick infill, the μ values Akkuzugil (1997) determined for mud brick and the μ values Akyazı (1998) determined for historic exterior finishing layers were used (Table 2.13). Eventually, the typical contemporary AAC wall sections were compared with the historical timber skeleton wall with mud brick infill in terms of water vapor permeability. The AAC wall section that presented the closest *SD* value to those of the historical wall section was selected.

$$SD_{total} = (\mu_1 x\ S_{o\,1}) + (\mu_2 x\ S_{o\,2}) + (\mu_3 x\ S_{o\,3}) + \ldots + (\mu_n x\ S_{o\,n}) \quad \ldots\ldots\ldots\ldots\ldots\ldots (8)$$

The water vapor permeability tests were also conducted to comment on the adherences between AAC and BC, BC and UC, UC and FC. For this, *SD* values were determined for the plastered AAC samples shown in Table 3.02 by laboratory tests and the obtained values were recorded as their *experimental SD* values. The *SD* values of the same samples were also calculated by the Equation 8, which includes the μ values and application thickness (S_o) of each layer. The obtained values were then recorded as their *calculated SD* values.

In case that the *experimental SD* value was found to be higher than the *calculated SD*, it was assumed that this difference would be due to the improper adherence between the layers resulting in air gaps in between. On the other hand, the similar results were to be considered as the signal for good adherence between the layers.

3.1.4. Determination of Capillary Suction

The test samples were dried in the oven at 45°C to a constant weight. They were then located into a humidity chamber of 65±5 constant relative humidity on a grid located in a basin that was filled with water, so that the water reached up to 1 or 2 mm height of the samples. The bottom surfaces of the samples were ensured to totally touch the water. The samples were regularly weighed with a balance sensitive to 0.01, while the height of the capillary rise was recorded at the same time. The results were expressed as the following diagrams:

1. water absorption per unit area (kg/m^2) versus square root time ($\sqrt{t}$,s$^{0.5}$)
2. moisture content (θ, % volume) versus square root time ($\sqrt{t}$, s$^{0.5}$)
3. moisture content at the level of capillary rise (θ, g/cm^3) versus square root time ($\sqrt{t}$, s$^{0.5}$)
4. moisture content at the level of capillary rise (θ, g/cm^3) versus the level of capillary rise (mm)
5. level of capillary rise (h, mm) versus time (t) (s)
6. level of capillary rise (h, mm) versus square root time ($\sqrt{t}$) (s$^{0.5}$)

In addition, capillary water absorption coefficients (A) and suction speeds (V_s) of the AAC samples were also determined. In water absorption per unit area (kg/m^2) versus square root time ($\sqrt{t}$, $s^{0.5}$) diagram, the slope of the line corresponds to the water absorption coefficient, *A*, which can be calculated with Equation 9 (RILEM, 1980a).

$$A = m / \sqrt{t} \quad \text{.....(9)}$$

where,

A: water absorption coefficient [$kg/ (m^2.s^{0.5})$]

m: the mass of water absorbed per unit area until time t (kg/m^2)

t: time passed after the capillary rise starts (s)

Suction speed, V_S, is the capillary rise per unit time and it is calculated by the Equation 10.

$$V_S = h / t^{0.5} \quad \text{.....(10)}$$

where,

V_S : suction speed ($mm/s^{0.5}$)

h: level of capillary rise (mm)

t: time allotted (s)

3.2. Basic Mechanical Properties

Analyses of basic mechanical properties covered the determination of ultrasonic pulse velocity (UPV), modulus of elasticity (E_{mod}), uniaxial compressive strength (UCS), point load strength index (I_s) and the correction factor (k) values of the test samples. In this section, preparation of test samples and the experimental methods used for the determination of basic mechanical properties were described. For the

analyses described in this section, AAC cubes of 5 cm x 5 cm x 5 cm and the cement based plaster samples of 1 cm x 3.5 cm x 3.5 cm and 2.5 cm x 3.5 cm x 3.5 cm were used.

3.2.1. Determination of Modulus of Elasticity (Young's Modulus)

The Modulus of Elasticity (E_{mod}) is defined as the ratio of stress to strain and shows deformation ability of a material under external forces (Timoshenko, 1970). E_{mod} values of both the AAC and the cement based plaster samples were determined indirectly by ultrasonic pulse velocity measurements (UPV) (ASTM, 1990; RILEM, 1980a). For this purpose, a portable PUNDIT Plus CNS Farnell Instrument with 54 kHz and 220 kHz transducers were used in the direct transmission mode (cross direction) to produce ultrasonic velocity data. In this method, the impulse is imparted to the specimen and, the time required for the ultrasonic waves to travel the minimum cross section of the specimen is measured. The ultrasonic pulse velocity of the waves is calculated by using the following Equation 11 (RILEM, 1980a; ASTM, 1990).

$$UPV = l / t \quad \text{.....(11)}$$

where,
UPV: ultrasonic pulse velocity (m/s)
l: the distance traveled by the wave (m)
t: travel time (s)

E_{mod} values were then calculated by means of the Equation 12, including both their ρ and *UPV* values (RILEM, 1980a; ASTM, 2003).

$$E_{mod} = \rho \times UPV^2 \times (1+V_{dyn})(1-2V_{dyn})/(1-V_{dyn}) \quad \text{.....(12)}$$

In Equation 12,

E_{mod} : modulus of elasticity (GN/ m^2)

ρ: density of the specimen (kg/m^3)

UPV: ultrasonic pulse velocity (m/s)

V_{dyn}: Poisson's ratio

In Equation 12, Poisson's ratio refers to the ratio of lateral expansion to the longitudinal reduction of the material under compression (Timoshenko, 1970). Poisson's ratio differs between 0.1 and 0.5 in relation to the elasticity of different building materials. Since AAC is a lightweight concrete and plasters are cement-based materials, V_{dyn} is taken as 0.18 to be used in the calculations of E_{mod} value for both AAC and its plasters.

The values obtained in GN/m^2 were used in tables and/or graphs after being converted into GPa.

3.2.2. Determination of Uniaxial Compressive Strength, Point Load Index and the Correction Factor

UCS values were determined for AAC samples with an ELE International Compact-1500 UCS Instrument as direct measurement. In addition, point load strength index (I_s) was also determined by using Point Load Testing method using appropriate equations as indirect measurement (ISRM, 1985).

Point load strength indexes (I_s) of the AAC samples were determined by the use of point load tests by Equation 13:

$$I_s = P / D_e^2 \quad \text{.....(13)}$$

In Equation 13,

P: applied load (kN)

D_e: equivalent core diameter (mm)

Equivalent core diameter (D_e) is calculated with Equation 14 for the axial tests, which is suggested for blocks and lumps.

$$D_e = \sqrt{4A/\pi} \quad \text{.....(14)}$$

The correction factor, *k*, was then determined by using UCS measurements and the I_s values by the Equation 15 (Broch and Franklin, 1972; Bieniawski, 1975; Anon, 1977; Beavis, Roberts and Minskaya, 1982; Foster, 1983; I.S.R.M., 1985; Topal, 1995; Norbury, 1986; Topal, 1999/2000).

$$k = UCS / I_s \quad \text{.....(15)}$$

where,

k: correction factor

UCS: uniaxial compressive strength value (MPa)

I_s: point load strength index (MPa)

3.3. Determination of Durability Properties

Durability properties of AAC samples were examined in terms of saturation coefficient (*S*) and wet-to-dry strength ratio based on *UCS* (R_{UCS}) and E_{mod} (Winkler, 1986; 1997; Topal, 1995; Topal and Doyuran, 1997).

3.3.1. Determination of Saturation Coefficient

Saturation coefficient (*S*) is the volume of water that a porous material absorbs by complete immersion under atmospheric pressure for a definite time (V_1) in relation

to the total volume of pores accessible to water (V_0) (RILEM, 1980a). It is a dimensionless coefficient and expressed with a number between 0 and 1.

In this study, *S* values were determined for the samples after 48 hours of complete immersion and Equation 16 was used for the calculations.

$$S = V_1 / V_0 \quad (16)$$

According to BRE (1997), the saturation coefficients less than 0.65 indicate extreme durability. However, it is also expressed in literature that saturation coefficient on its own is an unreliable guide to durability (BRE, 1997; RILEM, 1980a; Winkler, 1997).

In BRE (1997), it is also stated that a high saturation coefficient indicates the presence of high proportion of fine pores allowing water to be absorbed by capillary action. Saturation coefficient, *S*, values of AAC samples were, therefore, evaluated in terms of pore size distribution and the conclusions supported the results of the capillary suction and drying rate tests as well as the cross and thin section analyses.

3.3.2. Determination of Wet to Dry Strength Ratio

Wet to dry strength ratio (R_{UCS}) value is expressed as the ratio of the *UCS* value of a saturated sample to its *UCS* value at dry state in percentage. The R_{UCS} value is calculated by the Equation 17.

$$R_{UCS} = 100 \text{ x } (UCS_{wet} / UCS_{dry}) \quad (17)$$

In Equation 17,

R_{UCS} : wet to dry strength ratio (%)

UCS_{wet}: uniaxial compressive strength value of the saturated sample (MPa)

UCS_{dry}: Uniaxial compressive strength value of the dry sample (MPa)

In this study, R_{UCS} values were determined for the samples, which were left in water for 5 days after being saturated under vacuum. In addition, the changes in E_{mod} values of the AAC samples due to water were also followed. For this purpose, AAC samples were saturated under vacuum, left in water for 20 days and then dried. The E_{mod} values of these samples were determined indirectly by ultrasonic velocity measurements. The E_{mod} values were also determined for the dry samples during two cycles of wetting drying and the changes were presented in graphs.

According to Winkler (1993), the R_{ucs} values are classified as follows:

80%- 90% good and safe ,

70%- 80% further testing required

60%- 70% unsafe for frost and hygric forces

below %60 very poor quality

The R_{ucs} values obtained for the AAC samples were evaluated with respect to this classification and their durability was discussed.

3.4. Determination of Compositional Properties

The compositional properties of AAC samples were studied through the analysis of pozzolanic activity, examination on cross sections and on polished thin sections by optical microscopy and X-Ray Diffraction (XRD) analyses.

3.4.1. Determination of Pozzolanic Activity

Pozzolanic activity indicates the reaction ability of the material with calcium hydroxide by producing the calcium–silicate-hydrate (C-S-H) network. The higher the pozzolanic activity of AAC, the higher its bonding capacity with lime plasters (Tuncoku, 2001; Davey, 1961; Lea, 1970; Ashurst and Dimes, 1990). The pozzolanic activity of AAC samples were measured by using its powder lower than 125μ diameter. For the analysis, a 1.25 gr sample of powder was mixed with 50 ml saturated $Ca(OH)_2$ solution and the change in electrical conductivity of the mixture was measured by using Metrohm AG Herisau, Konduktometer E382 (Luxan, Madruga, Saavedra, 1989). The decrease in electrical conductivity (ΔEC in mS/cm) within 2 minutes was recorded for the evaluation of pozzolanic activity. Results were interpreted to find out whether AAC surfaces have sufficient bonding ability with lime mortars or not. The pozzolanic activity of the aggregates used in the production of AAC were also determined for the particles lower than 125μ diameter with the Luxan method (Luxan, *et al*, 1989). The results of the pozzolanic activity tests were then evaluated according to Luxan's classification. According to Luxan (1989), ΔEC values higher than 1.2 mS/cm refer to good pozzolanicity, ΔEC values between 0.4 mS/cm and 1.2 mS/cm refer to medium pozzolanicity and the ΔEC values lower than 0.4mS/cm refers to low pozzolanicity.

3.4.2. Cross and Thin Section Analyses

Cross and thin sections were prepared from both types of AAC, being G2 and G4 in order to investigate the pore and mineral structure of AAC. It was also aimed to explain its very high water-absorption capacity. A further aim was to gather the preliminary data for further discussions on the adherence between AAC and its plasters under the microscope. Thin sections of G2 and G4 were analyzed by optical microscope in x2.5, x10 and x20 magnification of single and cross nicols. During the analysis, the term *artificial air pores* was used for the definition of the

pores formed by the release of the hydrogen gas during the production process of AAC and the rest of the structure was defined as the cementitious micro porous matrix.

3.4.3. X-Ray Diffraction Analyses

The thin section analyses were supported by XRD analyses. For the analysis, powder G2 and G4 samples of <125 μ size were examined by using a Phillips Model PV 3710 X-Ray Diffractometer with Cu K α X-Rays.

CHAPTER 4

RESULTS

The results of all experiments are summarized in the following sections and they are expressed with the figures and tables.

4.1. Basic Physical Properties

In this section are presented the experimental results on basic physical properties, such as the bulk density *(ρ)*, effective porosity *(ϕ)*, water absorption capacity *(θ_{max})*, critical moisture content (θ_c), density of vapor flow rate (R_E), water vapor diffusion resistance index (μ), equivalent air thickness of vapor permeability (*SD*) and capillary water absorption coefficient (*A*).

4.1.1 Effective Porosity, Bulk Density, Water Absorption Capacity

The effective porosity, bulk density and water absorption capacity values determined for the AAC (G2 and G4), its plasters (BC, UC, FC and WRFC) and jointing adhesive (JA) were given in Table 4.01a and for the historical materials, such as infill (AdIB) and masonry brick (KMB), exterior (AdEP) and interior plasters (AIP) and timber samples (ST and AT) were given in Table 4.01b.

The ρ and ϕ of G2 and G4 samples were found to be 0.40 g/cm^3, 78%, and 0.60 gr/cm^3, 68%, respectively. The θ_{max} by weight for both G2 and G4 was found to be extremely high with values of 193% and 114%, respectively. While both the G2 and the G4 types of AAC were found to be very porous and lightweight materials, G4 was, expectedly, denser and less porous than G2 (Table 4.01a).

Table 4.01. The Bulk Density *(ρ),* Effective Porosity (*ϕ)* and Water Absorption Capacity (θ_{max}) values of: **(a)** AAC, its cement based plasters and jointing adhesive; and **(b)** and the historic materials of bricks, plasters and timbers.

(a)	Properties	G2	G4	BC	UC	FC	WRFC	JA
	ρ (gr/cm^3)	0.40	0.60	1.88	1.80	1.73	1.72	1.46
	ϕ (%)	78	69	23	25	29	32	34
	θ_{max} (% by weight)	193	114	12	14	17	18	24

(b)	Properties	AIB	KMB	AdEP	AIP	ST	AT
	ρ (gr/cm^3)	1.63	1.34	1.74	1.13	0.30	0.53
	ϕ (%)	40.53	53.26	32.45	54.10	31.97	21.74
	θ_{max} (% by weight)	24.92	39.90	18.69	48.17	100.68	40.99

AAC blocks showed variations in terms of their physical properties along their thickness. The samples taken from the wire-cut (exposed) surfaces of AAC blocks within the 2.5 cm thickness were found to have slightly less porosity as shown in the Figure 4.01.

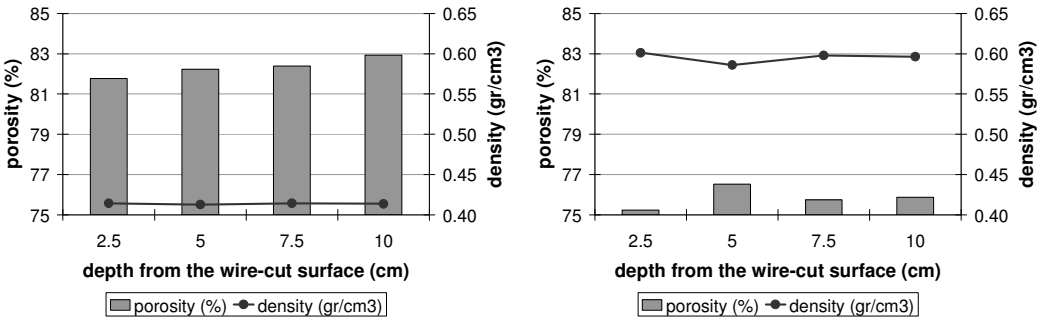

(a) **(b)**

Figure 4.01. Bulk density and effective porosity values for the 2.5 cm thick **(a)** G2 samples and **(b)** G4 samples taken from 2.5 cm, 5 cm., 7.5 cm and 10 cm depth from the wire-cut surfaces. The samples taken from the wire-cut surfaces up to 2.5 cm depth have the lowest porosity.

The plasters and the jointing adhesive were found to have ρ, ϕ and θ_{max} values of 1.88 g/cm^3, 23% and 12% for the BC, 1.80 g/cm^3, 25% and 14% for the UC, 1.73 g/cm^3, 29% and 17% for the FC, 1.72 g/cm^3, 32% and 18% for WRFC and 1.46

g/cm^3, 34% and 24% for the JA, respectively (Table 4.01a). These values showed that the plasters and jointing adhesive were considerably denser, less porous and less water absorptive when compared to AAC.

The ρ, ϕ and θ_{max} values of the historical materials were determined to be 1.63 g/cm^3, 40.53%, 24.92% for infill fired brick (AdIB); 1.34 g/cm^3, 53.26%, 39.90% for masonry fired brick (KMB); 1.74 g/cm^3, 32.45%, 18.69% for exterior plaster (AdEP); 1.13 g/cm^3, 54.10%, 48.17% for interior plaster (AIP); 0.30 g/cm^3, 31.97%, 100.68% for Safranbolu timber (ST) and 0.53 g/cm^3, 21.74%, 40.99% for Amasya timber (AT). The historical materials examined in this study seemed to be denser, less porous and less water absorptive when compared to AAC samples. On the other hand, the plasters seemed to be denser and less porous when compared to historical materials.

4.1.2. Drying Rate

The drying curves of AAC, its plasters and the historical materials were given in Figure 4.02 and Figure 4.03. For comparisons, the R_{Emax} values for all samples were given in Figure 4.04. In addition, the maximum vapor flow rates (R_{Emax}), the approximate duration of drying (T_d) and the critical moisture contents (θ_c) of the same materials were summarized in Table 4.02.

Drying rate curve showed that at the constant boundary conditions of 20±2^{o}C and 40±5% RH, G2 and G4 had similar R_{Emax} values of 0.0723 kg/m^{2}h and 0.0777 kg/m^{2}h, respectively (Figure 4.04 and Table 4.02) and G4 exhibited slightly slower drying than G2 samples below the θ_c level (Figure 4.02a). For instance, G4 dried in 25 days, while G2 dried in 24 days (Figure 4.02a). The θ_c of G2 and G4 were found to be almost the same with the values <22.79 and 23.84 for an average thickness of 1.6 cm, respectively (Figure 4.03a, Table 4.02).

Among the plaster samples, WRFC exhibited the fastest drying of 8 days with R_{Emax} value of 0.085 kg/m^{2}h. Base coat (BC), under coat (UC) and rendering (FC) dried in about 10 days with the average R_{Emax} values of 0.078 kg/m^{2}h, 0.059 kg/m^{2}h and 0.106 kg/m^{2}h respectively (Figure 4.04). The drying of AAC was concluded to take 2.5 times longer than those of its plasters. In addition, the θ_c levels were found to be 14.5% for 0.90 cm thick BC, 13.6% for 0.83 cm thick UC, 13.0% for 1.6 cm thick FC, 9.0% for 1.2 cm WRFC samples (Figure 4.04 and Table 4.02).

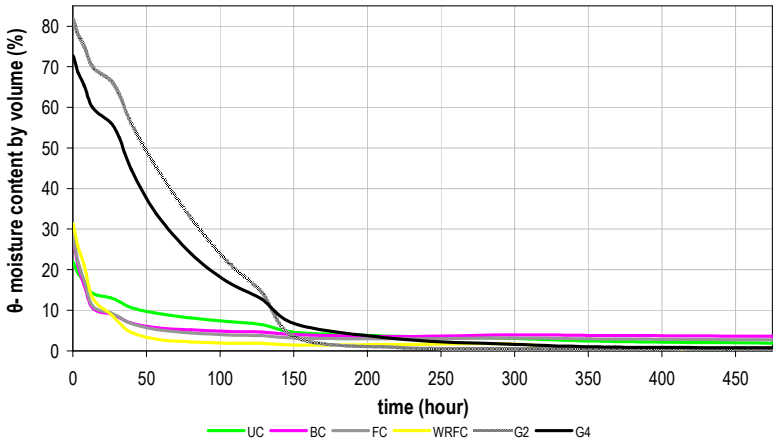

(a)

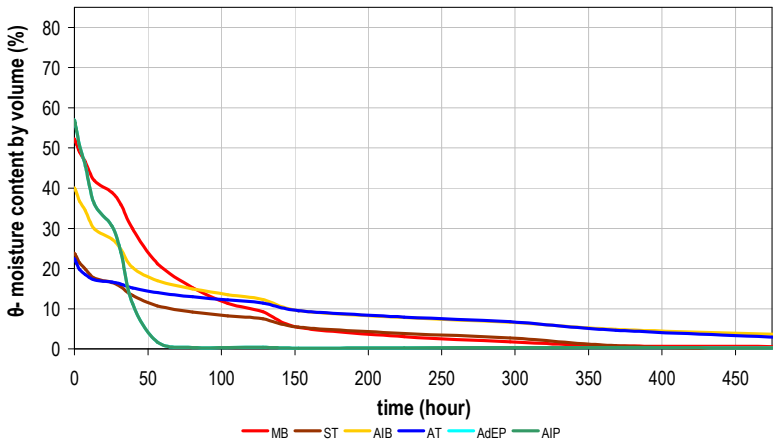

(b)

Figure 4.02. The drying curves showing moisture content as a function of time for **(a)** AAC (G2 and G4), its plasters (BC, UC, FC and WRFC) and **(b)** some historic materials (AdEP, AIP, KMB, AIB, ST and AT)

The historical materials of masonry brick (KMB), infill brick (AIB), exterior plaster (AdEP), interior plaster (AIP), timber from Safranbolu (ST) and timber from Amasya (AT) were determined to have R_{Emax} values of 0.124 kg/m^{2}h, 0.077 kg/m^{2}h, 0.075 kg/m^{2}h, 0.078 kg/m^{2}h, 0.141 kg/m^{2}h and 0.164 kg/m^{2}h respectively (Figure 4.04). These values showed that the drying rates of AAC samples were found to be almost the same with those of historic infill brick, exterior and interior plasters, while those of timber and masonry brick samples were distinctively higher. On the other hand, the drying periods of AAC and historic masonry bricks were found to be similar around 25 and 29 days respectively.

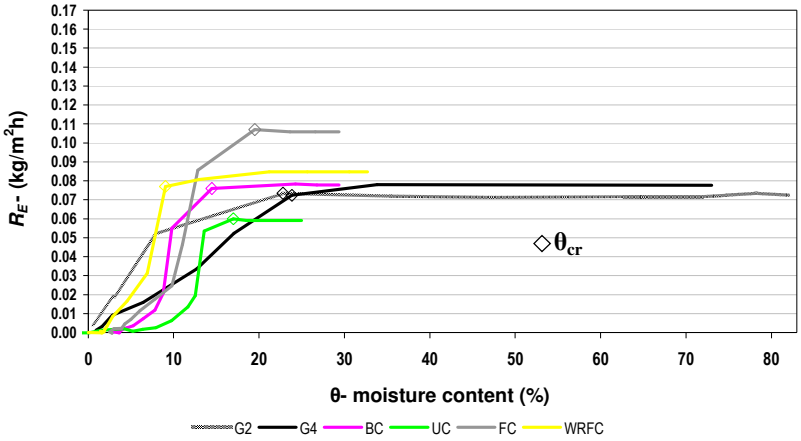

(a)

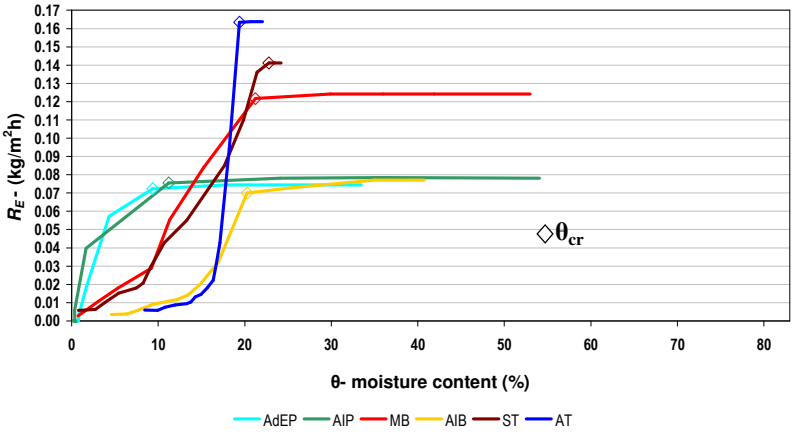

(b)

Figure 4.03. The drying curves showing evaporation rate, R_E (kg/m^{2}h), versus moisture content (% volume) **(a)** AAC (G2 and G4) and its plasters (BC, UC, FC and WRFC); **(b)** historical materials (AdEP, AIP, KMB, AIB, ST and AT).

The evaporation rates of AAC samples, base coat, finish coat and the water repellent finish coat were found to be close to those of historic infill brick, exterior plaster and interior plaster samples; however, under coat had a slightly lower evaporation rate. On the other hand, all of the cement-based plasters had lower evaporation rates when compared to historical masonry bricks and timber samples (Figure 4.04).

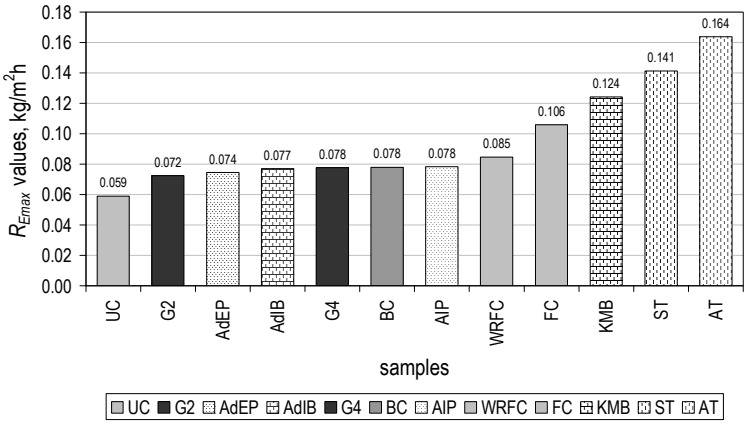

Figure 4.04. The results of evaporation rates (R_{Emax}) of AAC, its cement based plasters and some historical materials of infill brick (AIB), masonry brick (KMB), exterior plaster (AdEP), interior plaster (AIP) and timber samples from Safranbolu (ST) and Amasya (AT)

Table 4.02. The results showing the maximum density of water vapor flow rates (R_{Emax}) above θ_c, the total drying period (T_d) and the critical moisture content by volume (θ_c %): **(a)** for AAC (G2 and G4) and its plasters (BC, UC, FC and WRFC); and **(b)** for the historical materials (AdEP, AIP, KMB, AIB, ST and AT)

(a	Properties	G2	G4	BC	UC	FC	WRFC
	R_{Emax} (kg/m^{2}h)	0.0723	0.0777	0.0779	0.0591	0.1058	0.0847
	T_d (days)	24	25	10	10	10	8
	θ_c (%)	<22.79	23.84	14.47	16.00	13.00	9.04

(b	Properties	AIB	KMB	AdEP	AIP	ST	AT
	R_{Emax} (kg/m^{2}h)	0.0770	0.1241	0.0745	0.0782	0.1411	0.1637
	T_d (days)	36	29	4	4	46	43
	θ_c (%)	20.30*	21.23*	9.380	11.24	22.78*	19.40*

* θ_c of the samples were determined for the samples higher than 1 cm and in varying thickness. The data of their θ_c together with their thickness were given in Appendix B.

4.1.3. Water Vapor Permeability

The results of water vapor permeability tests on AAC samples were given in Figure 4.5. In Figure 4.05, the abscissa represented an AAC wall of 20 cm thickness having wire-cut surfaces on both sides and plastered typically as shown in Figure 2.15a. Wire-cut surfaces were found to have higher μ values within the first 5 cm depth for G4 and within the first 2.5 cm depth for G2 and to be almost constant beyond these depths. The highest μ values for both types of AAC blocks were obtained up to 1.25 cm depth from the wire-cut surfaces, with a value of 9.8 for G4 and 7.6 for G2. G4 apparently had higher μ values at the wire-cut surfaces when compared to G2. For G4 blocks, μ values sharply fell from 9.8 to 4.4 within the depth of 5 cm and the core beyond a depth of 5 cm showed similar μ values with an average of 3.3. For G2 blocks, μ value decreased from 7.6 to 5.7 within the depth of 2.5 cm and μ values were similar beyond this depth with an average of 4.1. The *SD* values for 2.5 cm thick slices taken along the 20 cm thickness of an AAC block were summed up. By this way, the total *SD* values of 20 cm thick G2 and G4 type AAC blocks were found to be 0.89m and 0.87m respectively (Table 4.03). The total *SD* values of 10 cm thick G2 and G4 type AAC walls, which can be representative for an infill wall of a timber framed historical buildings were calculated as 0.45m and 0.44m, respectively (Appendix C).

On the other hand, the μ values of BC, UC, FC, WRFC and JA were found to be 11.56, 13.99, 11.50, 5.86 and 13.37 respectively (Figure 4.05 and Table 4.03). The *SD* values for their recommended thickness of application were calculated to be <0.05m, 0.21m, 0.12m and 0.029 m, respectively. The *SD* value of JA was also found to be in the range of 0.01 to 0.04. According to the classification given in the standards (TSE, 1999), BC, FC, WRFC and JA were defined as high vapor permeable materials due to their *SD* values below 0.14m while UC seemed to be medium permeable due to its *SD* value between 0.14m and 1.4m.

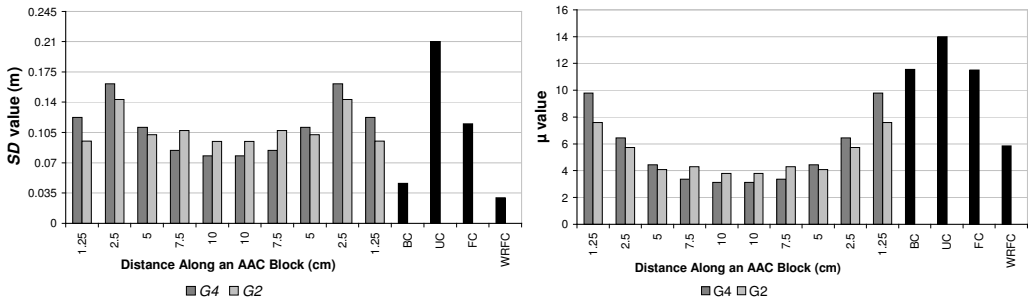

(a) **(b)**

Figure 4.05. Charts showing the changes in **(a)** *SD* and **(b)** μ values through an AAC wall of 20 cm thickness having wire-cut surfaces at both sides which were plastered typically as shown in Figure 2.15a. Two segments taken from the wire-cut surfaces up to a depth of 1.25 cm were located in the chart at both sides of the AAC block in order to show the effect of the wire-cutting process. The rest are the 2.5 cm thick segments taken along the 20 cm thickness of an AAC block from one wire-cut surface to the other.

Table 4.03. The water vapor diffusion resistance index (μ) and the equivalent air thickness of water vapor permeability (*SD*) values for AAC, its cement based plasters and jointing adhesive

Properties	G2	G4	BC	UC	FC	WRFC	JA
μ	3.78–5.73	3.13–6.44	11.56	13.99	11.50	5.86	13.37
SD	0.894[(1)]	0.869[(1)]	0-0.046[(2)]	0.210[(3)]	0.115[(4)]	0.029[(5)]	0.013 – 0.040[(6)]

[(1)] for 20 cm thick AAC wall; [(2)] for varying thickness between 0-4 mm; [(3)] for 15 mm thickness; [(4)] for 10 mm thickness; [(5)] for 5 mm thickness; [(6)] for varying thickness between 1-3 mm

The typical exterior finishing system shown in Figure 2.15a was found to have a total *SD* value of 0.37m where FC is the last layer, and to have a total *SD* value of 0.29m where WRFC is the last layer. On the other hand, the other application where WRFC is directly applied on the BC as shown in Figure 2.15b, was found have a total *SD* value of 0.08 m. According to TSE (1999), the typical application shown in Figure 2.15b seemed to be a high permeable exterior finishing system while the others without the application of an undercoat layer were found to be medium permeable ones.

The adherence between the surfaces of AAC and BC, BC and UC, UC and FC were analyzed by the comparison of experimental and calculated *SD* values. The experimental and calculated *SD* values given in Table 4.04 were found to be the same, signaling good adherence between all layers.

Table 4.04 The experimental and calculated *SD* values for the AAC samples in combination with its plasters.

Sample	Experimental *SD* (m)	Calculated *SD* (m)	Overall thickness of the samples (cm)
AAC/ G2	0.096		1.25
AAC/ G2 + BC	0.132	0.119	1.46
AAC/ G2 + BC+ UC	0.185	0.188	1.84
AAC/ G2 + BC+ UC+ FC	0.227	0.231	2.24

The total *SD* value of the historical timber skeleton wall with mud brick infill finished with lime and mud plaster was calculated to be 0.56 m. The total *SD* values of the AAC walls were calculated for each of the typical exterior finishing application shown in Figure 2.15. The total *SD* value for the successive application of BC, UC and FC (Figure 2.15a) onto a 10 cm thick AAC wall was found to be 0.82m, while that for the successive application of BC, UC and WRFC (Figure 2.15b) was 0.74m. The successive application of BC and WRFC on 10 cm thick AAC wall, on the other hand, was found to have a total *SD* value of 0.53m, which was very close to that of timber skeleton wall with mud brick infill.

4.1.4. Capillary Suction

The capillary water absorption coefficient, *A,* of G4 was found to be higher than that of G2 with values of 0.0367 $kg/m^2.s^{0.5}$ and 0.0255 $kg/m^2.s^{0.5}$ respectively as the slopes of the lines in Figure 4.06a indicated. At the level of capillary rise the moisture content, θ, of G4 was found to be higher than that of G2 with the constant values of 42% and 25%, respectively, as a function of time (Figure 4.07a) and as a

function of height (Figure 4.07b). However, the suction speeds, V_S, of G4 and G2 samples were found to be close to each other with the values of 0.09 mm/s$^{0.5}$ and 0.11 mm/s$^{0.5}$ respectively (Figure 4.08).

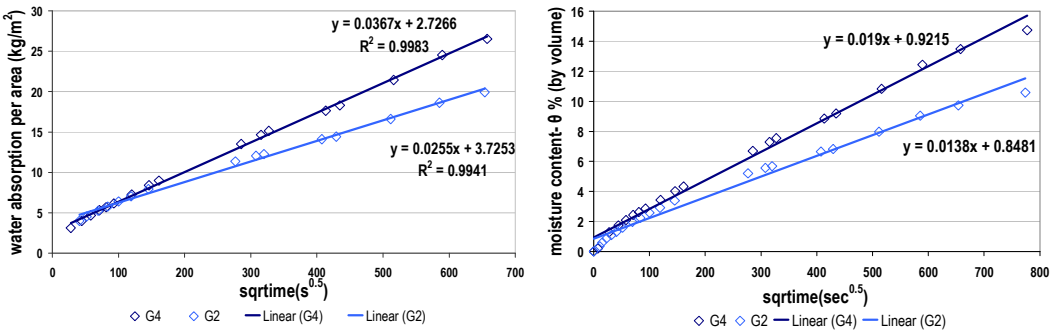

(a) **(b)**

Figure 4.06. The trend lines for G4 and G2 samples showing: **(a)** water absorption per unit area (kg/m^2) versus square root time ($\sqrt{t}$) (s$^{0.5}$); and **(b)** moisture content (θ) (% by volume) versus square root time ($\sqrt{t}$) (s$^{0.5}$)

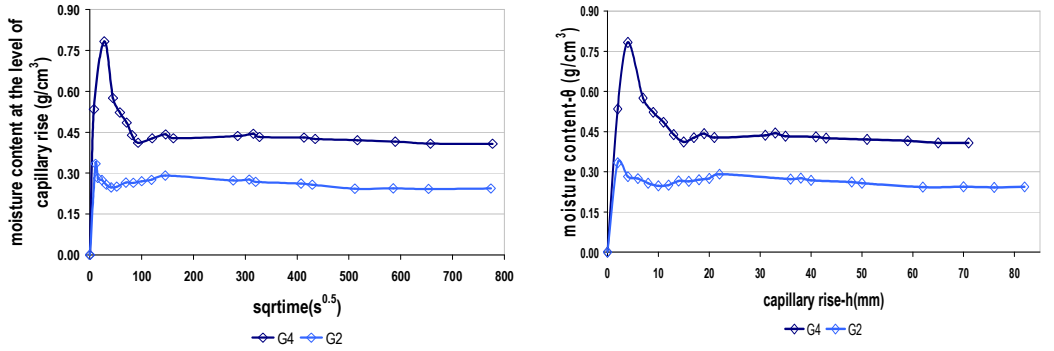

(a) **(b)**

Figure 4.07. **(a)** The curve showing the moisture content at the level of capillary rise (g/cm^3) versus square root time ($\sqrt{t}$) (s$^{0.5}$) **(b)** the trend line showing the moisture content at the level of capillary rise versus the level of capillary rise (mm), for G4 and G2 samples.

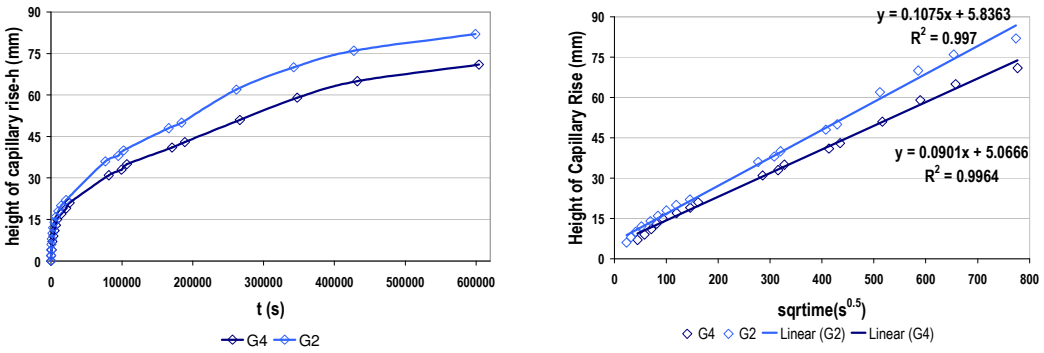

Figure 4.08. (a) The curve showing the level of capillary rise (*h*, mm) versus time (t) (sec); and **(b)** the trendline showing the level of capillary rise (*h*, mm) versus square root time ($\sqrt{t}$) ($s^{0.5}$)

4.2. Basic Mechanical Properties

In this section were given the modulus of elasticity and uniaxial compressive strength values, point load strength index and correction factors of the AAC and its cement based plasters.

4.2.1. Modulus of Elasticity (Young's Modulus)

The basic mechanical properties of AAC, its plasters and jointing adhesive were given in Table 4.5. Ultrasonic pulse velocity values (UPV) and E_{mod} were found to be 1965 m/s and 1.4 GPa for G2, while 1962 m/s and 2.1 GPa for G4, respectively. The E_{mod} values for the BC, UC, FC, WRFC and JA were found to be 3.9 GPa, 3.4 GPa, 3.7 GPa, 2.0 GPa and 3.0 GPa for thickness 1 cm to 3.5 cm as shown in Table 4.05. Among these plasters, WRFC seemed to be the closest one to the AAC material in terms of E_{mod} values.

The results of Felekoglu (2004) obtained by direct testing method for E_{mod} were compared with the results of this study obtained by indirect testing method (Table 4.06). It was seen that the E_{mod} values obtained in this study were three times lower than those of Felekoğlu.

Table 4.05. The results of mechanical properties of AAC, its cement based plasters and jointing adhesive in terms of ultrasonic velocity (*UPV*), modulus of elasticity (E_{mod}) and uniaxial compressive strength (*UCS*).

Properties	G2[(1)]	G4[(1)]	BC[(2)]	UC[(2)]	FC[(2)]	WRFC[(2)]	JA[(2)]
UV (m/s)	1965	1962	1512	1418	1516	1492	1501
E_{mod} **(GPa)**	1.4	2.1	3.9	3.4	3.7	2.0	3.0

[(1)] for the samples of 5x5x5 cm, [(2)] for the samples of samples of 1.0x3.5x3.5 and 2.5x3.5x3.5cm.

Table 4.06 –Modulus of Elasticity values, E_{mod}, of cement-based plasters found in this study by indirect testing method [(1)] and examined by direct testing method by Felekoğlu [(2)].

E_{mod} **(GPa) for different sample thickness**	BC	UC	FC	WRFC	JA
[1]1 cm to 3.5 cm thick samples	3.9	3.4	3.7	2.0	3.0
[2]Felekoglu, 2004: Cubic samples of 10 x 10 x 10 cm	7.6	7.5	3.0	4.7	NA

4.2.2. Uniaxial Compressive Strength, Point Load Strength Index and Correction Factor

Uniaxial compressive strength (UCS), point load strength (I_s) and correction factor (k) of G2 and G4 were 1.88 MPa, 0.4 MPa, 4.7 and 2.76 MPa, 0.7 MPa, 3.9 respectively.

4.3. Durability Properties

Durability properties of AAC samples were given in this section in terms of Saturation Coefficient (*S*) and wet to dry strength ratio (R_{UCS}).

4.3.1. Saturation Coefficient

The results on saturation coefficient, *S*, of AAC, its plasters and jointing adhesive were given in Table 4.10. The *S* of G2 was found to be lower than that of G4, with the values of 0.46 and 0.62, respectively. The saturation coefficients of BC, UC, FC, WRFC and JA were found to be 0.92, 0.95, 0.86, 0.71 and 0.98 respectively.

The *S* value of all plasters and jointing adhesive were higher than those of both G2 and G4. In addition, among the plasters, WRFC was found to have the lowest *S* value.

Table 4.07. The results on saturation coefficients (S) of AAC and its cement based plasters.

Properties	G2	G4	BC	UC	FC	WRFC	JA
***S* (0-1)**	0.46	0.62	0.92	0.95	0.86	0.71	0.98

4.3.2. Wet to Dry Strength Ratio

Considerable changes in mechanical properties were determined on saturated AAC samples. Wet-to-dry strength ratio based on *UCS* (R_{UCS}) for the G2 and G4 samples, which were left in water for 5 days after being saturated, were found to be 58.5% and 54.4% respectively. According to Winkler's (1993) classification, both G2 and G4 samples seemed to be in the category of unsafe materials against frost and hygric forces.

A slight increase was observed in the E_{mod} values of AAC after the first cycle of wetting and drying, especially for G4 with an increase of 0.53 GPa, while no considerable difference was observed after the second cycle. On the other hand, a significant reduction was determined in their E_{mod} values of the dry samples left in water for 20 days after being saturated under vacuum. For instance, the E_{mod} values dropped from 1.54 GPa to 0.76 GPa for G2 samples and from 2.66 GPa to 1.20 GPa for G4 (Figure 4.9). Considering the significant reduction in *UCS* and E_{mod} values of AAC when exposed to water for a long period of time, serious precautions seemed to be essential to be taken in order to keep AAC away from the risk of wet/soaking conditions in buildings.

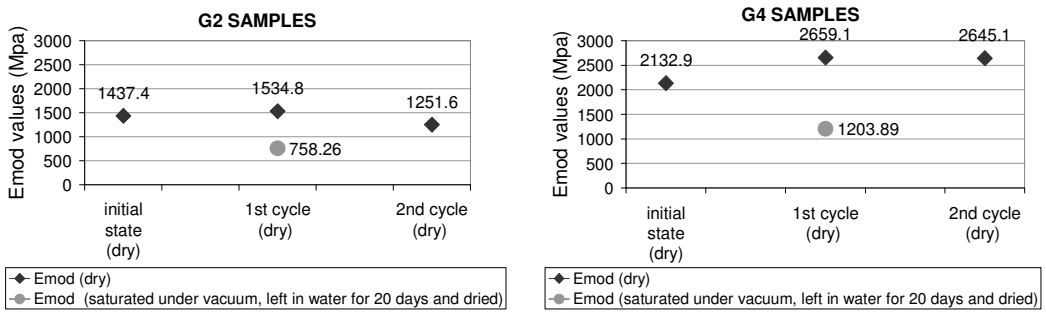

(a) **(b)**

Figure 4.09. The graphs showing the modulus of elasticity values, E_{mod}, of the initial state, after the first and second cycles of wetting and drying and when left in water for 20 days after being saturated under vacuum: for **(a)** G2; and **(b)** G4 samples.

4.4. Compositional Properties

In this section were presented the results of the laboratory experiments on pozzolanic activity, cross and thin section analyses of the AAC samples.

4.4.1. Pozzolanic Activity Measurements by Electrical Conductivity

The pozzolanic activity values of G2 and G4 samples were found to be 0.85 mS/cm and 0.95 mS/cm, respectively. The pozzolanic activity of aggregate, which was used in the production of AAC as raw material, was found to be 0.27 mS/cm. According to the classification defined by Luxan *et.al* (1989), the powdered AAC samples were determined as variable pozzolanic, while its aggregate was defined as of non-pozzolanic material. This indicated that the adhesion of AAC with lime mortars appeared to have a weak bonding.

4.4.2. Cross and Thin Section Analyses

The results of cross sections for AAC samples were given in Figure 4.10 and the results of thin sections were given in Figure 4.11 for G2 and in Figure 4.12 for G4 samples. Their combined interpretation showed that structure of AAC contained a

high proportion of pores and G2 was observed to have higher proportion of pores. The structure of both G2 and G4 had two components: the artificially induced air pores and a micro porous matrix. In addition, it was observed that a few of artificial pores had connection with each other while the others seemed to be totally impermeable on the 2D plane.

The mineral compositions of G2 and G4 were also determined by thin section analyses. G2 samples were found to contain angled aggregates with varied sizes of around 0.1 mm, 0.25 mm and 0.5 mm, while the aggregates of G4 samples were only 0.1 mm and 0.25 mm in size (Figure 4.11 and Figure 4.12). The minerals observed in both types of AAC were identical (Figure 4.11c and Figure 4.12c). They were quartz, orthoclase, muscovite, biotite, mica and opaque mineral. In addition, micritic limestone and quartzite were identified. These grains were within a matrix of finer grains which were ~5-10μ in size. The minerals identified within this matrix were calcite (C), opaque mineral of either hematite or limonite (L) and a majority of clay-size submicroscopic mineral (S). This submicroscopic mineral was identified as the mineral Tobermorite.

4.4.3. X-Ray Diffraction (XRD) Analyses

The results of thin section analysis were also supported by the *XRD* traces of G2 and G4 showing that the main minerals detected were 11 A^o Tobermorite and quartz (Figure 4.13).

(a) G2

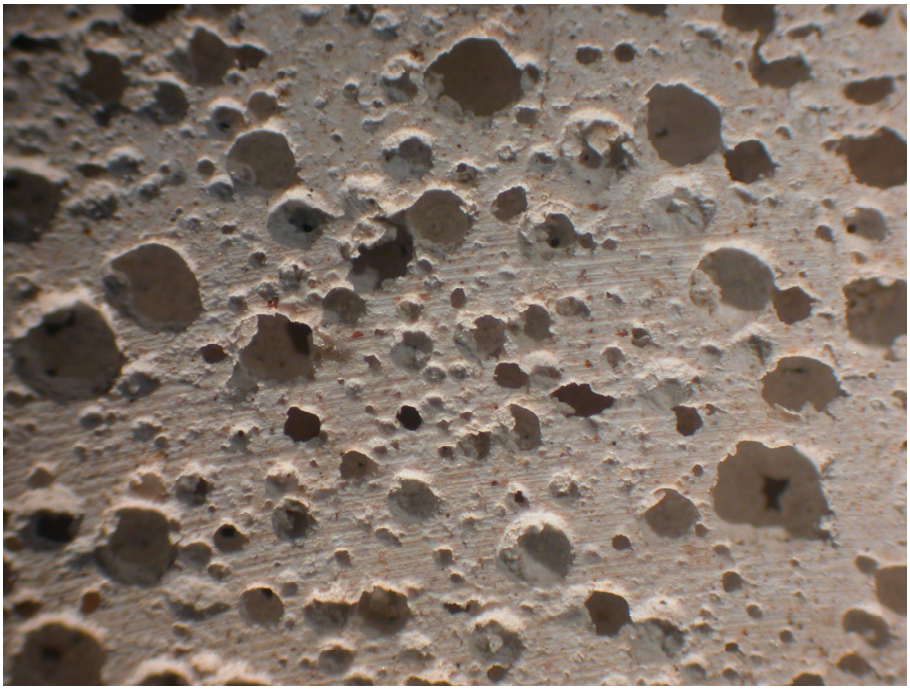

(b) G4

Figure 4.10. Cross sections showing the pore size distribution of AAC. Longer side of the micrograph = 1 cm.

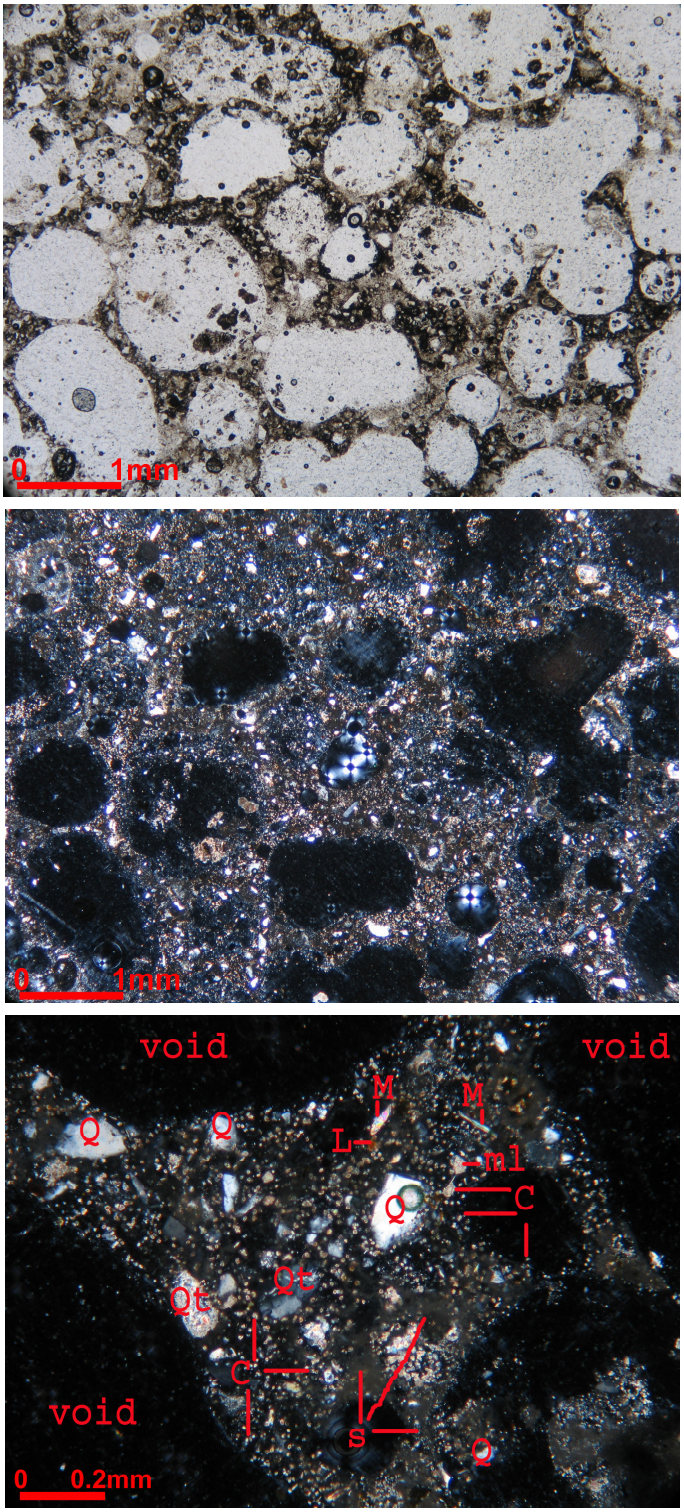

(a) x2.5 objective
single nicol

(b) x2.5 objective
cross nicol

(c) x10 objective
cross nicol. The minerals: quartz (Q), muscovite (mu), mica (M), micritic limestone (ml), quartzite (Qt), calcite (C), opaque mineral of limonite (L) and clay-size submicroscopic mineral (S)

Figure 4.11. Thin section of G2 showing the porous structure mineral composition and) the matrix in detail **(a)** under single nicol with x2.5 magnification; **(b)** under cross nicol with x2.5 magnification; and **(c)** under cross nicol with x10 magnification

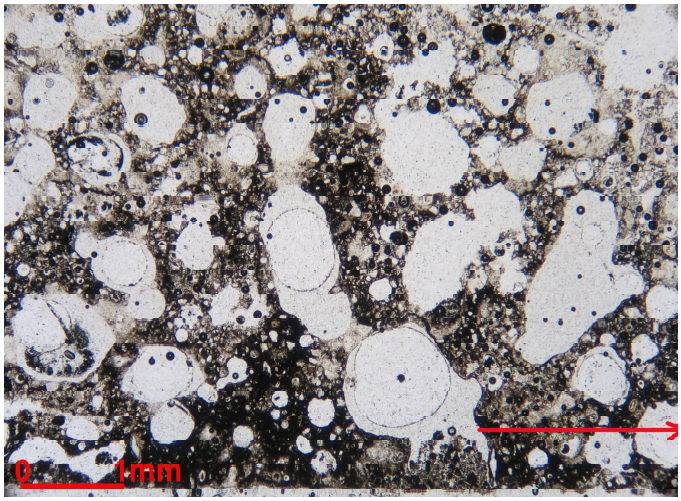

(a) x2.5 objective

single nicol

Air escape channels

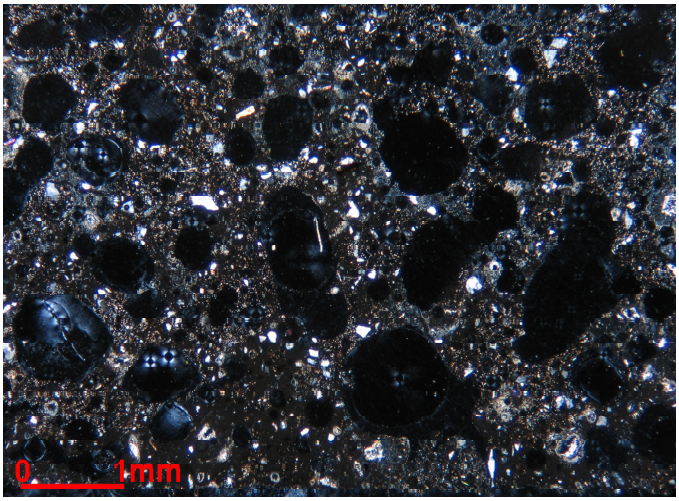

(b) x2.5 objective

cross nicol

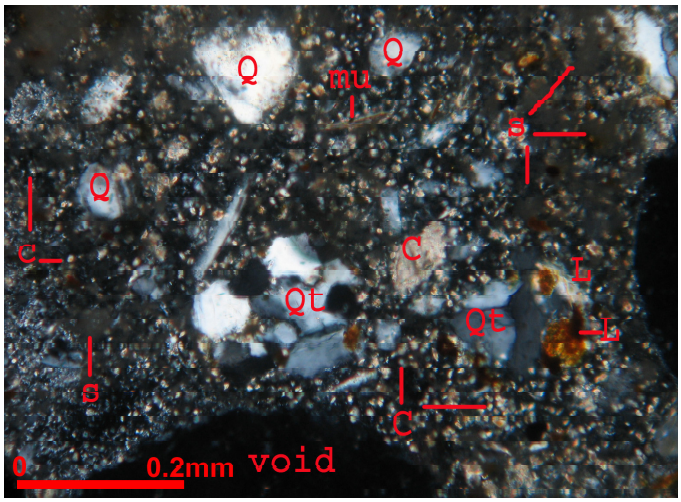

(c) x20 objective

cross nicol. x10 objective cross nicol. The minerals: quartz (Q), muscovite (mu), mica (M), micritic limestone (ml), quartzite (Qt), calcite (C), opaque mineral of limonite (L) and clay-size submicroscopic mineral (S)

Figure 4.12. Thin section of G4 showing the porous structure mineral composition and) the matrix in detail **(a)** under single nicol with x2.5 magnification; **(b)** under cross nicol with x2.5 magnification; and **(c)** under cross nicol with x20 magnification

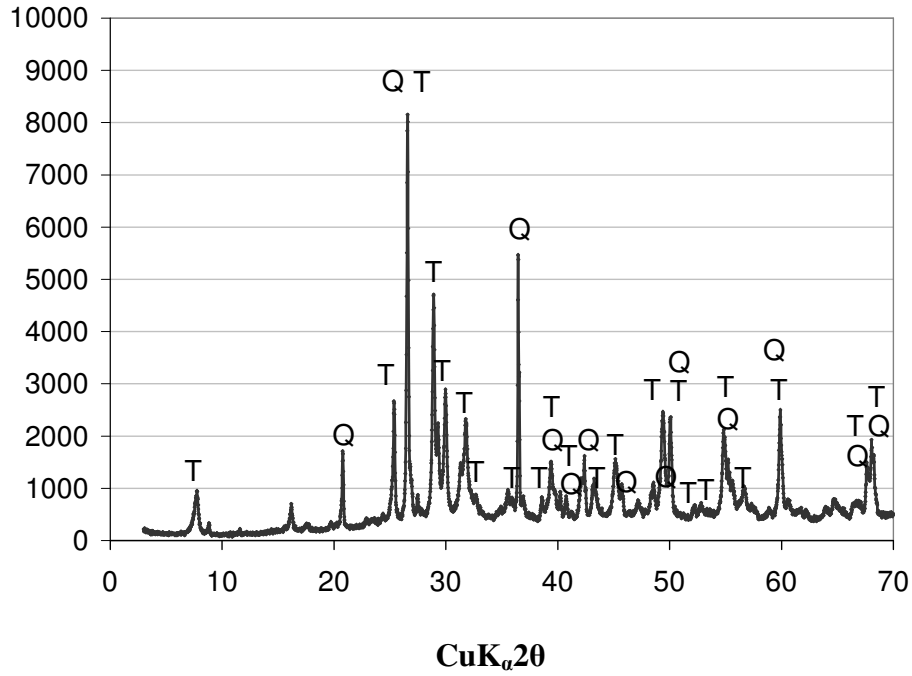

(a)

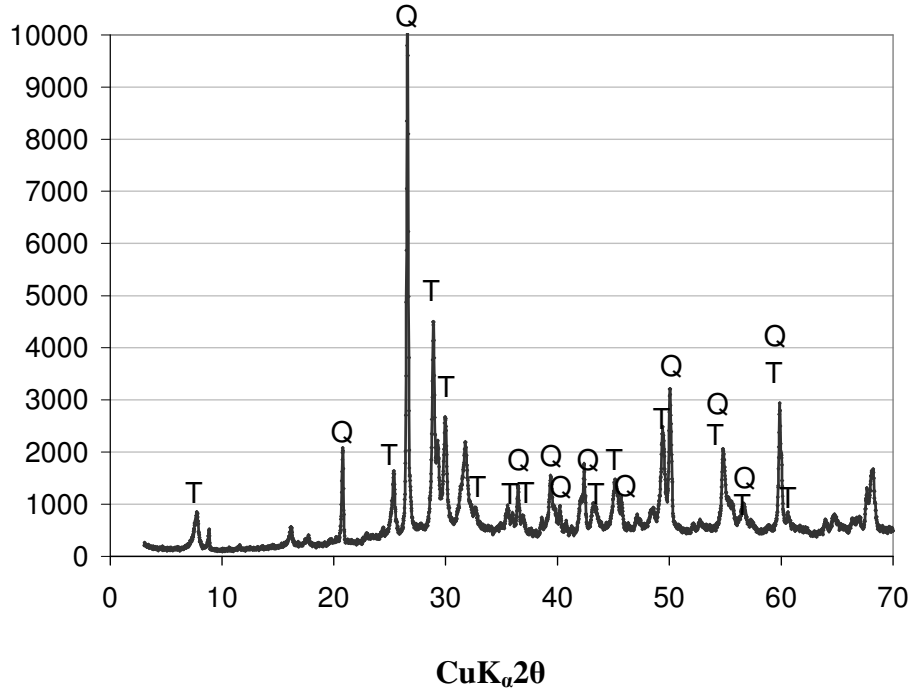

(b)

Figure 4.13. The XRD traces of **(a)** G2 and **(b)** G4 powder samples

CHAPTER 5

DISCUSSION

In this chapter are presented the basic discussions of the study under three basic titles. Under the first title, combined interpretation of the experimental results together with the data in literature was given in order to discuss the material properties of AAC. The second and the third title covered the discussions on the compatibility of AAC with its plasters inside a contemporary wall section and the compatibility of AAC and its plasters with the historical materials within the historic fabric respectively. The compatibility discussions were made through comparisons on the basic physical, mechanical and compositional properties of the materials.

5.1. Discussion on The Material Properties of AAC

In terms of their basic physical and mechanical properties, the AAC samples examined in this study were found to be within the acceptable ranges defined for AAC products by the standards. Both types of AAC samples (G2 and G4) were determined to be low dense, high porous and high water absorptive materials (Table 4.1). According to their densities, G2 and G4 were concluded to belong to the density classes of 400 and 600 defined by European Norms with their bulk density values of 0.4 g/cm^3 and 0.6 g/cm^3 respectively (prEN 12602, 1999). G2 and G4, at dry state, were also within the rages defined by the standards in terms of their uniaxial compressive strength (RILEM, 1993, CEB, 1978) and modulus of elasticity (DIN 4166) values and they were found to be in the compressive strength classes of 2 and 4 (DIN 4165) respectively.

Despite their different densities, the water vapor permeability characteristics of G2 and G4 were found to be similar to each other with average SD and μ values of

0.88m and 4.4, respectively, for a 20 cm thick AAC wall. In agreement with their similar water vapor permeability properties, both G2 and G4 were found to have similar evaporation rates (R_{Emax}) around 0.075 kg/m^{2}h. On the other hand, the μ value of AAC block was observed to drop sharply from the wire-surfaces up to a depth of 2.5 cm for G2 and up to a depth of 5 cm for G4 samples within the range of 9.8 and 3.3. Such difference was also followed with a slight decrease in porosity from the core towards the wire-cut surfaces. The range of μ values obtained for AAC in this study is, in fact, parallel to the range of μ values given in literature for the same material (RILEM, 1993). The differences at the wire-cut surfaces of AAC might be due to the wire cutting process during its production.

G2 and G4 were found to have very similar critical moisture content θ_c levels and evaporation rates, R_{Emax}, however, drying took longer time for G4 below the θ_c level when compared to G2. In addition, G4 was determined to retain more water at the level of capillary rise when compared to G2 with its higher capillary water absorption coefficient (A). The saturation coefficient (S) of G4 was also found to be higher when compared to G2. These results, in agreement, indicated that G4 had higher proportion of fine pores in its structure (BRE, 1997). This conclusion was also in agreement with the findings of Schober (2005) and Jacob & Mayer (1992) who observed that the higher the bulk density of AAC is, the higher the proportion of fine pores it contains (Table 2.02, Figure 2.03).

Observations under microscope showed that the pore structure of AAC contained high proportion of pores. The structure had two components: the artificially induced air pores and a micro porous matrix. In addition, some of the artificial pores were observed to overlap with each other, while the others seemed to be totally impermeable on the 2D plane. It is also known from the literature that the artificial pores are partly penetrable by water (Kadashevich, Schneider & Stoyan, 2004; Jacob & Mayer, 1992). These indicated that water might travel through the micro pores inside the cementitious matrix of AAC, rather than through the artificial air pores.

This conclusion was in agreement with F. Jacobs and G. Mayer (1992), Narayanan *et al*. (2000a), Kadashevich *et al.* (2004) who all state that the artificial air pores have little influence on the water permeability.

Uniaxial compressive strength (UCS) values for both types of AAC samples were found to be within the acceptable range defined for AAC products by RILEM (1993) (Figure 2.5a). According to prEN 12602 standards (1999), G2 was in the class of AAC 2, while G4 was in the class of AAC 3 (Table 2.05). Their *UCS* values were, in fact, found to be lower than the values stated by the manufacturer for the same types of AAC especially for G4 almost 0.6 of the data stated in the brochures (Table 2.10). Remembering that the compressive strength values for AAC samples vary according to the specimen size and shape and also the direction of loading (Narayanan *et.al.,* 2000a) the difference between the *UCS* values obtained with this study and the ones stated by the manufacturer might be due to the differences in any/both of these variables.

On the other hand, wet-to-dry strength ratios (R_{UCS}) determined for the wet samples which were left in water for 5 days after being saturated were out of the range defined by RILEM (1993) for the AAC products (Figure 2.5 b). According to CEB Manual of Design and Technology (1978), the wet-to-dry strength ratio in terms of *UCS* values cannot be lower than 65 %, however, the wet-to dry strength ratio of AAC was found to have 57%. According to Winkler's (1993) classification, a % 57 wet-to-dry strength ratios is in the category for the rocks, which are considerably weak against frost and hygric forces. Similarly, a significant reduction was also observed on the E_{mod} values of the dry samples, which were previously left in water for 20 days at saturated state (see Figure 4.9). In addition, another parameter related to the mechanical strength of natural rocks, namely *k value (UCS/* I_s*)* of the AAC samples were found to be 4.7 and 3.9 for G2 and G4, respectively. Those values were observed to be close to those for the weak rocks (Topal, 1999/2000; Topal, 1995). Considering all above, AAC should be

avoided from any risk of soaking and it should be well protected from water in its applications. Therefore, AAC should not be used in foundations or basement walls as recommended by the manufacturers (Borhan, 1990).

In this study, the capillary suction tests were conducted on AAC samples all surfaces of which were open to evaporation. Because this condition was thought to be more representative for the real case. Some of the water absorbed by capillary suction was lost due to evaporation and thereby, the capillary absorption coefficient (*A*) values were found to be considerably lower than those stated in literature (Pražák *et.al*., 1992; RILEM, 1993).

5.2. Discussion on The Compatibility of Autoclaved Aerated Concrete (AAC) With its Complementary Wall Elements

Under this title was discussed the compatibility of AAC with its complementary wall elements such as its cement based plasters and jointing adhesive for their use both in contemporary and historic wall sections. For this purpose, the material properties of these materials were compared with each other with the emphasis on their water vapor permeability properties and modulus of elasticity values. The plasters of AAC, were found to be denser and less porous when compared to AAC (Table 4.1a). Except the water repellent finish coat, all plasters and jointing adhesive were found to have higher μ values when compared to AAC samples (Figure 4.5). Due to their high density, low porosity, low water absorption capacity and high resistance to water vapor permeability, the plaster layers specifically produced for AAC seemed to protect AAC masonry from rain penetration.

On the other hand, according to the classification given in the standards (TSE, 1999) the plasters of BC, FC, WRFC and the jointing adhesive, *JA*, were determined as high water vapor permeable layers, while the undercoat was medium permeable considering the thickness recommended for their application. Similarly, the plasters, except the undercoat, *UC*, were found to have higher

evaporation rates at saturated state, R_{Emax}, when compared to AAC. Due to its lower evaporation rate, R_{Emax}, and lower water vapor permeability, the undercoat, *UC*, seemed to be the intermediate layer interrupting the removal of moisture/water, which is entrapped in AAC and/or basecoat. Finishing applications require preliminary wetting of the AAC surfaces and the plastering application is also a wet construction application. Therefore, new constructions keep water in their finishing system. It seemed that the plastering layers, except the UC, allow the drying of this water/moisture in the material. Therefore, the permeability properties of UC need to be improved to achieve a continuous vapor flow along the finishing layers.

Three typical exterior finishing systems, the first two being the successive applications of BC, UC, FC and of BC, UC, WRFC (Figure 2.15a) respectively and the third one being the direct application of WRFC on BC (Figure 2.15b), were compared with each other in terms of their total water vapor permeability. Due to the application of the UC, the first two applications were found to be medium water vapor permeable systems according to the standards (TSE, 1999). The second application, where WRFC is applied instead of the FC, seemed to be slightly more permeable than the first one. On the other hand, the third system where WRFC is applied directly on BC was found to have the highest water vapor permeability with a total *SD* value of 0.08m (TSE, 1999). Thinking of all, WRFC seemed to be a proper selection as a finishing for AAC and the application of WRFC directly on BC seemed to be the proper exterior finishing system for AAC masonry (Sasse *et al*., 1997).

Moreover, the coherence between the *experimental SD* and the *calculated SD* values examined for AAC wall plastered with the successive application of BC, UC and FC signaled the good adherence between the AAC and its finishing system and also between the layers of BC, UC and FC individually (Table 4.4). In any case,

further studies are required for the investigation of the adherence between the layers of this finishing system and for the adherence of this finishing system to the AAC surfaces.

The E_{mod} values of the plasters seemed to be in the range of E_{mod} values for the historical plasters and mortars (Yıldırım Esen *et. al*., 2004; Tuncoku, 2001). Since historical plasters have survived for long period of times, the range of their E_{mod} values were thought to express enough strength to cope up with the exposed conditions. It seemed that the E_{mod} values of the plasters specifically produced for AAC seemed to have enough strength.

Among all plasters studied, WRFC seemed to have E_{mod} values close to those of G2 and G4 while BC, UC and FC had higher E_{mod} values. Owing to the fact that the use of a layer stronger than its backing material may cause mechanical failures in the plastering system (Sasse & Snethlage, 1997), WRFC seemed to be more compatible with the AAC masonry than the others in terms of its modulus of elasticity values. On the other hand, the E_{mod} values obtained in this study were found to be considerably lower than the results determined by Felekoğlu (2004) for the same materials, even reaching to one third of his values. In this study, the indirect method (RILEM 1980a, ISRM, 1985) of using UPV and density values in some equations (see Section 3.2.2) was conducted on the samples of 1.5x3.5x3.5cm and 2.5x3.5x3.5cm, while Felekoğlu used direct testing method (ASTM, 2000) for the plasters of 10 x 10 x 10 cm, as shown in Table 4.6. In order to prevent misleading interpretations, it was concluded that some further studies were necessary to reveal the relation between the sample dimensions and E_{mod} values and to compare these two different testing methods. The experimental testing methods need to be improved to get a reliable data for the materials applied in thin layers.

5.3. The Compatibility of Autoclaved Aerated Concrete (AAC) and Its Complementary Wall Elements With Historic Building Materials

In Turkey, for repair purposes, AAC is used as substitute of the original mud brick, fired brick and stone infill of the historical timber framed structures and the system is finished with the cement-based plasters of AAC (see Section 2.3.3). Under this title was discussed whether the AAC and its complementary wall elements are suitable to be used as repair materials for the historic timber framed structures of Anatolia. Above all, it should strongly be emphasized that replacing AAC with the original infill material is unacceptable if the original infill material is still existing and functioning properly within the structure. This principle is significant for preserving the authenticity of the historic structure. Therefore, the use of ACC as an infill material for repair purposes can only be discussed only if the original material is not existing or so deteriorated that it cannot fulfill its function. In addition, the plasters of AAC are cement-based; therefore, they are not acceptable to be used within the historic fabric since they introduce severe salt problems resulting in considerable damage to historic fabric.

Due to the necessity of a void filler material where the original material is lost, in Turkey, restoration firms have recently been using AAC within the historic fabric as the infill material mostly because of its lightweight. In these applications, the finishing and jointing elements of AAC masonry wall construction are also introduced into the system. Hereunder was discussed the compatibility of these contemporary building materials with the historic fabric in terms of the similarities between their material properties.

The properties of AAC and some historic materials were summarized in Appendix C. According to the results, AAC was found to be less dense and more porous with very high water absorption capacity when compared to historical fired brick, mud brick, mortar and plaster (Tuncoku, 2001; Tuncoku *et al.*, 1993; Akkuzugil, 1997; Güdücü, 2003; Eriç, 1980; Yıldırım Esen *et.al*., 2004; Akyazı, 1998; Caner, 2003).

The evaporation rates, R_{Emax}, of both AAC samples, base coat and the water repellent finish coat were found to be in the same range for those of historic infill brick, exterior plaster and interior plaster samples; while the under coat had slightly lower evaporation rate (Figure 4.4). On the other hand, AAC and its plasters seemed to have lower evaporation rates than historical masonry brick and timber samples (Figure 4.4). In terms of vapor permeability and evaporation rate, except undercoat, all plasters, BC, FC and WRFC seemed to have similar breathing capability with historical infill brick. These plasters, on the other hand, seemed to be incompatible with historic masonry brick and timber samples since they had much lower R_{Emax} values when compared to masonry brick and timber.

The *SD* values for AAC, historic infill brick and mud brick for the thickness of 10 cm (Akyazı, 1998) showed that AAC was similar to historic mud brick infill used at timber framed historical buildings in terms of its water vapor permeability (Akkuzugil, 1997; Akyazı, 1998). The E_{mod} values of AAC samples were found to be within the range for those of some historic brick, brick mortars, plasters and burnt mud brick (Güdücü, 2003; Tuncoku 2001; Yıldırım Esen *et al*, 2004; METU MCL, 2004; Caner, 2003), while they were a bit lower than those of historic bricks (Yıldırım Esen *et al*, 2004). In terms of *UCS* values, AAC was found to be within the range for those of historic mud brick (METU MCL Studies, 2004; Eriç, 1980; Olivier & Mesbah, 1993; Eriç *et. al*., 1980), however, they had lower values when compared to historic brick (Kahya, 1991). AAC appeared to be close to the historic mud brick in terms of its water vapor permeability, E_{mod} and *UCS* values but further studies are required to conclude its use as a repair material alternative to the original infill of timber framed historical buildings.

Similar to historic mud brick, significant reduction in the mechanical properties of AAC was observed in soaking conditions (see Section 4.3.2; Houben & Guillaud, 1989). Therefore, also in its use for repairs of historic buildings, it should be well protected from direct water exposure and accumulation of water in the immediate periphery of buildings in order to maintain its inherent mechanical properties.

AAC was found to be medium pozzolanic, even its aggregates nonpozzolanic, while the historical mud brick, mortars and plasters were high pozzolanic materials (Yıldırım Esen *et.al*., 2004; Tuncoku, 2001; Caner, 2003; Güdücü, 2003). Therefore, bonding problems may occur at the interface of AAC with repair materials such as pozzolanic lime mortars and plasters within the historical structure.

The cement based exterior plasters of AAC and its jointing adhesive were mostly denser and less porous than the historical materials, while still remaining within the range of values for the historical plasters given in literature (Tuncoku, 2001; Tuncoku *et al.*, 1993; Akkuzugil, 1997; Güdücü, 2003; Eriç, 1980; Yıldırım Esen *et.al*., 2004; Akyazı, 1998; Caner, 2003). In terms of water vapor permeability properties, except the undercoat, the cement based plasters and the jointing adhesive seemed to have μ and *SD* values in the range for those of historic plasters (Figure 4.5, Yıldırım Esen *et.al*., 2004; Akkuzugil, 1997; Akyazı, 1998). Among the typical applications of AAC only the AAC wall with successive application of BC and WRFC seemed to exhibit similar total *SD* values with the mud brick infill wall plastered with mud plaster and lime plaster (Akyazı, 1998; Akkuzugil, 1997; Table 4.3). In any case, more comprehensive studies were required to investigate the total *SD* values of timber framed historical walls and their comparison with AAC walls.

Among the cement based plasters of AAC, only the WRFC seemed to fall into the range of E_{mod} values for brick mortars and historic plasters (Caner, 2003).

CHAPTER 6

CONCLUSION

Some physical, mechanical, durability and compositional properties of Autoclaved Aerated Concrete (AAC) produced in Turkey were defined and evaluated in comparison to the standards. Two types of AAC block, one produced as infill (G2) and the other as load-bearing material (G4) were examined in the study. Three types of typical exterior finishing systems for AAC, consisting of cement based plasters, specifically produced for AAC by using some additives, were also compared with each other and the most appropriate one was selected for the AAC masonry depending upon their water vapor permeability properties and modulus of elasticity values. Together with its plasters, the use of AAC as an infill material for repairs of the timber framed historical buildings was discussed by the comparison of some material properties. Further studies were suggested in the end.

The results showed that, AAC examined in the study was in the ranges defined by the standards for AAC in terms of its density, resistance to water vapor diffusion index, uniaxial compressive strength and modulus of elasticity values.

Both G2 and G4 were determined to be low dense, high porous and very high water absorptive materials. Both of them were found to have similar permeability properties in terms of equivalent air thickness of water vapor permeability (*SD*), water vapor diffusion resistance index (μ) and vapor flow rate (R_{Emax}). In addition, wire-cut surfaces of G2 and G4 were found to present some differences in terms of porosity and μ value. For instance, porosity slightly decreases at the wire-cut surfaces of AAC. The wire-cut surfaces were determined to have the highest μ value and this value sharply decreased up to a depth of 2.5 cm for G2 and up to a depth of 5 cm for G4.

The pore structure was found to consist of artificially induced air pores partly penetrable by water and the micro porous matrix. Water seemed to travel through the micro pores inside the cementicious matrix of AAC rather than through the artificial air pores.

Considering the significant reduction in the strength of AAC when exposed to soaking conditions, it should not be used in foundations or basement walls where there is risk of water accumulation and it should also be well protected from water exposure during its applications.

The cement-based plasters of AAC were found to be denser and less porous than AAC. Due to their higher density, lower porosity, lower water absorption capacity and higher μ value, they seemed to protect AAC from rain penetration. In terms of their *SD* values, the plasters of base coat (BC), finish coat (FC), water repellent finish coat (WRFC) and the jointing adhesive (JA) were determined to be high water vapor permeable layers. The undercoat (UC), on the other hand, was found to be medium permeable. The UC also had the lowest evaporation rate among the plasters of AAC and it appeared to be the intermediate layer interrupting the removal of moisture/water entrapped in AAC and/or base coat. It seemed that except the UC, the plaster layers permit a continuous vapor transmission along the layers of finishing system of AAC wall and also let the drying of water/moisture retained in especially the new constructions from their exposed surfaces.

The adherence between the AAC and the BC, the BC and the UC, the UC and the FC seemed to be good according to the consistency obtained between the *experimental SD* and *calculated SD* values of the same wall sections.

Among the cement-based plasters studied, WRFC was found to be a proper finishing for AAC masonry due to its E_{mod} value similar to that of AAC and its high vapor permeability. Due to such advantageous properties of WRFC, the finishing system where WRFC is directly applied on BC was determined to be the most proper exterior finishing system for AAC masonry.

The use of AAC within the historic structure as an alternative infill material for repairs of historic structures can only be discussed only if the original infill material is lost or it cannot fulfill its function within the structure.

AAC was found to be less dense and more porous with very high water absorption capacity when compared to historic fired brick, mud brick, historic mortar and plaster. On the other hand, AAC, especially G4, presented similarities to the historic infill fired brick in terms of water vapor permeability, evaporation rate, E_{mod} values. Similar to historic mud brick, significant reductions in mechanical properties of AAC were observed in soaking condition. Therefore, in use for repairs of historic buildings, it should be well protected from direct exposure to water and accumulation of water in the immediate periphery of buildings.

AAC was found to be medium pozzolanic and, therefore, bonding problems may occur at the interface of AAC with repair materials, such as pozzolanic lime mortars/plasters within the historical structure.

The plasters of AAC are cement-based; therefore, they are not acceptable to be used within the historic fabric since they introduce severe salt problems resulting in considerable damage to historic fabric. When compared with the historical plasters in terms of their material properties, the cement based exterior plasters of AAC and its jointing adhesive was mostly denser and less porous than the historical infill materials, such as historical mud brick and fired-brick, while still remaining within the range of values for the historical plasters given in literature. On the other hand, except the UC, the cement based plasters exhibited similar vapor permeability with historic plasters.

It was concluded that AAC exhibited some similarities with the historical materials in terms of its water vapor permeability and modulus of elasticity values. Among the plasters of AAC, WRFC appeared to be the most similar one with AAC and the historical materials in terms of its water vapor permeability properties and E_{mod}

values. WRFC is, however, cement based and, definitely cannot be used as a repair material in historic structures. As a result, a new repair mortar/plaster compatible with the historical materials seemed to be required in order to provide a good integrity between AAC and the historic fabric. In addition, the pozzolanic activity of AAC blocks needed to be improved to ensure this integrity by means of a good adherence between AAC and lime-based repair mortars/plasters.

Further studies should be conducted on some other compatibility parameters, especially the thermal and moisture dilatation properties, for AAC and its neighboring materials in order to decide on their compatibility both in contemporary and historical wall sections. In addition, water permeability properties of cement-based plasters still need to be determined for the assessment of its performance under rainwater exposure. Furthermore, the experimental testing methods need to be improved to clarify the effect of sample dimensions on the modulus of elasticity E_{mod} values, especially for the plasters applied in thin layers.

LITERATURE CITED

AKG GAZBETON. http://www.akg-gazbeton.com. Last accessed date: 20 July 2006.

AKKUZUGIL, E. 1997. A study in historical plasters. Unpublished Master's Thesis. METU Ankara.

AKYAZI, M. 1998. A proposal for the repair and conservation of Haraçoğlu Konak in Bursa. Unpublished MSc. Thesis, Department of Architecture – Restoration, METU, Supervisor: Neriman Şahin Güçhan, Co-supervisor: E. N. Caner-Saltık.

ALEXANDERSON, J. 1979. Relations between structure and mechanical properties of autoclaved aerated concrete, in: *Cement and Concrete Research* (p. 507-514, v.9).

ANDOLSUN, S., A. Tavukçuoğlu, E. N. Caner-Saltik, 2005. Evaluation of autoclaved aerated concrete (AAC) as a repair material for timber framed historical structures, in: *Proceedings of Postgraduate Researchers of the Built and Natural Environment (PROBE) 2005 Conference* (p.505-519), 16-17 November, 2005. Glasgow, Scotland. (ISBN 1-903661-82-X).

ANON, 1977. The description of rock masses for engineering purposes, in: *Q. J. Eng. Geology* (p. 355-389, v.10).

ASHURST J. & F. G. Dimes 1990. Mortars of Stone Buildings, in: *Conservation of Building and Decorative Stone* (p. 78-93, v.2). Butterworth-Heinemann.

ASTM, 2003. D 2845-00. Standard test method for laboratory determination of pulse velocities and ultrasonic elastic constants of rock, in: *American society for testing and materials* (p. 361-365).

ASTM, 2000. C 349. Standard Specification for Compressive Strength of Hydraulic Cement Mortars (Using Portions of Prism Broken in Flexure), in: *Annual Book of ASTM Standards*
.

ASTM, 1993. E 96-93. Standard Test Methods for Water Vapor Transmission of Materials, in: *American Society for Testing and Materials*.

ASTM, 1990. D 2845-90. Standard Test Method for Laboratory Determination of Pulse Velocities and Ultrasonic Elastic Constants for Rock, in: *American Society for Testing and Materials*, (p. 361-365).

BEAVIS, F.C., F.I. Roberts & L. Minskaya. 1982. Engineering aspects of weathering of low grade metapelites in an arid climatic zone, in: *Q. J. Engineering Geology* (p.29-45, v.15).

BORHAN, B. 1990. Ytong Yapı Elemanlarının Tanımı Kullanma Yöntemleri, in: *Ytong El Kitabı 2*.

BRE (Building Research Establishment). 1997. Selecting Natural Building Stones, in: *Digest 420*. 8p.

BRIESEMANN, D. 1976. Einfluss der feuchtigkeit auf die druckfestigkeit dampfgeharteten gasbetons, in: *Cement and Concrete Research* (p.561-570, v.6).

BROCH, E. & J.A. Franklin, 1972. The Point Load Strength Test, in: *Int. J. Rock Mech. Min. Sci.* (p.669-697, v.9).

BS, 2002. EN ISO 13788. Hygrothermal Performance of Building Components and Building Elements- Internal Surface Temperature to Avoid Critical Surface Humidity and Interstitial Condensation- Calculation Methods. British Standards Institute.

CANER, E. 2003. Archaeometrical investigation of some Seljuk plasters, Unpublished MSc Thesis, Archaeometry Program, METU, Supervisor: Şahinde Demirci, Co-supervisor: E. N. Caner-Saltık.

CEB, 1978. Autoclaved Aerated Concrete, in: *CEB Manual of Design and Technology*, The Construction Press, Lancaster, London, New York. (ISBN 0904406768.)

CEB, 1977. Autoclaved Aerated Concrete, in: *Manual of Design and Technology*. The Construction Press, Lancaster, London, New York. (ISBN 0904406768.)

ÇİÇEK, Y. E., 2002. Pişmiş toprak tuğla, bimsbeton, gazbeton ve perlitli yapı malzemelerinin fiziksel, kimyasal ve mekanik özelliklerinin karşılaştırmalı olarak incelenmesi. Unpublished Master's Thesis.

DAVEY, N. 1961. Gypsum plaster-limes and cement-stucco-mortar and concrete, in: *A History of Building Materials* (p.86-128). Phoenix House, London.

ERIÇ, M., 1980. Kerpiç eski eserlerin onarımı ve korunmasında bir araştırma, *in: Proceedings of Üçüncü Uluslararası Koruma Sempozyumu*. 29 Eylül-4 Ekim, 1980. Ankara.

ERIÇ, M., Ü. Anil, K. Çorapçioğlu, 1980. Kerpiç malzemenin türkiye koşullarında rasyonel kullanımını sağlamak amacıyla kalitesinin yükseltilmesi konusunda bir araştırma, T.D.G.S.A. Mim. Fak.

ESEN, S., N. Tunç, S. Telatar, A. Tavukçuoğlu, E. N. Caner-Saltik & Ş. Demirci, 2004. Manisa Çukur Hamam'ın Onarımına Yönelik Malzeme Çalışmaları, in: *Proceedings of 2. Ulusal Yapı Malzemesi Kongresi ve Sergisi* (p.494-505) 6-8 Ekim, 2004. İstanbul, Türkiye. TMMOB Chamber of Architects - Istanbul Branch.

FELEKOĞLU, B. 2004. Gazbeton ile geleneksel ve softharç serisi katkılı sıvaların uyumu sonuç raporu. Yayınlanmamış araştırma sonuç raporu. Dokuz Eylül Üniversitesi Mühendislik Fakültesi İnşaat Mühendisliği Bölümü, İzmir.

FOSTER, I. R. 1983. The Influence of core sample geometry on the axial point load test, in: *Int. J. Rock Mech. Min. Sci. and Geomech. Abstr*. (p.291-295, v. 20).

FREY, E. 1992. Recent results on thermal conductivity and hygroscopic moisture content of AAC, in: *Proceedings of the Third RILEM International Symposium on Autoclaved Aerated Concrete* (p.89-92). 14-16 October, 1992. Advances in Autoclaved Aerated Concrete, F.H. Wittmann, ed. A.A. Balkema, Rotterdam, Brookfield. (ISBN 90-5410-086-9).

GOODIER, A. & S. Matthews. 1997. In-service behavior of reinforced autoclaved aerated concrete planks, in: *Spec. Publ. Am. Concr. Inst.* (p. 1197-1214, v.2, no. SP-170).

GÜDÜCÜ, G. 2003. Archeometrical Investigation of Mud Plasters on Hittite Buildings in Şapinuwa-Çorum. Unpublished Master's Thesis. Middle East Technical University.

HAMA, Y., E. Kamada, M. Tabata, T. Watanabe. 1992. Frost resistance of increased density autoclaved aerated concrete, in: *Proceedings of the Third RILEM International Symposium on Autoclaved Aerated Concrete* (p.157-163). 14-16 October, 1992. Advances in Autoclaved Aerated Concrete, F.H. Wittmann, ed. A.A. Balkema, Rotterdam, Brookfield. (ISBN 90-5410-086-9).

HANECKA, K., O. Koronthályová & P. Matiašovský. 1997. The carbonation of autoclaved aerated concrete, in: *Cement and Concrete Research* (p.589-599, v.27, no.4). Elsevier.

HOUBEN, H & H. Guillaud. 1989. Earth Construction. London, UK: Intermediate Technology Publications.

HOUSE, Y., F. Alou and F.H. Wittmann. 1983. Influence of moisture content on mechanical properties of autoclaved aerated concrete, in: in F.H. Wittmann ed. (p.219-234).

I.S.R.M., 1985, Suggested method for determining point load strength, in: *Int. J. Rock Mech. Min. Sci. and Geomech. Abstr.* (p.51-60, v.22, No.2).

ISU N., H. Ishida, T. Mitsuda. 1995. Influence of quartz particle size on the chemical and mechanical properties of autoclaved aerated concrete-tobermorite formation, in: *Cement and Concrete Research* (p.243- 248, v.25).

JACOBS, F. & G. Mayer. 1992. Porosity and permeability of autoclaved aerated concrete, in: *Proceedings of the Third RILEM International Symposium on Autoclaved Aerated Concrete* (p.71-75). 14-16 October, 1992. Advances in Autoclaved Aerated Concrete, F.H. Wittmann, ed. A.A. Balkema, Rotterdam, Brookfield (ISBN 90-5410-086-9).

KADASHEVICH, I., H-J. Schneider, D. Stoyan. 2004. Statistical modeling of the geometrical structure of the system of artificial air pores in autoclaved aerated concrete, in: *Cement and Concrete Research* xx(2004) xxx-xxx.

KAHYA, 1991. İstanbul Bizans Mimarisinde Kullanılan Tuğlanın Fiziksel ve Mekanik Özellikleri. Unpublished PhD Thesis, İTÜ.

KUMARAN, M. K., G. P. Mitalas, M. T. Bomberg, 1994. Fundamentals of transport and storage of moisture in building materials and components, in: *Moisture Control in Buildings.* H. R. Trechsel, ed. Philadelphia: ASTM.

KUŞ, H. 2002. Long-Term Performance of Water Repellants on Rendered Autoclaved Aerated Concrete. Unpublished Ph.D. Thesis. Royal Institute of Technology, Stockholm

LEA, F. M. 1970. The chemistry of cement, 3rd ed. (p.414-453). Edward Arnold ed. London.

LEGATSKI, L.A. Cellular concrete, significance of tests and properties of concrete and concrete making materials, in: *ASTM Special Technical Publication*. (p.533- 539, no. 169C). Klinger PK, JF Lamond ed. Philadelphia.

LEITCH FN. 1980. The properties of aerated concrete in service, in: *Proceedings of the Second International Conference on Lightweight Concretes*. London.

LIPPE, K. F. 1992. The effect of moisture on the thermal conductivity of AAC. in: *Proceedings of the Third RILEM International Symposium on Autoclaved Aerated Concrete* (p.99-102). 14-16 October, 1992. Advances in Autoclaved Aerated Concrete, F.H. Wittmann, ed. A.A. Balkema, Rotterdam, Brookfield. (ISBN 90-5410-086-9.)

LUXAN, M. P., F. Madruga, & J. Saavedra, 1989. Rapid evaluation of pozzolanic activity of natural products by conductivity measurement, in: *Cement and Concrete Research* (p.63-68, v.19).

MASSARI, G. & M. Massari, 1993. *Damp Buildings, Old and New*. Rome: ICCROM.

MATSUSHITA, F., Y. Aono & S. Shibata. 2004. Calcium silicate structure and carbonation shrinkage of a tobermorite-based material, in: *Cement and Concrete Resesarch* (p.xxx, v.xx).

MATSUSHITA, F., Y. Aono. & S. Shibata. 2000. Carbonation Degree of Autoclaved Aerated Concrete, in: *Cement and Concrete Research* (p.1741- 1745, v.30).

MATSUSHITA, F. & S. Shibata. 2000. Carbonation degree as a durability criteria for autoclaved aerated concrete, in: *Proceedings of 5th CANMET/ ACI International Conference on Durability of Concrete* (p.1123- 1134, no. SP-192) V.M. Malhotra ed. Am. Concr. Inst.

MERTZ, J. D. 2004. Effect of water repellent treatments on the hydric dilatation of sandstone during water capillary absorption and drying stages, in: *Proceedings of the 10th International Congress on Deterioration and Conservation of Stone* (p.355-362). 27 June-2 July, 2004, Stockholm, ICOMOSSWEDEN.

METU MCL Studies. 2004. Materials Conservation Laboratory Studies for the course coded REST 556. Faculty of Architecture, Department of Architecture, Middle East Technical University.

MITSUDA T., C.F. Chan. 1977. Anomalous tobermorite in autoclaved aerated concrete, in: *Cement and Concrete Research* (p.191- 194, v.7).

MITSUDA T., T. Kiribayashi, K. Sasaki, H. Ishida. 1992. Influence of hydrothermal processing on the properties of autoclaved aerated concrete, in: *Proceedings of the Third RILEM International Symposium on Autoclaved Aerated Concrete* (p.11-18). 14-16 October, 1992. Advances in Autoclaved Aerated Concrete, F.H. Wittmann, ed. A.A. Balkema, Rotterdam, Brookfield. (ISBN 90-5410-086-9.)

NARAYANAN N. 1999. Influence of Composition on the Structure and Properties of Aerated Concrete. Unpublished Master's Thesis. IIT Madras.

NARAYANAN N., K. Ramamurthy, 2000a. Structure and properties of aerated autoclaved concrete: a review. In: *Cement and Concrete Composites* (p.321-329, v.22).

NARAYANAN N., K. Ramamurthy, 2000b . Microstructural investigations on aerated concrete, in: *Cement and Concrete Research* (p.457-464, v.30)

NIELSEN A. 1983. Shrinkage and creep deformation parameters of aerated autoclaved concrete, in: *Autoclaved Aerated Concrete, Moisture and Properties* (p.189-205). F.H. Wittmann, ed. Elsevier. (ISBN 0444421173.)

NORBURY, D.R. 1986. The point load test, site investigation practice: assessing BS 5930, in: *Geol. Soc. Engineering Geol. Special Pub* (No.2). 423 p.

ODLER I., M. Robler. 1985. Investigation on the relationship between porosity, structure and strength of hydrated portland cement pastes: effect of pore structure and degree of hydration, in: *Cement and Concrete Research* (p.401- 410, v.15).

OLIVIER, M. & A. Mesbah. 1993. Behavior of ancient and new structures made out of raw earth, in: *Proceedings of the Third International Conference on Structural Studies, Repairs and Maintenance of Historical Buildings*. Brebbia C.A, Frewer R. J. B. ed.

POSPISIL F., J. Jambor, J. Belko. 1992. Unit weight reduction of fly ash aerated concrete, in: *Proceedings of the Third RILEM International Symposium on Autoclaved Aerated Concrete* (p.43-52). 14-16 October, 1992. Advances in Autoclaved Aerated Concrete, F.H. Wittmann, ed. A.A. Balkema, Rotterdam, Brookfield. (ISBN 90-5410-086-9).

PRAŽÁK J. & P. Lunk. 1992. Capillary Suction of AAC, in: *Proceedings of the Third RILEM International Symposium on Autoclaved Aerated Concrete* (p.119-123). 14-16 October, 1992. Advances in Autoclaved Aerated Concrete, F.H. Wittmann, ed. A.A. Balkema, Rotterdam, Brookfield. (ISBN 90-5410-086-9).

prEN 12602. 1999. Prefabricated Reinforced Components of Autoclaved Aerated Concrete, February, 128 pp.

PRIM P. & F.H. Wittmann. 1983. Structure and water absorption of aerated concrete, in: *Autoclaved Aerated Concrete, Moisture and Properties* (p.43-53). F.H. Wittmann, ed. Elsevier. (ISBN 0444421173.)

RAMAMURTHY, K., N. Narayanan. Factors ınfluencing the density and compressive strength of aerated concrete, in: *Mag. Concr. Res.*, in press.

RILEM, 1993. Recommended practice- RILEM Technical Commities: 78-MCA and 51-ALC. Autoclaved Aerated Concrete- Properties, Testing and Design. S. Aroni, G. J. de Groot, M. J. Robinson, G. Svanholm and F.H. Wittman ed. Taylor & Francis Group, London and New York, 1993.

RILEM. 1980a. Tentative Recommendations, Commission – 25 – PEM, Recommended Test to Measure the Deterioration of Stone and to Assess the Effectiveness of Treatment Methods. Materials and Structures (p.173-253, v.13, no.73).

RILEM, 1980b. RILEM TC 25-PEM: Protection and Erosion of Monuments, Test No. 11.6, Water Absorption Coefficient (Capillarity), in: *Materials and Structures* (v.13, p.209).

ROULET CA. 1983. Expansion of aerated concrete due to frost- determination of critical saturation, in: *Autoclaved Aerated Concrete, Moisture and Properties* (p.157-169). F.H. Wittmann, ed. Elsevier. (ISBN 0444421173.)

RUDNAI, G. 1963. Lightweight Concretes. Budapest: Akademi Kiado.

SASSE & Snethlage. 1997. Methods for the Evaluation of Stone Conservation Treatments, Saving Our Architectural Heritage, in: *The Conservation of Historic Stone Structures* (p.223-243) (Derleyenler: N. S. Baer ve R. Snethlage). John Wiley and Sons, New York.

SCHUBERT P. 1983. Shrinkage behavior of aerated concrete, in: *Autoclaved Aerated Concrete, Moisture and Properties* (p.207-217). F.H. Wittmann, ed. Elsevier. (ISBN 0444421173.)

SENBU, O. & E. Kamada. 1992. Mechanism of frost deterioration of AAC, in: *Proceedings of the Third RILEM International Symposium on Autoclaved Aerated Concrete* (p.153-156). 14-16 October, 1992. Advances in Autoclaved Aerated Concrete, F.H. Wittmann, ed. A.A. Balkema, Rotterdam, Brookfield. (ISBN 90-5410-086-9.)

SCHOBER, G. 2005. The most important aspects of microstructure influencing the strength of AAC, in: *Proceedings of 4th International Conference on Autoclaved Aerated Concrete* (p.145-153). 8-9 September, 2005. Limbachiya and Roberts ed. Taylor & Francis Group, London. (ISBN 0 415 38356 0.)

SVANHOLM, G. 1983. Influence of water content on properties, in: F.H. Wittmann ed. (p.119-130).

TADA S. 1986. Material design of aerated concrete, in: *An Optimum Performance Design., Materials and Construction* (p.21- 26, v.19).

TADA, S., S. Nakano. 1983. Microstructural approach to properties of moist cellular concrete, in: *Autoclaved Aerated Concrete, Moisture and Properties* (p.71-88). F.H. Wittmann, ed. Elsevier. (ISBN 0444421173.)

TAŞDEMIR, C. & N. Ertokat, 2002. Gazbetonun Fiziksel ve Mekanik Özellikleri Üzerine Bir Değerlendirme, in: *Proceedings of 1. Ulusal Yapı Malzemesi Kongresi ve Sergisi* (p.425-437, v.2). İstanbul: TMMOB Mimarlar Odası İstanbul Büyükkent Şubesi.

TAVUKÇUOĞLU, A. & E. Grinzato. 2006. Determination of Critical Moisture Content in Porous Materials by IR Thermography, in press.

TEUTONICO, J.M. 1988. A Laboratory Manual for Architectural Conservators, Rome: ICCROM.

TEUTONICO, J.M., A.E. Charola , E. De Witte, , G. Grassegger, , R.J. Koestler, , M. Laurenzi Tabasso, H.R. Sasse, & R. Snethlage, 1997.'Group Report: How Can We Ensured the Responsible and Effective Use of Treatments (Cleaning, Consolidation, Protection)?', Report of the Dahlem Workshop on 'Saving our architectural heritage: the conservation of historic stone structures.'(p.292-313) N.S. Baer and R. Snethlage eds., John Willey & Sons Ltd.

TIMOSHENKO S. 1970. Strength of Materials, in: Analysis of Stress and Strain (p.53, chapter 2). Van Nostrand Reinhold Company, Holland.

TOPAL, T., 1995. Formation and Deterioration of Fairy Chimneys of Kavak Tuff in Ürgüp-Göreme Area (Nevşehir-Turkey), Unpublished Ph. D. Thesis. (p.61-67) Geological Engineering Department, METU.

TOPAL, T., 1999/2000. Nokta yükleme deneyi ile ilgili uygulamalarda karşılaşılan problemler, in: *Jeoloji Mühendisliği Dergisi* (p.73-86, v. 23-24, No.1).

TOPAL, T., V. Doyuran, 1997. Engineering geological properties and durability assessment of the Cappadocian tuff, in: *Engineering Geology* (p.175-187, v.47).

TORRACA, G., 1988. *Porous Building Materials - Materials Science for Architectural Conservation* (3rd ed.). Rome, Italy: ICCROM.

TORRACA, G., 1982. *Porous Building Materials - Materials Science for Architectural Conservation* (2nd ed.). Rome, Italy: ICCROM.

TSE, 1988. TS 453. Gas and Foam Concrete Material and Elements for Building.

TSE, 1995. TS EN 678 Determination of the Dry Density of Autoclaved Aerated Concrete.

TSE, 1999. TS prEN ISO 7783-2. Paint and Varnishes- Coating Materials and Coating Systems For Exterior Masonry- Part 2: Determination and Classification of Water-Vapour Transmission Rate (Permeability)

TUNCOKU, S. S., E. N. Caner-Saltık & H. Böke 1993. Definition of the materials and related problems of a XIIIth century Anatolian Seljuk 'mescid': a case study in Konya city, in: *Proceedings of The International RILEM/ UNESCO Congress on Conservation of Stone and Other Materials* (p. 368-375, v. 1).

TUNCOKU, S. S. 1993. The Restoration Project of a XIIIth Century Anatolian Seljuk "Mescid" In Konya With The Emphasis on the Materials and Related Problems. Unpublished Master's Thesis.

TUNCOKU, S. S. 2001. Characterization of Masonry Mortars Used in Some Anatolian Seljuk Monuments in Konya, Beyşehir and Akşehir. Unpublishes PhD Thesis. Middle East Technical University.

VALEK, J. 17 February 2005. Compatibility of new mortars with historic masonry, mortars, renders and plasters. Institute of Theoretical and Applied Mechanics.http://www.itam.cas.cz/static-presentation/contents/pdf/valek/valek_Compatibility%20of%20new%20mortars%20with%20historic%20masonry.pdf. Last accessed date: 5 September 2006

VALORE RC. 1954a. Cellular concretes-composition and methods of preparation, in: *J Am Concr Inst* (p.773-795, v.25).

VALORE RC. 1954b. Cellular Concretes- Physical Properties, in: *J Am Concr Inst* (p.817-836, v.25).

VAN HEES, R.P.J. 1999. Damage diagnosis and compatible repair mortars, in: *RILEM International Workshop, 'Historic Mortars: Characteristics and tests* (p.27-36). Paisley P. J. M. Bartos, C. J. W. P Groot and J. J. Hughes eds. RILEM 2000.

WINKLER, E. M. 1986. A durability index for stone, in: *Bulletin of Association of Engineering Geologists* (p.344-347, v.23).

WINKLER, E. M. 1993. Discussion and reply on the durability of sandstone as a building stone, especially in urban environments, in: *Bulletin of Association of Engineering Geologists* (p.99-101, v.30, no.1).

WINKLER, E. M. 1997. Stone in Architecture Properties and Durability. 3rd Third Edition. Springer-Verlag Berlin Heidelberg New York (ISBN 3-540-57626-6.)

ZIEMBIKA H. 1977. Effect of micro pore structure on cellular concrete shrinkage, in: *Cement and Concrete Research* (p.323-332, v.7).

APPENDIX A

BASIC PHYSICAL AND MECHANICAL PROPERTIES OF AAC, EXTERIOR FINISHING PLASTERS AND JOINTING ADHESIVE

Properties	G2	G4	BC	UC	FC	WRFC	JA
ρ (gr/cm^3)	0.40	0.60	1.88	1.80	1.73	1.72	1.46
θ_{max} (% by mass)	193	114	12	14	17	18	24
S (0-1)	0.46	0.62	0.92	0.95	0.86	0.71	0.98
ϕ (%)	78	69	23	25	29	32	34
μ	3.4–7.0	2.9–7.0	11.56	13.99	11.5	5.86	13.37
SD	0.89[1]	0.87[1]	0-0.046[2]	0.021[3]	0.115[4]	0.029[5]	0.013 – 0.04[6]
E_{mod} (GPa)	1.4	2.1	3.9[7]	3.4[7]	3.7[7]	2.0[7]	3.0[7]
UCS (Mpa)	1.88	2.76	NA	NA	NA	NA	NA
R_{Emax} (kg/m^{2}h)	0.0723	0.0777	0.0779	0.0590	0.1058	0.0847	NA
Drying time	24	25	~10	~10	~10	~8	NA

(1) for 20 cm thick AAC wall; (2) for varying thickness between 0-4 mm; (3) for 15 mm thickness; (4) for 10 mm thickness; (5) for 5 mm thickness; (6) for varying thickness between 1-3 mm (7) for 10 to 35 mm thickness.

APPENDIX B

DRYING RATE SAMPLES

CODE	$SA_{(AV)}$(cm^2)	$h_{(AV)}$(cm)	ρ (gr/cm^3)	ϕ (%)	θ_{max} (% by mass)	θ_c (%)	θ_c/ϕ (%)	R_{Emax} (kg/m^2.h)
G2	23.01	1.54	0.40	78	193	<23	<29	0.07232
G4	20.10	1.76	0.60	69	114	24	35	0.07769
BC	11.15	0.91	1.87	23	12	15	65	0.07788
UC	11.83	0.83	1.96	25	14	16.00	64	0.05906
FC	11.07	1.56	1.73	29	17	13	45	0.10581
WRFC	9.48	1.18	1.72	32	18	9	28	0.08473
AIB	19.82	2.33	1.63	41	25	20	49	0.07701
KMB	11.02	3.37	1.34	53	40	21	40	0.12413
AdEP	15.50	0.78	1.74	33	19	9	27	0.07445
AIP	20.03	1.00	1.13	54	48	11	20	0.07823
ST	20.62	4.68	0.30	32	101	22.78	72	0.14114
AT	19.26	4.74	0.53	22	41	19	86	0.16373

APPENDIX C

MATERIAL PROPERTIES OF AAC, ITS COMPLEMENTARY ELEMENTS AND SOME HISTORICAL MATERIALS

VALUE	AAC	BC, UC, FC, WRFC & JA	HISTORIC MUDBRICK	HISTORIC FIRED BRICKS	HISTORIC MORTARS	PLASTERS	TIMBER
ρ (gr/cm^3)	0.4 for G2 0.6 for G4	1.88 for BC, 1.80 for UC, 1.73 for FC, 1.72 for WRFC, 1.46 for JA	1.2-1.6 (Eriç, 1980) 1.17-1.57 for burnt mud brick (Güdücü, 2003)	1.34-1.82 (Tuncoku *et al.*, 1993); 1.38-1.47 (Tuncoku, 1993), 1.18- 1.61 for masonry brick (Tuncoku, 2001); average 1.67 (Yıldırım Esen *et al.*, 2004); 1.57-1.78 (Akyazı, 1998); 1.6 for infill brick; 1.30- 1.36 for masonry brick	1.51 for burnt mud-mortar (Güdücü, 2003); 1.39-1.85 for stone mortars; 1.25-1.74 for brick mortar (Tuncoku, 2001) 1.63 for stone masonry mortar, 1.53 for brick masonry mortar (Tuncoku, 1993); 1.52-2.07 for brick masonry mortars, 1.62-2.22 for stone masonry mortars (Yıldırım Esen *et al.*, 2004)	0.97–1.84 for lime plasters (Yıldırım Esen *et al.*, 2004); 1.28-1.67 for lime plasters, 1.35-1.70 for gypsum plasters (Akkuzugil, 1997); 1.17-1.32 for burnt mud plaster (Güdücü, 2003); 1.23-1.90 for Seljukid plasters (Caner, 2003); 1.18-1.43 for horasan plasters and 0.98-1.65 for lime plasters (Akyazı,1998); 1.66- 1.84 for exterior plasters from Adana; 1.1- 1.2 for exterior plasters from Ankara; 1.1 for interior plasters from Amasya;	0.5 for samples from Amasya and 0.2–0.4 for samples from Safranbolu
ϕ (%)	78.0 for G2 68.0 for G4	23 for BC, 25 for UC, 29 for FC, 32 for WRFC, 34 for JA	35- 50 for burnt mud brick (Güdücü, 2003)	45-48 (Tuncoku, 1993); 35.58-56.91 for masonry brick (Tuncoku, 2001); 28.1-49.6 (Tuncoku *et. al.* 1993); 34 (Yıldırım Esen *et al.*, 2004); 30.69-40.10 (Akyazı, 1998); 40.4- 40.7 for infill brick from Adana; 52.0- 54.2 for masonry brick;	40.1 for burnt mud-mortar (Güdücü, 2003), 27.36-45.88 for stone mortars; 27.81-52.26 for brick mortars (Tuncoku, 2001); 30-47 for brick masonry mortars, 29-32 for stone masonry mortars (Yıldırım Esen *et al.*, 2004)	32.05-47.82 for lime plasters; 23.52-41.38 for gypsum plasters (Akkuzugil, 1997); 40.7-56.2 for burnt mud plaster (Güdücü, 2003); 19.67-49.03 for Seljukid plasters (Caner, 2003); 33.67-55.30 for horasan plasters, 24.76-57.64 for lime plasters (Akyazı, 1998);29-59 (Yıldırım Esen *et al.*, 2004); 30- 34 for exterior plasters from Adana; 54 for interior plasters from Amasya; 44-48 for exterior plasters from Ankara;	19-53 for samples from Safranbolu; 20-23 for samples from Amasya
θ_{max} (% by weight)	192 for G2 114 for G4	12 for BC, 14 for UC, 17 for FC, 18 for WRFC, 24 for JA	39.1-69.4 for burnt mud brick (Güdücü, 2003)	15.2-36.7 (Tuncoku *et. al.* 1993); 30-35 (Tuncoku, 1993); 17.20-25.49 (Akyazı, 1998); 38.5- 41.3 for masonry brick from Konya.; 24.6-25.1 for infill brick from Adana	44 for burnt mud mortar (Güdücü, 2003)	21.94-37.06 for lime plasters, 13.90- 30.78 for gypsum plasters (Akkuzugil, 1997); 55.9-76.8 for burnt mud plaster (Güdücü, 2003); 10.3-39.8 for Seljukid plasters (Caner, 2003); 23.71 and 46.80 for horasan plasters, 15.84-58.88 for lime plasters (Akyazı, 1998); 17.72-19.38 for exterior plaster samples from Adana; 47.6-48.7 for interior plaster samples from Amasya; 36.0-43.6 for exterior plaster samples from Ankara;	78.6-137.4 for samples from Safranbolu; 37.6-44.2 for samples from Amasya
***SD* (m)**	0.45 for G2 0.44 for G4 **S_o:** 10 cm	0-0.046 for BC, 0.210 for UC, 0.115 for FC, 0.029 for WRFC and 0.013-0.040 for JA, S_O= 0-0.4cm, 1.5 cm, 0.8-1 cm, 0.5 cm, 0.1-0.3 cm for BC,UC,FC,WRFC and JA respectively.	0.28-0.32, **S_o:** 10 cm	0.91 & 1.29, **S_o:** 10 cm	0.033 for mud mortars of 0.0163 m thickness (Akkuzugil, 1997)	0.020-0.069 for Seljukid plasters (Caner, 2003); 0.04-0.15 for lime plasters (Yıldırım Esen *et al.*, 2004); 0.026-0.059 for lime coats, 0.014-0.051 for mud plasters, 0.013-0.050 for gypsum plasters (Akkuzugil, 1997); 0.052-0.152 for horasan, 0.051-0.113 for lime plasters, 0.043, 0.044 and 0.057 for mud plasters (Akyazı, 1998)	0.8, **S_o:** 10 cm
μ	3.4-7.0 for G2 2.9-7.0 for G4	11.56 for BC, 13.99 for UC, 11.50 for FC, 5.86 for WRFC, 13.37 for JA	2.75- 3.23 (Akkuzugil, 1997) 0.57-0.99 for burnt mud brick (Güdücü, 2003)	9.06 &12.85 (Akyazı, 1998)	1.92-2.70 for mud mortars (Akkuzugil, 1997)	2.3-16.2 for lime plasters (Yıldırım Esen *et al.*, 2004), 3.04-18.27 for lime plasters, 2.88-13.33 for gypsum plasters, 1.19-3.16 for mud plasters (Akkuzugil, 1997); 0.51 & 0.64 for burnt mud plaster (Güdücü, 2003); 1.79-9.22 for Seljukid plasters (Caner, 2003); 2.878 and 12.790 for horasan plasters, 6.444 and 23.704 for lime plasters and 3.043, 5.507 and 2.519 for mud plasters (Akyazı, 1998)	8 (Kumaran *et. al.*, 1994)
T_{drying} (days)	24 for G2 25 for G4	10 for BC, 10 for UC, 10 for FC, 8 for WRFC	NA	~10 for historic bricks (Tuncoku *et. al.*, 1993); ~29 for masonry bricks; ~36 for infill bricks	5 or 6 for some stone and brick mortars (Tuncoku, 2001)	4 days for exterior plasters from Adana, 4 days for interior plasters from Amasya, 3 days for exterior plasters from Ankara	~43 days for Amasya timber, ~46 days for timber samples from Safranbolu
R_E (kg/m^2.h)	0.0723 for G2 0.0777 for G4	0.0779 for BC, 0.0591 for UC, 0.1058 for FC, 0.0847 for WRFC	NA	0.0770 for infill brick samples from Adana; 0.1241 for masonry brick samples from Konya	NA	0.0745 for exterior plasters from Adana; 0.0782 for interior plaster samples from Amasya	0.1411 for samples from Safranbolu; 0.1637 for samples from Amasya
E_{mod} (GPa)	1.4 for G2 2.1 for G4	3.9 for BC, 3.4 for UC, 3.7 for FC, 2.0 for WRFC, 3.0 for JA 7.6 for BC, 7.5 for UC, 3 for FC, 4.7 for WRFC (Felekoğlu, 2004)	0.7 (METU-MCL studies Fall 04'-REST 556), 1.170- 2.068 (Güdücü, 2003)	3.1-5.2 for bricks (Yıldırım Esen *et al.*, 2004)	1.2-3.6 for brick mortars (Yıldırım Esen *et al.*, 2004), 0.71-8.32 for stone mortars, 0.70-2.99 for brick mortars (Tuncoku, 2001)	0.7-6.6 for lime plasters (Yıldırım Esen *et al.*, 2004); 0.6-1.7 for burnt mud plaster (Güdücü, 2003); 2.855 average for Seljukid plasters (Caner, 2003)	NA
UCS (Mpa)	1.88 for G2 2.76 for G4	26.2 for BC, 15.6 for UC, 11.9 for FC, 12.8 for WRFC (Felekoğlu, 2004)	5.69 Mpa (METU-MCL studies Fall 04'-REST 556), 0.3-2Mpa (Eriç, 1980), 0.5-2 Mpa for non stabilized earth (Olivier & Mesbah, 1993), 1Mpa for normal mud brick according to T.S. 2514 (Eriç, Anıl & Çorapçıoğlu, 1980)	17 (Kahya, 1991)	NA	NA	NA
$Is_{(50)}$(Mpa)	0.4 for G2 0.7 for G4	NA	0.10- 1.51 for burnt mud brick (Güdücü, 2003)	NA	0.52-1.38 for stone mortars 0.10-0.59 for brick mortars (Tuncoku, 2001)	0.02-0.15 for burnt mud plasters (Güdücü, 2003)	NA
ΔEC (mS/cm)	0.85 for G2; 0.95 for G4; 0.27 for the aggregate	NA	3-5.7 for burnt mud brick (Güdücü, 2003)	NA	9 for the aggregates of stone and brick mortars (Yıldırım Esen *et al.*, 2004), 0.4-1.5 for brick mortars (Tuncoku, 2001); 1.7- 3.3 for stone mortars (Tuncoku, 2001)	7 for the aggregates of plasters (Yıldırım Esen *et al.*, 2004); 1.8- 6.4 for burnt mud plasters (Güdücü, 2003); 42 mS/cm for Alanya Byzantine plaster (Caner, 2003)	NA